Epigenetic and posttranslational regulation of the disintegrin and metalloproteases ADAM17 and ADAMTS-16

Dissertation

zur Erlangung des Doktorgrades

der Mathematisch-Naturwissenschaftlichen Fakultät

der Christian-Albrechts-Universität zu Kiel

vorgelegt von

Felix Kordowski

Kiel, 2015

Erste Gutachterin: **Prof. Dr. rer. nat. Karina Reiss**

Zweiter Gutachter: **Prof. Dr. rer. nat. Thomas Roeder**

Tag der mündlichen Prüfung: **02.12.2015**

Zum Druck genehmigt: **02.12.2015**

gez. Prof. Dr. rer. nat. Wolfgang J. Duschl, Dekan

Table of content

1 Introduction

1.1 The Adamalysine protease family

Physiological processes in higher organisms need to be precisely orchestrated and tightly regulated. Proteolysis is one of the many biological processes that regulate and control physiological functions of the cell. Proteolysis is the breakdown of proteins into smaller polypeptides or amino acids. In addition to the pure breakdown and recycling of proteins, it plays a crucial role in the maturation of proteins, activation and deactivation of enzymes and proteins, and the release of signaling molecules, such as growth factors and cytokines. Proteases are the enzymes realizing this function. A specialized case of proteolysis is the proteolytic processing of transmembrane proteins followed by their ectodomain release. This process is known as *shedding* (Reiss and Saftig, 2009) and enzymes mediating this process are known as *sheddases*. Shedding serves diverse functions, such as releasing soluble factors from the cell surface, rapidly decreasing selective proteins on cells and inactivating cell surface receptors, and detaching cell adhesion proteins (Reiss and Saftig, 2009). The major proteinase family that mediates shedding is the *A Disintegrin And Metalloproteases (ADAMs)* family. The name is derived from two major functional domains of ADAMs: a disintegrin domain and a metalloprotease domain. ADAMs belong to the family of Adamalysines which are part of the Metzincin family of metalloproteases. The *Snake venom metalloproteinase (SVMPs)* and *ADAMs with thrombospondin motifs (ADAMTSs)* are also part of the Adamalysine family. ADAMs and ADAMTSs are both strongly related with similar domain structure, but distinct functions. While the ADAM family comprises mostly transmembrane proteases with very important functions as sheddases, the ADAMTSs are lacking the transmembrane domain and are therefore secreted proteases with major functions in remodeling the extracellular matrix (Apte, 2004). Both families are involved in inflammatory (Demircan et al., 2014) and cancerous diseases (Cal and López-Otín, 2015) and will be introduced in the following chapters.

1.1.1 The ADAMs

ADAMs are zinc-dependent metalloproteases as they need zinc as co-factor for their proteolytic activity. Interestingly, about half of the 21 identified human members of the ADAM family do not express the typical metalloprotease zinc-binding active site (HExxHxxGxxH) and as a consequence are proteolytically inactive (Bode et al., 1993). These proteolytically inactive ADAM members are suggested to fulfill functions through mediating protein-protein interactions with their disintegrin and cysteine-rich domains (White, 2003). ADAMs are type-I-transmembrane proteins located in the plasma membrane of cells where they carry out their major function as sheddases. However, most ADAMs are found predominantly in the Golgi (Lammich et al., 1999; Schlöndorff et al., 2000) and to a lesser degree on the cell surface (Gutwein et al., 2003). ADAMs were identified in a broad range of species, such as *C. elegans*, *Drosophila, Xenopus,* as well as in vertebrates, but not in *E. coli*, *S. cerevisiae* or plants (Seals and Courtneidge, 2003). Interestingly, the mouse genome encodes nearly double the amount of ADAM genes compared to the human genome (Puente and Lo, 2004). All ADAMs follow a comparable modular design: The ADAM prototype consists of a prodomain, a metalloprotease domain, a disintegrin domain, a cysteine-rich domain, an *epidermal growth factor (EGF)*-like domain, a transmembrane domain and a cytoplasmic tail. The functions of these domains will be further discussed in chapter 1.1.1.1. The major importance of ADAMs is reflected by the phenotypes of ADAM knock-out mice. For instance, ADAM10 or ADAM17 deficiency leads to prenatal and perinatal lethality, respectively (Hartmann et al., 2002; Peschon, 1998). In contrast, deletion of some ADAM members does not result in any pathologies suggesting redundancy with other ADAM proteases (Seals and Courtneidge, 2003). Just recently, the second known case of ADAM17 loss in humans was published. This homozygous loss-of-function mutation was associated with severe multiorgan dysfunction, eventually leading to the death of this patient 10 months after birth (Bandsma et al., 2015). The importance of the ADAMs is further reflected by the enormous substrate variety they shed. For the best studied member, ADAM17, more than 75 substrates were identified, comprising diverse molecule classes, including cytokines, e.g. *tumor necrosis factor alpha (TNF-α)*, cytokine receptors, e.g. *TNF receptor I (TNFRI)*, as well as growth factors, e.g. *transforming growth factor alpha (TGF-α)* (Scheller et al., 2011). Additionally, cell adhesion molecules such as E-cadherin are important ADAM substrates. In the process of ectodomain shedding ADAMs are processing other transmembrane proteins or membrane-associated proteins resulting in the release of their ectodomain. Shedding of these molecules not only provides the possibility for down-regulation, but also for initiating or inhibiting autocrine or

paracrine signaling via soluble proteins (Figure 1). Many ADAM members shed more than only one substrate and also commonly share some substrates. Interestingly, there is no consensus sequence in the cleavage site of different substrates shed by the same ADAM, although some ADAMs show preferences in their cleavage site specifity for some amino acids (Tucher et al., 2014). Nevertheless, the common feature is that all proteins are shed in close proximity to the membrane. The ADAM-mediated ectodomain shedding gives rise to two major biological concepts: the fast and rapid remodeling of the cell surface changing the phenotype of the cell, and the release of soluble mediators from the cell surface. The physiological consequence is strongly dependent on the functions of the shed protein in the biological system. For instance, growth-factors are often transported in an inactive state to the cell surface where they rest in the plasma membrane until they are shed. The released ectodomain then functions as a paracrine signaling molecule and can activate other cells through binding to their receptors. A typical example for this type of signaling is the release of proTGF-α by ADAM17. After activation, soluble TGF-α can bind to *epidermal growth factor-receptors (EGFRs)* of other cells and stimulate the cells to proliferate and migrate. Due to the broad variety of substrates, ADAMs control a wide spectrum of biological processes: cell migration and adhesion, cell proliferation, fertilization, central nervous system and cardiovascular system development, immunity, and wound healing. Moreover, these proteases are involved in pathophysiological processes such as inflammation and cancer as well. This thesis will focus on the regulation of ADAM17, one of the most important ADAMs.

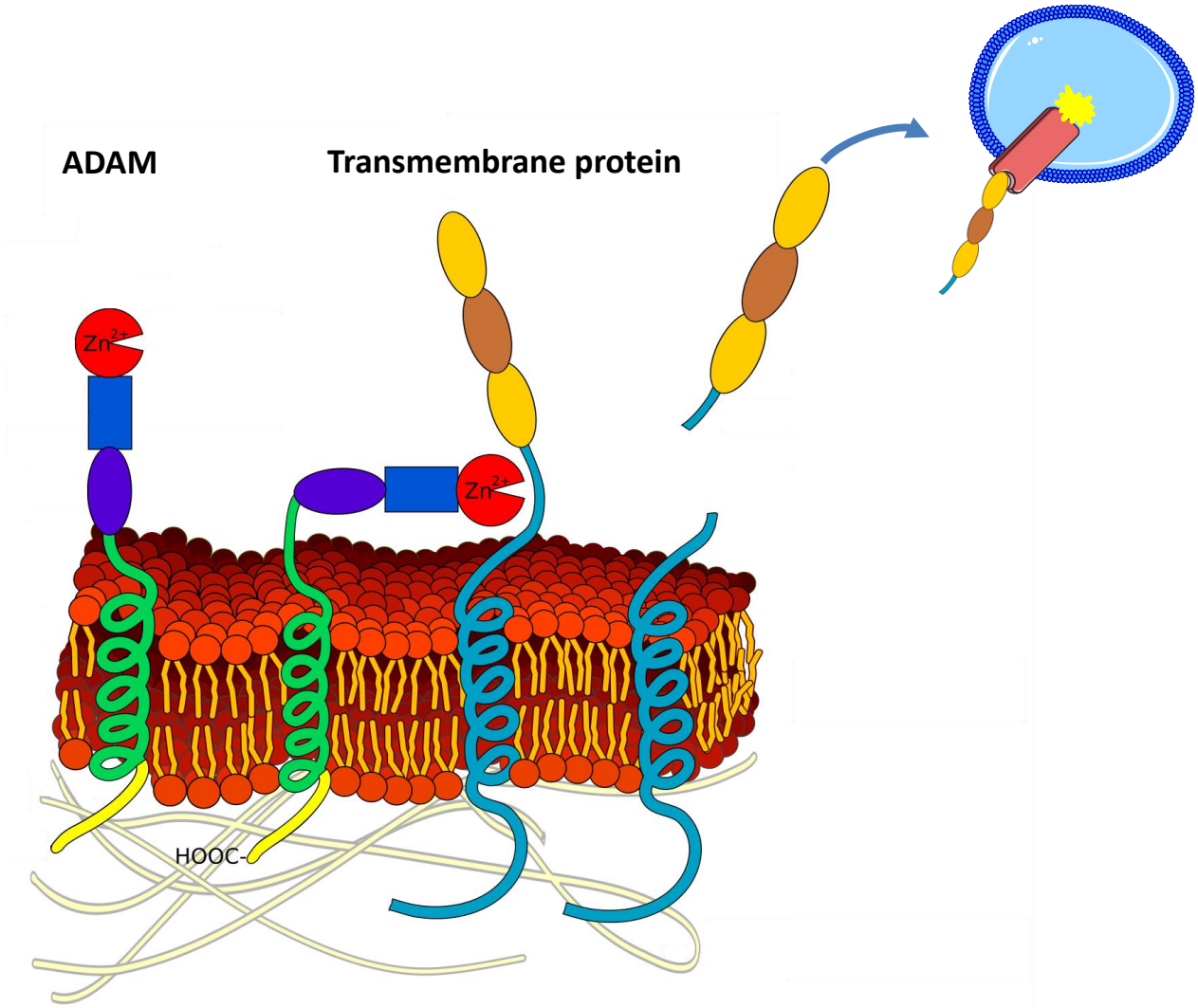

Figure 1. Schematic view of ADAM-mediated substrate shedding. Shedding is the proteolytic processing of transmembrane proteins followed by their ectodomain release. Shedding serves diverse functions, such as releasing soluble factors from the cell surface, rapidly decreasing selective proteins on cells and inactivating cell surface receptors. The major proteinase family that mediates shedding is the A Disintegrin And Metalloproteases (ADAMs) family. Depicted is a generalized shedding event of a transmembrane substrate (e.g., TNF-α) by an ADAM (e.g., ADAM17). The substrate is cleaved in close proximity to the cell membrane releasing its ectodomain. The soluble ectodomain may then function as a signaling molecule and activate other cells in a paracrine manner. The modified picture is licensed under *CC BY-SA 3.0* and based on work from Armin Kuebelbeck.

1.1.1.1 The metalloprotease ADAM17

ADAM17 was initially identified as the ADAM member that releases the pro-inflammatory cytokine TNF-α from the cell surface. For this reason it was named *tumor necrosis factor converting enzyme (TACE)* (Black et al., 1997). Later on, many more substrates of ADAM17 were identified (Seals and Courtneidge, 2003).

ADAM17 and its closest relative ADAM10 are two atypical ADAM members regarding their domain organization. The canonical modular design of ADAMs is: a prodomain, a metalloprotease domain, a disintegrin domain, a cysteine-rich domain, an EGF-like domain, a transmembrane domain and a cytoplasmic tail (Figure 2). While ADAM17 and ADAM10 in general follow this design, they differ in comprising a membrane-proximal domain (MPD) and a flexible stalk region, instead of the cysteine-rich and EGF-like domain (Düsterhöft et al., 2014; Takeda, 2009). The N-terminus of ADAMs contains a signal sequence that directs the protease into the secretory pathway. This sequence is later cleaved off. The following prodomain is involved in the maturation process and acts as a chaperone during the transit through the secretory pathway. Studies show that the prodomain is essential for proper folding of the metalloprotease domain. Mutants lacking the prodomain are proteolytically inactive, but can be rescued by coexpression of the prodomain (Anders et al., 2001). The metalloprotease domain gives rise to the proteolytic function of ADAMs, although not all ADAMs comprise the catalytic motif HExxHxGxxH, rendering them proteolytic inactive. Crystallization of the metalloprotease domain revealed the structure of the active site (Maskos et al., 1998). The disintegrin domain was first identified in *snake venom metalloproteases*, where it binds to integrin receptors inhibiting the association of platelets with the integrin receptors. This leads to abolished coagulation at the wound site after a snake bite. Integrins are transmembrane receptors mediating cell to cell-interactions and cell to matrix-interactions, thus providing cell adhesiveness. Several ADAM members bind to integrin receptors. ADAM17 mediates cell-cell contacts by binding to $\alpha_5\beta_1$-integrins (Bax et al., 2004). The MPD and the adjacent stalk region of ADAM17 were shown to be involved in substrate binding, ADAM17 multimerization and ADAM17 activation/deactivation (Düsterhöft et al., 2013, 2014; Lorenzen et al., 2011, 2012). Since the studies were conducted *in vitro*, the *in vivo* relevance of these findings remains to be shown. The MPD and the stalk region will be discussed in more detail in chapter 1.2.3.1. The transmembrane domain anchors the ADAMs in the plasma membrane. Interestingly, this domain does not only function as a pure membrane anchor, but is also important for the

shedding activity. ADAM17 lacking the transmembrane domain, but instead anchored through a glycosylphosphatidylinositol (GPI)-anchor, is not able to shed TGF-α, TNF-α and L-selectin anymore (Li et al., 2007). The transmembrane domain seems to be also important for substrate selectivity (Li et al., 2007). The importance and functions of the intracellular cytotail are introduced in 1.2.3.1.

ADAM17 has a crucial role in inflammation because of its genuine function in releasing the pro-inflammatory cytokine TNF-α. This type II-transmembrane protein acts as an important signaling molecule in the immune system. After shedding of the membrane-bound TNF-α, the released soluble TNF-α can bind to TNFR1 and TNFR2. Binding to the TNFRs leads to the activation of various intracellular pathways e.g., NF-κ-B activation which promotes an inflammatory response. In many inflammatory diseases, such as rheumatoid arthritis, inflammatory bowel disease and multiple sclerosis, TNF-α promotes the inflammation. In line with this, ADAM17 dysregulation could be identified in these diseases (Edwards et al., 2008).

Many ligands of the EGF receptor family are ADAM10 and ADAM17 substrates. TGF-α represents a prototype of such ligands released from the membrane by ADAM17. This cytokine belongs to the EGF family and is a ligand of the EGFR family. Similar to TNF-α, TGF-α is synthetized as a membrane bound precursor which is shed from the cell surface by ADAM17. Soluble TGF-α can then bind to EGFRs and induce signaling in the respective cell in an autocrine or paracrine manner. The downstream signaling network is amazingly complex, but in principle leads to activation of genes regulating cell proliferation, survival, cell migration and differentiation (Oda et al., 2005). The importance of ADAM17-mediated EGFR ligand shedding is also reflected in the phenotype of mice lacking functional ADAM17: Both, EGFR knock-out mice and ADAM17 knock-out mice show similar phenotypes, e.g. defects in epithelial maturation and differentiation (Peschon, 1998) and perinatal death (Miettinen et al., 1995).

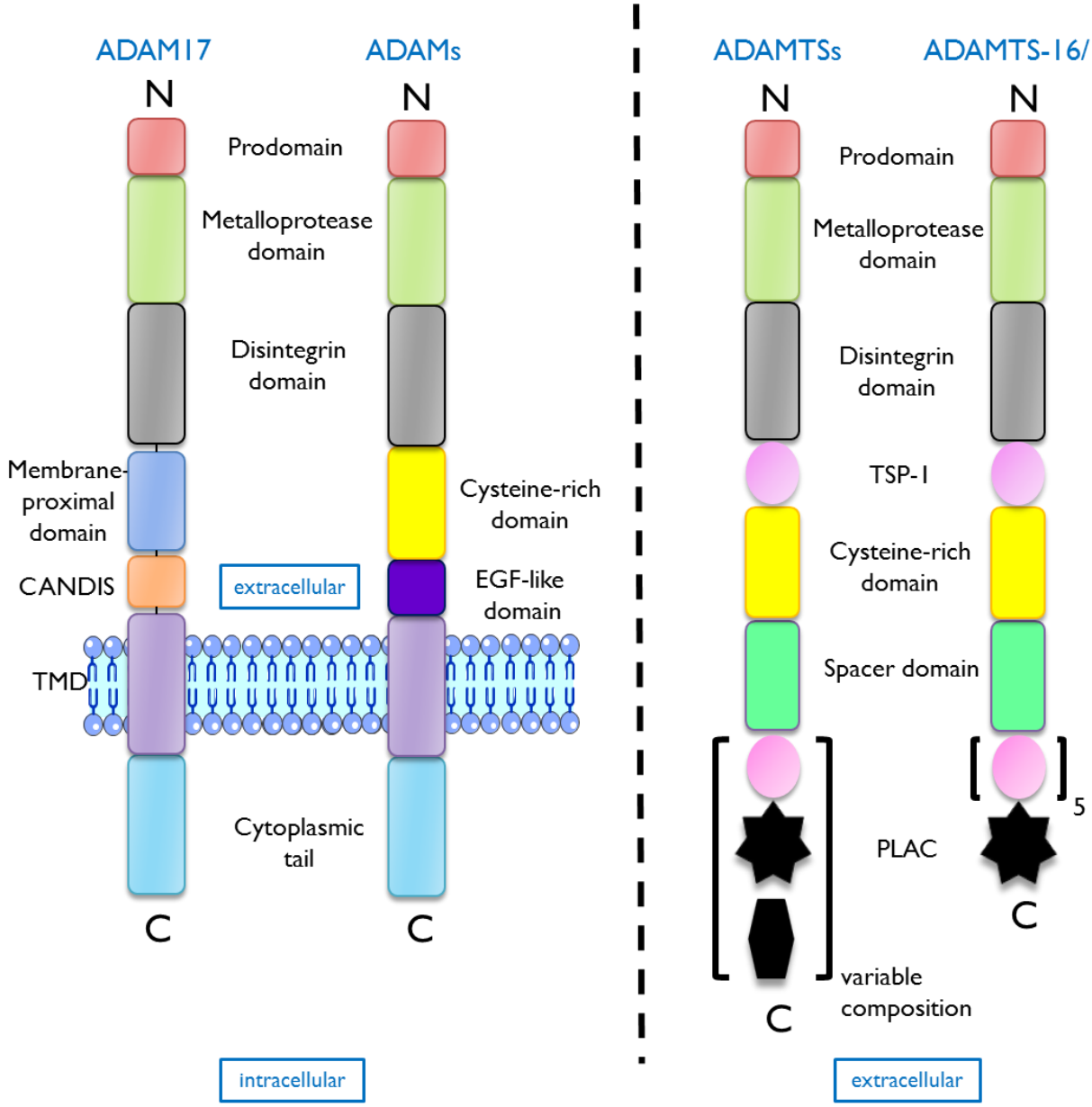

Figure 2. Modular design of ADAMs and ADAMTSs. ADAMs and ADAMTSs follow a similar modular design. The major difference between both is that ADAMTSs comprise thrombospondin type 1 (TSP-1) repeats and lack the transmembrane domain (TMD). Therefore, ADAMTSs are secreted proteases with functions in the extracellular matrix, whereas ADAMs function as sheddases on the cell surface. Member-specific domain organization is shown for ADAM17 and ADAMTS-16/18. N=N-terminus; C=C-terminus; PLAC=protease and lacunin domain. According to (Apte, 2004; Cal et al., 2002; Takeda, 2009).

1.1.2 The ADAMTSs

Another important Adamalysine subfamily is the *ADAM with thrombospondin motifs (ADAMTS)* family. The ADAMTSs and the ADAMs share many features. ADAMTSs have the characteristic ADAM-like metalloprotease domain, prodomain, disintegrin-like domain and cysteine-rich domain. However, ADAMTSs differ from ADAMs in two important features: They comprise *thrombospondin type 1 (TSP-1)* repeats and they lack the transmembrane domain (Tang, 2001) (see Figure 2). Thus, they are secreted into the extracellular space. The TSP-1 repeats adhere them to components of the *extracellular matrix (ECM)*, a collection of extracellular molecules secreted by cells that provides structural and biochemical support to the surrounding cells. Therefore, ADAMTSs differ from the ADAMs in their localization and also in their substrates. Since most of the ADAMTSs substrates are components of the ECM, such as procollagen and aggrecan, ADAMTSs have major functions in the remodeling of the ECM (Apte, 2004).

Nineteen members of this relative new protease family have been identified in humans so far. Interestingly, all are presumed to be proteolytically active, but many of them are still marked as *orphan ADAMTSs*, since there is no known function or substrate yet identified. More recently, a homologous subfamily, of *ADAMTS-like proteases (ADAMTSLs)* which lack the enzyme activity was identified (Le Goff and Cormier-Daire, 2011). The mammalian ADAMTS members can be classified regarding their major substrates into aggrecanases (ADAMTS-1, -4, -5, -8, -9, -15, -20), procollagen N-proteinases (ADAMTS-2, -3, -14), the *Von Willebrand factor-cleaving protease (vWFCP/ADAMTS-13)* and the orphan ADAMTSs (-6, -7, -10, -12, -17-19) with no known substrate (Jones and Riley, 2005). ADAMTS-16, which will be introduced in chapter 1.1.2.1 in detail, used to belong to the group of orphan ADAMTSs. Only recently, some of its functions have been identified.

The prototypic design of ADAMTSs is: an N-terminal signal peptide, followed by a prodomain, a metalloprotease domain and an ancillary domain. The ancillary domain comprises a disintegrin-like domain, a central TSP-1 repeat, a cysteine-rich domain and a *spacer domain (SD)*. The C-terminal part of the ADAMTSs is the most variable part and can include additional TSP-1 repeats and various other domains e.g., *protease and lacunin (PLAC)* domains (Apte, 2004). The disintegrin-like domain found in ADAMTSs differs from those found in the *snake venom metalloproteases* and has not been yet shown to bind integrins as the ADAM-disintegrin-like domain does (Brocker et al., 2009). It is suggested that the ADAMTS-disintegrin-like domain is

important for the enzyme activity and substrate specifity, as evidenced for ADAMTS-13 (De Groot et al., 2009). ADAMTSs lack the EGF-like domain, the transmembrane domain and the cytotail, that ADAMs are comprising. Instead, they have a central TSP-1 repeat, optional additional C-terminal TSP-1 repeats and a SD. The C-terminal TSP-1 repeats are involved in cell-cell interactions, angiogenesis and induction of apoptosis (Guo et al., 1997; Iruela-Arispe et al., 1999). Supported by studies of ADAMTS-1, the central TSP-1 repeat is thought to be a functional heparin-binding motif, anchoring ADAMTSs to the ECM. The C-terminal TSP-1 repeats support this function, but show a lower affinity to heparin then the central repeat (Kuno and Matsushima, 1998). The SD mediates substrate-binding (De Groot et al., 2009) and is also involved in heparin binding (Kuno and Matsushima, 1998).

Since ADAMTSs process several important extracellular proteins, such as collagen and aggrecan, they are highly involved in connective tissue turnover, especially of the cartilage (Malfait et al., 2002; Pratta et al., 2003). Many mutations in ADAMTS genes are linked to diseases caused by a dysfunctional ECM with altered features, such as different stabilizing properties and altered network formation (Hubmacher and Apte, 2015). Moreover, ADAMTSs are also involved in angiogenesis, blood coagulation and cell migration. Therefore, the involvement of one of the ADAMTSs, ADAMTS-1, in cancer progression has been intensively studied (Tan et al., 2013). ADAMTS-1 facilitates tumor progression through promoting several critical tumor features, such as cell migration by degrading surrounding ECM molecules (versican and brevican), and angiogenesis by sequestration of pro-angiogenic factors (Kumar et al., 2012). Interestingly, several other ADAMTSs are anti-angiogenic or tumor suppressors. ADAMTS-9, for example, acts directly as a tumor suppressor and is associated with poor survival in gastric cancer (Du et al., 2012).

1.1.2.1 The metalloprotease ADAMTS-16

ADAMTS-16 is one of the less studied ADAMTS members. Until recently, ADAMTS-16 belonged to the orphan members of the ADAMTSs, where no substrate and function was known. Today, the only known substrate of ADAMTS-16 is α2-macroglobulin (Gao et al., 2007), a general inhibitor of proteases. Additionally, it was shown that recombinant truncated forms of ADAMTS-16 show low aggrecanase activity, although it is not known if this truncation occurs naturally (Zeng et al., 2006). In the recent years, more functions of ADAMTS-16 were proposed. It was shown that ADAMTS-16 is a regulator of blood pressure, probably by regulating the thickness of the arteries in *Adamts16*

knock-out rats. Homozygous *Adamts16* knock-out rats develop hypertension and renal damages (Gopalakrishnan et al., 2012). In further studies it was revealed that these knock-out rats have impaired development of the male testis, resulting in infertile males (Abdul-Majeed et al., 2014). In line with these findings, two genetic variants of *ADAMTS16* in humans could be linked to inherited hypertension supporting its role as a regulator of systolic blood pressure (Joe et al., 2009). A physiological role of ADAMTS-16 is suggested in the human ovarian follicle maturation. α2-macroglobulin binds and thereby inactivates the pro-angiogenic *vascular endothelial growth factor (VEGF)* (Soker et al., 1993). This inactivation could restrict the development of small blood vessels until final maturation of the ovarian follicle (Gruemmer et al., 2005). The maturation of the ovarian follicles is regulated by increasing levels of *follicle-stimulating hormone (FSH)*. Since FSH also induces ADAMTS-16 expression, it was suggested that ADAMTS-16 expression inactivates α2-macroglobulin after increasing FSH levels. The consequence is that active α2-macroglobulin is released and promotes angiogenesis needed for proper maturation (Gao et al., 2007). The importance of ADAMTS-16 in ovarian maturation is also indicated by a gene variant associated with higher risk of premature ovarian failure (Pyun et al., 2014). *ADAMTS16* was the most upregulated metalloprotease in the inflammatory disease, osteoarthritis (Kevorkian et al., 2004). In the perspective of cancer, ADAMTS-16 was shown to be upregulated in esophageal squamous-cell carcinoma, where it was identified as an oncogene (Sakamoto et al., 2010). siRNA-mediated knock-down of *ADAMTS16* in esophageal cancer cell lines reduced invasiveness of these cells in an *in vitro* invasion assay (Sakamoto et al., 2010). By contrast, ADAMTS-16 overexpression in human chondrosarcoma cells led to decreased cell proliferation and migration (Surridge et al., 2009), therefore suggesting a cell type dependent effect. Interestingly, the closest relative of *ADAMTS16*, *ADAMTS18*, is a tumor suppressor gene (Wei et al., 2010; Xu et al., 2015).

1.2 Mechanisms of regulation for ADAMs and ADAMTSs

ADAMs and ADAMTSs have important functions in many physiological processes. These functions have to be tightly regulated and balanced. In general, a plethora of regulation mechanisms for proteins and their genes exist. In the following subchapter, three important mechanisms regarding ADAMs and ADAMTSs regulation, and in particular ADAM17 and ADAMTS-16, will be introduced.

1.2.1 Transcriptional regulation

Transcriptional regulation is the complex collection of diverse means that regulate the conversion of DNA to RNA. By controlling this vital process a cell orchestrates its gene activity by up and down-regulation of gene transcript levels and consequently protein levels.

1.2.1.1 Transcriptional regulation of ADAMs and *ADAM17*

The contribution of *ADAM17* gene expression changes to ADAM17 functions is poorly characterized. Altered expression of ADAM17 is described for breast cancer (Santiago-Josefat et al., 2007) and also for inflammatory diseases, such as ulcerative colitis (Arribas and Esselens, 2009) and rheumatoid arthritis (Charbonneau et al., 2007). Despite obvious functional implications of ADAM17 in inflammation (TNF-α) and cancer (EGFR-ligands), the effect of higher expression needs further investigation. The importance of ADAM17 expression levels was challenged by a recent publication: Transgenic overexpression of ADAM17 in mice clearly showed neither an elevated TNF-α shedding nor an elevated inflammatory response, thus clearly questioning that regulation of ADAM17 functions depends mainly on transcriptional regulation (Yoda et al., 2013). Nevertheless, extreme down-regulation or absence of ADAM17 expression is pathological as shown by knock-out mice. Additionally, a negative regulation of ADAM17 expression by microRNAs was identified (Doberstein et al., 2013).

1.2.1.2 Transcriptional regulation of ADAMTSs and *ADAMTS16*

Most ADAMTSs are expressed at low levels in mammals making it difficult to detect and study them (Tang, 2001). However, transcriptional regulation of expression seems to be an important regulatory step for the functions of ADAMTSs, since many studies show that diverse ADAMTS members are differentially expressed in various human cancers (Rocks et al., 2008). In many cases,

differential expression is correlated with methylation alterations in these ADAMTS genes (Kumar et al., 2012). Unfortunately, most studies lack functional analyses of this differential expression and their consequences remain uncertain.

ADAMTS expression is distributed over a broad range of adult tissues, but more limited in the fetal tissue. In case of distinct members, the expression is generally limited to selected tissues and not ubiquitous (Porter et al., 2005). Expression profile studies show that differential expression of many ADAMTS members is associated with different pathological processes, such as inflammatory or cancerous diseases. The only known dysregulations of *ADAMTS16* are reported for osteoarthritis (Kevorkian et al., 2004) and esophageal squamous-cell carcinoma (Sakamoto et al., 2010). *ADAMTS16* was originally identified to be expressed in the fetal lung and fetal kidney, and the adult brain and adult ovaries (Cal et al., 2002). More recently, it was reported that it is also expressed in the adult in the kidney, pancreas, spinal cord (Sakamoto et al., 2010) and colon muscle (Wilhelm et al., 2014). It should be noted that depending on the source, the reported tissue specific expression profiles differ in many cases which could possibly be attributed to different detection methods.

Regulation of ADAMTS gene expression is still poorly characterized, but several reports indicate that they are regulated by growth factors, hormones and inflammatory cytokines (Surridge et al., 2009). *ADAMTS16* expression is induced by FSH in the ovaries (see chapter 1.1.2.1) and can be induced by TGF-β, at least in a chondrocyte cell line (Surridge et al., 2009). Additionally, there was an inverse correlation of the *ADAMTS16* expression and *matrix metalloprotease-13 (MMP13)* expression in this cell line after *ADAMTS16* transfection.

Promoter studies of *ADAMTS16* could experimentally determine the promoter region and some transcription factors of *ADAMTS16* (Jacobi et al., 2013; Surridge et al., 2009). Several ADAMTS members are post-transcriptionally regulated by alternative splicing as several isoforms for ADAMTS proteins have been identified (Bevitt et al., 2005). Indeed, several transcript variants and isoforms of ADAMTS-16 were also reported. Unfortunately, so far there is no knowledge about the regulation and function of these isoforms. The present lack of knowledge about ADAMTS-16 is also reflected by the fact that there are only 23 publications about ADAMTS-16 available so far, urging for further research on this protease.

1.2.2 Epigenetic regulation

In the recent decades other general and very important regulatory mechanisms of gene transcription were identified: epigenetic mechanisms.

Epigenetic information is additional information encoded into the genome, by other means than the genetic code. In principle, all cells in the body share the same genetic code, but show divergent gene expression profiles and as a consequence can express different phenotypes. Epigenetic modifications are responsible for this diversity of gene expression by regulating the activity of genes. They decide which genes are actively transcribed and which are silent. Most of this epigenetic information is stored in structural modifications, such as histon modifications, DNA methylation and nucleosome positioning. It can also be mediated through non-coding regions in the DNA, which express e.g., microRNAs that silence mRNA transcripts.

Histon modification and DNA methylation are two key components of structural modifications as they alter the compactness of the chromatin and therefore the accessibility of genes for transcription. DNA methylation is the addition of a methyl (CH_3)-group to a cytosine at position 5. This methylation occurs in mammals nearly exclusively in the cytosine of CpG-dinucleotides (cytosine and guanine connected through a phosphate). CpG sites are in many cases enriched around the promoter region of genes. CpG-methylation in these regions has a tremendous effect on the activity of genes. Prototypically, actively transcribed genes show low methylation in CpG sites in the promoter region and the first exon, but high methylation in CpG sites in the gene body. Transcriptionally inactive genes show the inverse situation (Figure 3). This gene transcription modulation and gene silencing is important especially during development (Teif et al., 2014), as a host defense mechanism (Yoder et al., 1997) and in cancer (Esteller, 2007; Herman and Baylin, 2003). In cancer cells a global hypomethylation occurs, but strikingly, the CpG-sites in the promoter regions are instead hypermethylated. Consequently, the affected genes are silenced. These genes are in many cases tumor suppressor genes and their silencing contributes to the malignant development.

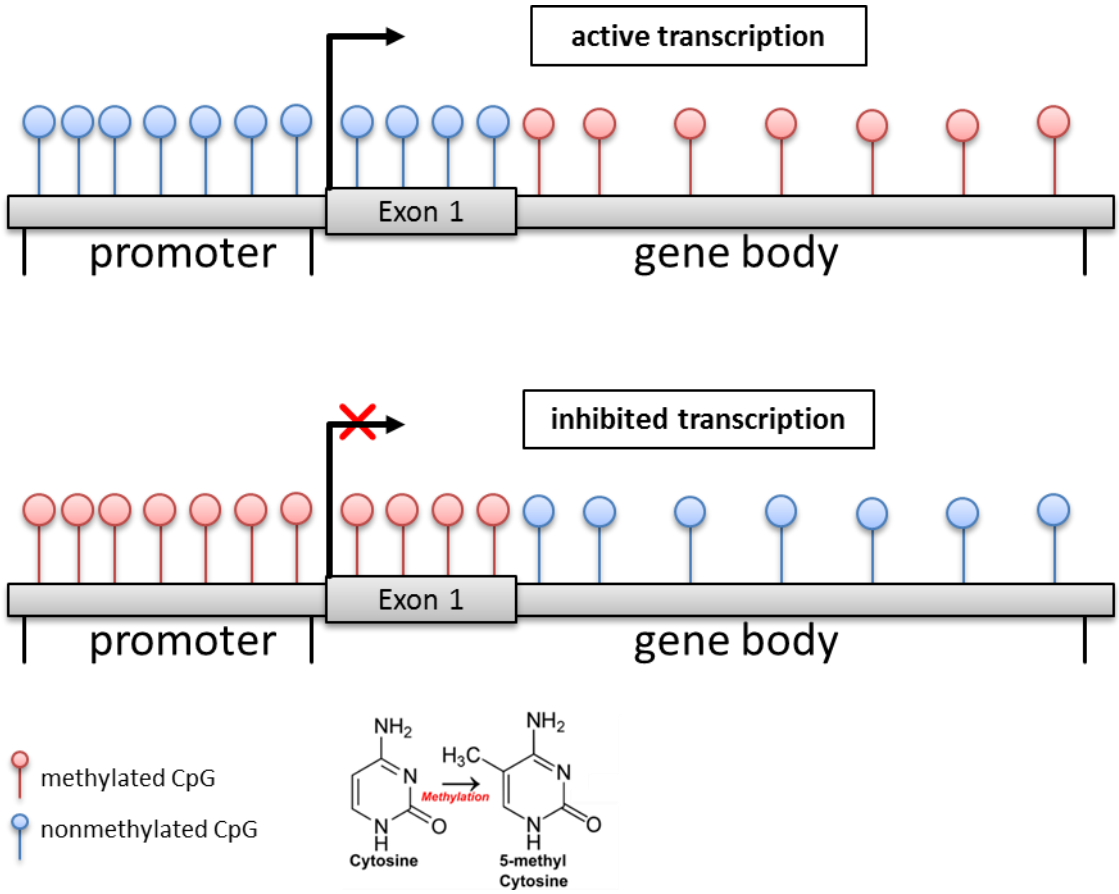

Figure 3. Regulation of gene activity by DNA methylation. CpG-dinucleotides are often clustered in the promoter region and around the first exon. Addition of a methyl group to the cytosine of a CpG can have a tremendous effect on the activity of genes. Prototypically, actively transcribed genes show low methylation in CpG sites in the promoter region and the first exon, but high methylation in CpG sites in the gene body. Transcriptionally inactive genes show the inverse methylation profile. This epigenetic regulatory mechanism is especially common in cancers. Promoter hypermethylation of tumor suppressor genes leads to their transcriptional inactivation. This contributes to many of the hallmarks of cancer. According to (Esteller, 2002, 2007).

1.2.2.1 Epigenetic regulation of ADAMs and ADAMTSs

Methylation changes for the two most important ADAMs, ADAM10 and ADAM17, are not described so far, but methylation changes for some ADAM (Seniski et al., 2009) and several ADAMTS (Kumar et al., 2012) members, especially in cancer, have been reported. Therefore, one aim of this thesis was to investigate whether methylation changes in inflammatory and cancerous diseases play a role for the regulation of ADAM and ADAMTS (ADAM/TS) proteases, particularly ADAM10 and ADAM17.

1.2.3 Posttranslational regulation

Posttranslational regulation refers to all means that regulate the levels of active proteins after their translation. These means include several known mechanisms, such as posttranslational modifications, proteolysis, protein folding and structural changes, which are either reversible or irreversible altering the properties and functions of these proteins. In the following, posttranslational regulation mechanisms for ADAMs and ADAMTSs will be introduced.

1.2.3.1 Posttranslational regulation of ADAMs and ADAM17

ADAMs are generally synthesized as zymogens, latent precursors which are later converted to the active form by removal of their prodomain. This is also the case for ADAM17. ADAM17 is translated at the outer face of the endoplasmic reticulum and the prodomain is cleaved by a furin-type proprotein convertase in the Golgi during its way through the secretory pathway (Schlöndorff et al., 2000). This generates mature, active ADAM17, since the prodomain acts as an inhibitory domain by coordinating the Zn^{2+} ion in the active site by a cysteine residue, blocking the catalytical site. An additional major function of the prodomain is its function as a chaperone, supporting the proper folding of ADAM17 during the secretory pathway (Milla et al., 1999).

A major question regarding the regulation of ADAM shedding activity is how the substrate selectivity is regulated. ADAM17 has a wide range of substrates, although there is no common consensus sequence for cleavage in its substrates. It is obvious that ADAM17 and its substrate need to be temporarily colocalized for the shedding event to take place, thus giving rise for a temporal and spatial regulation of the substrate accessibility to ADAM17. The majority of ADAM17 is localized in an intracellular compartment near the nucleus, but mature ADAM17 can be found on the cell surface (Schlöndorff et al., 2000). It was shown that mature ADAM17 is sequestered in lipid rafts during its way through the secretory pathway. Its shedding activity of TNF-α, TNFR1 and TNFR2, on the cell surface is then rate-limited by the entry of these substrates into the lipid raft microdomains. Substrates outside of the lipid rafts are not accessible to mature ADAM17 (Tellier et al., 2006). The hypothesis that regulation of the shedding activity occurs by limiting the substrate accessibility is also supported by studies showing, that lipid raft destruction through cholesterol depletion enhances ADAM17-mediated shedding (Matthews et al., 2003). Interestingly, not all ADAM17 substrates are cleaved on the cell surface. Amyloid precursor protein and ADAM17 are colocalized in the trans-Golgi-network while cleavage takes place there (Skovronsky et al., 2000).

The ectodomain shedding process of ADAM17 itself is also regulated: The protease is constitutively active, but strikingly its shedding activity can be rapidly induced by several physiological and unphysiological stimuli. Unphysiological stimuli, such as phorbol 12-myristate 13-acetate (PMA) and the ionophore ionomycin, can induce a rapid increase in ADAM17 shedding activity under experimental conditions (Horiuchi et al., 2007). Additionally, a broad variety of physiological stimuli, *inter alia,* thrombin, lysophosphatidic acid, lipopolysaccharides, acetylcholine, TNF-α, (Bz)ATP and EGF can induce the shedding of ADAM17 (Le Gall et al., 2010). These molecules are ligands of a broad range of different receptor types, such as G-protein coupled receptors, ligand gated ion channels, receptor tyrosine kinases and toll-like receptors. How all the different signaling pathways downstream of these receptors eventually lead to higher ADAM17 shedding activity is a central question in the research field and remains under intensive investigation. The involvement of the intracellular cytotail in the shedding activity is controversally discussed. Some studies show that ADAM17 shedding can be modulated through phosphorylation sites in the cytoplasmic tail (Schwarz et al., 2014; Xu and Derynck, 2010), but others show that ADAM17 lacking the cytoplasmic tail can still be activated (Le Gall et al., 2010). Recently, our research group (Sommer et al., 2015, in revision) proposed the distinctive step in the activation of stimulated ADAM17-mediated shedding: phosphatidylserine (PS)-exposure. It is proposed that a PS-binding motif in the MPD interacts with exposed PS after stimulation, and consecutively positions ADAM17 in the right orientation for proper shedding, thus enhancing its shedding activity. It is not yet clear, whether ADAM17 and ADAM10 share this mechanism, since some of the stimuli activate ADAM17 and ADAM10, e.g., ionomycin, but others only activate ADAM17 e.g., PMA (Le Gall et al., 2009).

In the recent years, importance was also attributed to the membrane-proximal domain of ADAM17. ADAM17 can principally multimerize, whereas it is not clear how many monomers are forming the multimer. Multimerization could have an important regulatory impact on the shedding activity like it is known for the *matrix metallopeptidase 14 (MT1-MMP)* (Lorenzen et al., 2011). In the case of ADAM17, the multimerization is most likely mediated by its MPD but the functional and biological relevance remains unclear.

Interestingly, a putative molecular turn-off switch was identified for ADAM17. The membrane-proximal domain (amino acids 581-642) comprises a thioredoxin motif ($C_{600}XXC_{603}$) which can be isomerized by a *protein-disulfide isomerase (PDI)*. The PDI rearranges the two disulfide linkages in

this motif. These disulfide bond changes restructure the MPD from a flexible, open conformation to a more closed and inflexible conformation (Düsterhöft et al., 2013). PDIs are found on the cell surface as ADAM17 and can indeed negatively regulate the ADAM17 shedding activity (Bennett et al., 2000; Willems et al., 2010) potentially by restructuring the MPD. So far, no reversion of this proposed inactivation has been identified.

Another feature of the MPD and the adjacent stalk region is the involvement in substrate binding. They recognize and bind the type-I transmembrane substrates *interleukin-6 receptor (IL-6R)* and *interleukin-1 receptor 2 (IL-1RII)*, but not the type-II transmembrane protein TNF-α (Lorenzen et al., 2012). Later on, it was revealed that a sequence in the stalk region, but not the MPD, was actually responsible for this interaction and named *Conserved ADAM seventeeN Dynamic Interaction Sequence* (*CANDIS,* amino acids 644-660), due to its high conservation between species and its substrate binding ability (Düsterhöft et al., 2014).

1.2.3.2 Posttranslational regulation of ADAMTSs and ADAMTS-16

All ADAMTS members undergo pro-protein processing similar to that of ADAMs, where the prodomain is cleaved off along the secretory pathway (Porter et al., 2005). In general, the prodomain mediates latency of the protein, however there are known exceptions e.g., ADAMTS-13 is active even with attached prodomain (Majerus et al., 2003).

An additional C-terminal processing is reported for several ADAMTSs regulating their activity. At least ADAMTS-1 and ADAMTS-4 can undergo cleavage in the SD, which alters their activity: Both processed forms have less affinity for heparin. Processed ADAMTS-1 is less anti-angiogenic and the processing of ADAMTS-4 alters its proteolytic activity against aggrecan (Gao et al., 2002; Rodríguez-Manzaneque et al., 2000). These changes have been attributed to loss or truncation of the SD and the following TSP-1 repeats. Whether this type of regulation can be applied to ADAMTS-16, needs further investigation. In principle, at least truncated recombinant forms of ADAMTS-16 show an enhanced aggrecanase activity, but if they occur under physiological situations is not reported (Zeng et al., 2006).

1.3 Aims of this thesis

ADAM17 is pivotal for a broad range of physiological and pathological processes, since it is a key regulator of substrates mediating these events. Although being intensively investigated, it still remains uncertain how this protease is regulated in detail, and how the shedding of such a broad substrate repertoire is tightly regulated and kept in balance not to result in pathological conditions. Modulating ADAM17 shedding activity is discussed as a potential target for therapeutic intervention in pathologies, in which ADAM17 substrates are involved. However, drugs directed against the active site of ADAM17 have not been a success to date. These inhibitors failed, since they were not substrate-specific and blocked the proteolysis of all ADAM17 substrates. As a consequence, treated patients suffered from severe side effects. Therefore, understanding the molecular mechanisms of ADAM17 regulation is essential and may aid to develop substrate-specific therapeutics. The stalk region of ADAM17, recently named *Conserved ADAM seventeeN Dynamic Interaction Sequence (CANDIS)*, has been shown to bind to a subset of ADAM17 substrates. Interestingly, it is also able to interact with lipids, suggesting a putative membrane interaction between CANDIS and the plasma membrane. This interaction could be an important modulatory step in the molecular mechanism of ADAM17-mediated shedding of certain substrates. The ① aim of this thesis was to evaluate whether this lipid binding ability of the CANDIS region contributes to the ADAM17 shedding activity.

Transcriptional regulatory mechanisms of ADAMs are even less characterized, although dysregulation of ADAMs was reported in inflammatory and cancerous diseases. Transcription levels are in general tightly regulated by epigenetic mechanisms such as DNA methylation. Consequently, the question arises whether DNA methylation contributes to the dysregulation of ADAMs in diseases. This is particularly interesting, since epigenetic modifications are reversible and can be potentially influenced by nutrition or drug intervention for therapeutic purposes. Epigenetic regulation of ADAM proteases in normal tissue has been poorly investigated and no reports exist describing the epigenetic patterns of these genes in diseases, except cancer. Surprisingly, despite being involved in shedding of inflammatory cytokines and cell adhesion molecules, epigenetic patterns of ADAM10 and ADAM17 in inflammatory and cancerous diseases have not been reported so far. The ② aim of this thesis was to investigate whether ADAMs, including ADAM17 and ADAM10, are epigenetically dysregulated in inflammatory diseases. Since methylation alterations in the related ADAMTS family have been previously reported, the study was expanded to ADAMTS genes as well. Furthermore, also cancerous tissues compared to normal tissues were investigated.

2 Material and Methods

2.1 Equipment and Consumables

Table 1. Consumables

Description	Manufacturer / Provider
96-well plates, flat bottom	Sarstedt AG & Co., GER
Cell culture dishes, 10 cm	Sarstedt AG & Co., GER
Cell culture plates, 12-, 24-, 96-well	Sarstedt AG & Co., GER
Cell scraper, 16 cm, 25 cm	Sarstedt AG & Co., GER
Falcon centrifuge tubes	Sarstedt AG & Co., GER
Glass flasks, 1000 ml, 300 ml	Schott AG, GER
MicroAMP Fast 96-well Reaction Plate (0.1 ml) for qPCR systems	Thermo Scientific, USA
Microtubes with thread	Sarstedt AG & Co., GER
Neubauer chamber	Brand GmbH & Co. KG, GER
Parafilm	American National Can Company, USA
Pasteur pipettes	Carl Roth GmbH & Co. KG, GER
Petri dishes	Sarstedt AG & Co., GER
Plastic box, airtight	EMSA GmbH, GER
PVDF membrane, 0.45 µm	Carl Roth GmbH & Co. KG
Serological pipettes, 5 ml, 10 ml, 25 ml	Sarstedt AG & Co., GER
Syringe filter, 0.45 µm pore size	Sarstedt AG & Co., GER
Whatman paper, 1.5 mm	Carl Roth GmbH & Co. KG

Table 2. Standard equipment

Description	Manufacturer
Analytical balance	Kern & Sohn GmbH, GER
Analytical balance	Denver Instruments, USA
Biophotometer	Eppendorf, GER
Centrifuge 5417R, fixed angle rotor F45-30-11	Eppendorf, GER
Centrifuge 5424, fixed angle rotor FA45-24-11	Eppendorf, GER
Centrifuge 5804R fixed angle rotor F34-6-38	Eppendorf, GER
Centrifuge 5810R, swing-out rotor A-4-62	Eppendorf, GER
Centrifuge Heraeus Multifuge X3R, fixed angle rotor F14-6x250LE	Thermo Scientific, USA
Chemiluminescence detector Fusion FX7	Peqlab, GER
Exhaust pump, BVC professional	Vacuubrand, GER
Flow cytometer BD Fortessa	BD, GER

Freezing container, Nalgene Mr. Frosty	Thermo Fisher Scientific Inc., USA
Heating block	Eppendorf, GER
Heating cabinet	Memmert, GER
Incubator Hera cell 150	Thermo Scientific, USA
iScan methylation array scanner	Illumina, NL
Light microscope, inverse	Hund, GER
Magnetic stirrer CB162	Stuart, USA
Microwave oven	Samsung, GER
NanoDrop 1000 spectrophotometer	Peqlab, GER
PH-meter pH211	HANNA Instruments GmbH, GER
Plate reader EL800	Biotek Instruments GmbH, GER
Plate reader FLx800	Biotek Instruments GmbH, GER
Power Supply EV231	Peqlab, GER
Power Supply PAC300	Bio-Rad Laboratories, Inc., GER
Real-Time PCR System StepOnePlus™	Thermo Fisher Scientific Inc., USA
Roller mixer, Stuart SRT6	Bibby Scientific Ltd., UK
Shaking incubator Minitron	Infors HT, GER
Single channel pipettes	Abimed GmbH, GER
Sonificator	Bandelin electronic GmbH, GER
Sterile work bench	Köttermann GmbH & Co. KG, GER
Tank electroblotter Web S	Peqlab, GER
Thermocycler peqSTAR 96 universal	Peqlab, GER
Tilting shaker Unitwist-RT	Uniequip, GER
Tube rotator MACSmix™	Miltenyi Biotech, GER
Vortexer Vortex Genie	IKA, GER
Water bath GFL1004	GFL, GER
Water purification system, TKA GenPure	TKA, GER

2.2 Chemicals

Table 3. Chemicals

Description	Manufacturer
1,10-Phenanthroline	Roth, GER
Accutase	Innovative Cell Technologies, USA
Acrylamide (Rotiphorese® Gel 30 (37,5:1))	Roth, GER
ADAM peptide substrate (soluble)	Enzo Life Sciences, USA
Agar Agar	Roth, GER
Ammoniumperoxidisulfate (APS)	Roth, GER

Ampicillin	Roth, GER
Bovine serum albumin (BSA)	Sigma, GER
Bradford *Coomassie Plus*	Fermentas, USA
Calciumchloride ($CaCl_2$)	Roth, GER
Dimethylsulfoxid (DMSO)	Roth, GER
Dulbecco´s Modified Eagle Medium (DMEM), High Glucose (4.5 g/l)	GE Healthcare, USA
ECL Select and ECL Prime	GE Healthcare, USA
Ethanol 96% (EtOH)	Roth, GER
Ethanolamine	Sigma, GER
Ethylenediaminetetraacetic acid (EDTA)	Roth, GER
Fc-Block (Purified Rat Anti-Mouse CD16/CD32)	BD, GER
Fetal calf serum (FCS)	GE Healthcare, USA
Glucose	Roth, GER
Glycerin	Roth, GER
Glycine	Roth, GER
Hydrochloric acid (HCl)	Roth, GER
Isopropanol	Roth, GER
Magnesiumchloride ($MgCl_2$)	Merck, GER
Magnesiumsulfate ($MgSO_4$)	Merck, GER
Mercaptoethanol	Roth, GER
Methanol (MeOH)	Roth, GER
Milk powder	Roth, GER
Penicillin/Streptomycin (100x)	GE Healthcare, USA
p-Nitrophenyl phosphate (pNPP) tablets	Sigma, GER
Potassiumchloride (KCl)	Merck, GER
Potassiumdihydrogenphosphate (KH_2PO_4)	Roth, GER
Protease-inhibitor mix *Complete*	Roche, GER
Proteinmarker PageRuler™ Plus	Thermo Scientific, USA
RNAse free water (Ampuwa)	Fresenius Kabi Deutschland GmbH, GER
Saccharose	Roth, GER
Sodiumchloride (NaCl)	Roth, GER
Sodiumdodecylsulfate (SDS)	Roth, GER
Tetramethylethylendiamin (TEMED)	Roth, GER
Transfectionreagent *Turbofect*	Thermo Scientific, USA
Tris	Roth, GER
Triton X-100	Roth, GER
Trypsin-EDTA	GE Healthcare, USA
Trypton/Pepton from Casein	Roth, GER

Tween®20	Roth, GER
Yeast extract	Roth, GER

2.3 Kits

All Kits were handled according to manufacturer´s instructions.

Table 4. Kits

Description	Manufacturer
DNeasy Kit	Qiagen, GER
EZ DNA Methylation™ Kit	Zymo Research, GER
Infinium Human Methylation 450k BeadChip Kit	Illumina, NL
PrimeScript RT Master Mix	Takara Bio Inc., USA
PureYield™ MidiPrep Kit	Promega, USA
QuikChange® II Site-directed Mutagenesis	Stratagene, USA
RNeasy Kit	Qiagen, GER
SYBR Select Master Mix	Thermo Scientific, USA

2.4 Software

Table 5. Software

Description	Company
Adobe Photoshop CS4	Adobe Systems, USA
Clone Manager 9	Scientific & Educational Software, USA
FlowJo 8.7.3	FlowJo, LLC, USA
FluoView FV10-ASW 4	Olympus corporation, JPN
GenomeStudio (Version2011.1, Methylation Analysis Module Version 1.9.0)	Illumina, NL
GETPrime	Gubelmann et al., 2011
GraphPad Prism 5.04	GraphPad Software Inc., USA
Mendeley	Mendeley Ltd., UK
Microsoft Office 2010	Microsoft Corp., USA
Primerblast	Ye et al., 2012
QuikChange® Primer Design Tool (http://stratagene.com/qcprimerdesign)	Stratagene, USA
R 3.2.2	R foundation
RStudio 0.98.501	RStudio, Inc, USA
StepOne Software 2.3 (qPCR)	Thermo Scientific, USA
Venny 2.0	Oliveros, 2007

2.5 Stimulants and inhibitors

Table 6. Stimulants and inhibitors

Name	Description	Manufacturer
Ionomycin (IO)	Ca^{2+}-ionophore	Calbiochem, GER
Marimastat (MM)	Broad range metalloprotease-inhibitor	Tocris Bioscience, UK
Phorbol 12-myristate 13-acetate (PMA)	PKC-activator	Sigma, GER

2.6 Antibodies

Table 7. Primary antibodies

Antigen/type	Reactivity	Provider	Species	Used dilution/concentration
ADAM17	h, m, r	Chemicon	rabbit	1:3000 (western blot)
GAPDH	h, m	Santa Cruz	rabbit	1:500 (western blot)
Hemagglutinin (HA)-Tag		Sigma-Aldrich	rabbit	1:1000 (western blot)
IgG_1 (Isotype control for K133 ADAM17)		Southern Biotechnology	rabbit	10 µg/mL (flow cytometry)
K133 anti-ADAM17	h, m	Department of Immunology, Group Koch-Nolte, UKE, Hamburg, Germany,	rabbit	10 µg/mL (flow cytometry)
β-Actin	h, m , r	Santa Cruz	rabbit	1:500 (western blot)

Table 8. Secondary antibodies

Type	Coupling	Provider	Used dilution /concentration
α-rabbit Alexa Fluor 488	Fluorescence dye	Life Technologies, GER	6.6 µg/mL (flow cytometry)
Goat-α-mouse IgG	Horseradish peroxidase (HRP)	Jackson ImmunoResearch, USA	1:10000 (western blot)
Goat-α-rabbit IgG	Horseradish peroxidase (HRP)	Jackson ImmunoResearch, USA	1:10000 (western blot)

2.7 Plasmids

Table 9. Plasmids

Name	Encoded protein	Vector	Provider
ADAM17 3Q	ADAM17 3Q mutant	pcDNA 3.1 (Invitrogen)	self generated
ADAM17 EA	Inactive ADAM17	pcDNA 3.1 (Invitrogen)	G. Murphy (University of Cambridge, UK)
ADAM17 EE	ADAM17 EE mutant	pcDNA 3.1 (Invitrogen)	self generated
ADAM17 WT	ADAM17 wildtype	pcDNA 3.1 (Invitrogen)	G. Murphy (University of Cambridge, UK)
TGF-α AP	TGF-α AP	pAPtag5 (GenHunter)	C. Blobel (Hospital for Special Surgery, USA)

2.8 Buffers

Table 10. Buffers

Name	Recipe
6x SDS sample buffer	0.75 M Tris 12% SDS 6.54 M Glycerin 6 mM EDTA 120 mM DTT 0.15% Bromphenole blue pH 6.8
Alkaline phosphatase (AP) buffer	100 mM NaCl 100 mM Tris 20 mM $MgCl_2$ pH 9.5
Cell lysis buffer for AP-assays	1 mM EDTA 10 mM 1,10-Phenanthroline* 2.5% (v/v) Triton-X-100 in H_2O
Cell lysis buffer for western blotting	5 mM Tris 1 mM EGTA 250 mM Saccharose 1% (v/v) Triton-X-100 10 mM 1,10-Phenanthroline* 1 x *Complete* protease inhibitor mix (Roche)*
Electrophoresis buffer	25.1 mM Tris 192 mM Glycin 0.1% SDS pH 8.8
FACS buffer	2 mM EDTA, 1% BSA in PBS
Phosphate-buffered saline (PBS)	137 mM NaCl 2.7 mM KCl 1.8 mM KH_2PO_4

	10.1 mM Na_2HPO_4
Resolving gel buffer	1.5 M Tris 0.4% SDS pH 8.8
Stacking gel buffer	0.5 M Tris 0.4% SDS pH 6.8
TBS	20 mM Tris 1.17 M NaCl 10 mM EDTA
TBST	20 mM Tris 1.17 M NaCl 10 mM EDTA 0.1% Tween-20
Transfer buffer	192 mM Glycin 25 mM Tris 10% MeOH pH 8.5

* Freshly added prior to use

2.9 Functional analysis of ADAM17

2.9.1 Cell lines

Table 11. Cell lines

Name	Cell type	Growth medium
COS-7	SV40 transformed cell line from kidney of *cercopithecus aethiops*, fibroblast cells	DMEM + 10% FCS + Pen/Strep (100 U/ml)
ADAM10/17-double deficient knockout murine embryonic fibroblasts (MEFs)	Murine fibroblasts generated from knock-out mice (Biochemistry Kiel)	DMEM + 10% FCS + Pen/Strep (100 U/ml)

2.9.2 Cultivation of eukaryotic cells

Cells were cultered at 37°C in a humidified, 5% CO_2 atmosphere. Standard culture medium was *Dulbecco´s Modified Eagle Medium (DMEM)* supplemented with 10% fetal calf serum (FCS) and Penicillin/Streptomycin (100 U/ml). Pure DMEM was used as indicated. Culture medium was preheated to 37°C prior to use. The adherent COS-7 cells and ADAM10/17-double deficient knockout murine embryonic fibroblasts (MEFs) were grown in cell culture dishes until 90% confluency was reached and then either seeded into a new culture dish for further propagation or

seeded into cell culture plates for experiments. Before seeding, the cells were washed once with phosphate-buffered saline (PBS) and incubated afterwards with trypsin-EDTA until detachment. The proteolytic activity of trypsin was then immediately inhibited by addition of serum-containing medium and the cells were split into new culture dishes or culture plates in the appropriate density.

2.9.3 Plasmid

The ADAM17 WT plasmid, which was used as a template for the mutagenesis reactions, consists of the *pcDNA3.1 expression vector* (*Invitrogen*) and a 2484 bp fragment which encodes for the murine ADAM17. The coding sequence contains the full-length ADAM17 with the prodomain as well as an additional *hemagglutinin (HA)*-tag. This tag was added to the cytoplasmic tail of ADAM17 and was used to detect ADAM17 expression by immunodetection with antibodies against HA. The ADAM17 WT plasmid was kindly provided by Prof. Gillian Murphy (University of Cambridge, Cambridge, UK) and was also used for the transfection of ADAM17 WT into eukaryotic cells.

2.9.4 Mutagenesis of ADAM17

For mutagenesis the *QuikChange® II Site-directed Mutagenesis* kit was used according to the manufacturer's instructions. Briefly, a polymerase chain reaction was performed with the *PfuUltra HF DNA-polymerase*, the ADAM17 WT plasmid as template and the mutagenesis primer pair (2.9.5). The primer pair carried mismatching bases, in regard to the target sequence, that introduce the intended mutation. The generated plasmids are in contrast to the template plasmid not methylated and are therefore protected against the subsequent performed digestion with the methylsensitive *DpnI* endonuclease. The template DNA is digested and only newly synthetized DNA remains. Such DNA was then circulized and amplified in *E. coli* XL1 blue (2.9.7), isolated (2.9.9) and sequenced (2.9.10). The ADAM17 EE (F652E F655E substitutions) plasmids were generated in one mutation reaction with ADAM17 WT plasmid as template. The ADAM17 3Q (D647Q E650Q D654Q substitutions) mutant was generated in two consecutive mutagenesis reactions, with first the D647Q E650Q substitutions followed by the D654Q substitution. See Table 13 for a list of the generated ADAM17 mutants and their mutated sequence.

2.9.5 Mutagenesis primers

The mutagenesis primer oligonucleotides that were used to introduce mutations in the ADAM17 WT plasmid were designed with the online tool *QuikChange Primer Design* (http://stratagene.com/qcprimerdesign). The primers were then ordered from *Sigma-Aldrich*. The sequences of the mutagenesis primer pair are depicted in Table 12.

Table 12. Mutagenesis primers

Name	Sequence (5'→3')
ADAM17 EE forward	gaaacgagtacaggacgtaattgagcgagagtgggatgagattgaccagctgagcatcaacacttttg
ADAM17 EE reverse	caaaagtgttgatgctcagctggtcaatctcatcccactctcgctcaattacgtcctgtactcgtttc
ADAM17 3Q forward (first mutagenesis)	caaatgtgagaaacgagtacagcaggtaattcagcgattttgggatttcattga
ADAM17 3Q reverse (first mutagenesis)	tcaatgaaatcccaaaatcgctgaattacctgctgtactcgtttctcacatttg
ADAM17 3Q forward (second mutagenesis)	ggtaattcagcgattttggcagttcattgaccagctgagca
ADAM17 3Q reverse (second mutagenesis)	tgctcagctggtcaatgaactgccaaaatcgctgaattacc

Table 13. List of ADAM17 variants

Name	CANDIS sequence	Substitutions
ADAM17 wildtype (A17 WT)	RVQDVIERFWDFIDQLS	none
ADAM17 EE (A17 EE)	RVQDVIEREWDEIDQLS	F652E F655E
ADAM17 3Q (A17 3Q)	RVQQVIQRFWQFIDQLS	D647Q E650Q D654Q

2.9.6 Preparation of chemical competent cells

To generate chemical competent *E. coli* bacteria, XL1 blue cells were treated with $CaCl_2$ as follows. Bacteria from an overnight culture were diluted 1:100 with LB medium and grown at 37°C and 200 rpm. When the optical density (OD_{600}) reached a value between 0.4 and 0.6, the cells were cooled down for 20 min on ice. Thereafter, the cells were separated in 50 ml aliquots and pelleted for 5 min at 5000 rcf. Each pellet was resuspended in 20 ml pre-chilled tris-buffer and centrifuged again for 10 min at 4°C at 5000 rcf. The pellets were then resuspended in 20 ml $CaCl_2$ solution and incubated for 20 min on ice. Subsequently, the cells were pelleted again and resuspended in 2 ml $CaCl_2$ solution. After another 1 h incubation 500 µl glycerol was added and the cell suspension immediately snap-frozen in liquid nitrogen and stored in aliquots of 50 µl at -80°C until further use.

Table 14. Buffer and solutions for the preparation of chemical competent cells

Name	Recipe
$CaCl_2$-solution	0.1 mM $CaCl_2$ 5 mM Tris 5 mM $MgCl_2$
LB medium	171 mM NaCl 10% (w/v) Trypton/Pepton 5% (w/v) Yeast extract
Tris buffer	0.1 mM NaCl 5 mM Tris 5 mM $MgCl_2$

2.9.7 Transformation of chemical competent bacteria

To transform bacteria with plasmids, 50 µl of chemical competent *E. coli* XL1 blue were thawed on ice and mixed with 1 µl of the respective plasmid. The mixture was incubated for 45 min on ice. The cells were heat shocked by warming them rapidly to 42°C for exactly 40 s. The cells were then immediately cooled down on ice for 5 min and mixed with 300 µl SOC medium. An incubation for 1 h at 37°C and shaking at 200 rpm followed. The bacteria suspension was plated onto LB-plates containing ampicillin as selection marker. The plates were incubated at 37°C overnight. Single colonies were picked with a sterile pipette tip and incubated in 5 ml LB-medium containing ampicillin for 6 h. Subsequently, the medium was used for preparation of glycerol stocks.

Table 15. Medium and solutions for the transformation of bacteria

Name	Recipe
LB-plates	171 mM NaCl 1% (w/v) Trypton/Pepton 0.5% (w/v) Yeast extract 1.5% (w/v) Agar Agar 0.1 mg/ml Ampicillin
SOC medium	0.5% (w/v) Yeast extract 2.0% (w/v) Trypton 10 mM NaCl 2.5 mM KCl 10 mM $MgCl_2$ 10 mM $MgSO_4$ 20 mM Glucose

2.9.8 Preparation of bacterial glycerol stocks

Glycerol stocks of all transformed bacteria were prepared for long storage and easy plasmid preparation. 850 µl of bacteria culture were mixed with 150 µl sterile glycerol, vortexed and snap-frozen in liquid nitrogen. They were afterwards stored at -80°C.

2.9.9 Isolation of plasmid DNA from *E.coli*

To amplify and isolate plasmids from transformed bacteria, 200 ml LB medium containing ampicillin, as selection marker, was inoculated with bacteria from glycerol stocks. This bacteria culture was incubated overnight at 37°C and 200 rpm. The plasmids were isolated with the *PureYield™ MidiPrep* kit (*Promega*) according to the manufacturer´s instructions and analyzed with *Nanodrop* for purity and quantity.

2.9.10 DNA sequencing

The successful mutation of ADAM17 was verified by commercial DNA sequencing (*Seqlab*). Therefor, 650 ng plasmid-DNA was mixed with 20 pmol of the sequencing primer Se-qpcDNA3.1BGHrev (5´-CTAGAAGGCACAGTCGAG-3´) in a volume of 7 µl and sent to *Seqlab*. The obtained results were then aligned with the wildtype sequence in *CloneManager* and verified for successful mutation.

2.9.11 Transient transfection of eukaryotic cells

Different variants of ADAM17 proteins were overexpressed in COS-7 cells and MEFs. This was achieved by transient transfection of plasmids encoding for these proteins. The plasmids were delivered through lipofection into the cells. In single transfections 0.5 µg plasmid and 1 µl *Turbofect* were added to 100 µl serum-free medium in a reaction tube. The tube was inverted a few times and incubated at room temperature for 20 min to form the DNA-lipid complexes. For double-transfections 0.5 µg of each plasmid was added to the serum-free media and 1.5 µl of *Turbofect*. The medium in the 12-well plate was replaced with 500 µl fresh serum-free medium. The transfection mix was then added dropwise to the wells. The cells were transfected at 60-80% confluency for 6 h. After the incubation, medium was exchanged with 1 ml of complete growth medium. 24 h after transfection, the cells were used for further experiments such as AP-assays.

2.9.12 Stimulation, cell lysis and collection of supernatants

Cell culture experiments for analyzing the ADAM17-mediated shedding using alkaline phosphatase (2.9.17) were conducted as follows. 24 h after transfection (see 2.9.11), cells were incubated for 1 h with fresh medium without serum. Thereafter, medium was renewed with serum-free medium and cells were treated or not treated with phorbol 12-myristate 13-acetate (PMA, 200 ng/mL) for 2 h or ionomycin (Iono, 1 µM) for 30 min. Marimastat was added 15 min before the stimulation started as indicated. For all stimulants, corresponding carrier controls with the solvent of the stimulant were carried along to exclude effects of the solvent on the cells. The medium was removed after the indicated stimulation time and centrifuged at 12.000 rcf at 4°C for 5 min to remove cell debris. Thereafter, supernatant was immediately used for AP-assays. To lyse the cells, different lysis buffers were used for western blotting and AP-assays (see Table 10). Cell lysis was performed on ice or at 4°C. For western blotting, cells were lysed by adding 150 µl ice-cooled lysis buffer and freezing and thawing them three times. The lysis solution was transferred to *Eppendorf reaction tubes* and incubated on ice. Every 10 min the solution was vortexed. After 30 min of incubation the lysis solution was cleared from cell debris by centrifugation at 12.000 rcf at 4°C for 5 min. The supernatants containing the proteins were immediately used for further analysis or stored at -20°C until use. For AP-assays the cells were lysed by adding 300 µl ice-cooled lysis buffer to each well and the plates were slowly rocked at 4°C for 30 min. The lysis solution was transferred to *Eppendorf tubes* and incubated for further 30 min on ice and vortexed every 10 min. Finally, the solution was cleared by centrifugation at 12.000 rcf at 4° C for 5 min. The solution was then directly used for the AP-assay.

2.9.13 Protein concentration determination using *Bradford* assay

Bradford protein concentration assay was used to determine the protein concentration in lysed cell solutions (Bradford, 1976). Therefor, 1 µl of the cell lysate was added to 200 µl of a *ready-to-use Coomassie Plus solution*. As blank control, 1 µl of lysis buffer without cells was used. The extinction was measured at 595 nm in a plate reader. Protein concentrations were calculated by interpolating with a bovine serum albumin (BSA) standard curve.

2.9.14 Protein separation by sodium dodecyl sulfate polyacrylamide gel electrophoresis

Sodium dodecyl sulfate polyacrylamide gel electrophoresis (SDS-PAGE) was used to separate proteins according to their size. Therefor, 50 µg of proteins per sample were first denaturated and linearized by boiling them in 1x SDS sample buffer for 5 min at 95°C. Thereafter, the denatured proteins were loaded onto a gel together with an extra lane containing the size marker *PageRuler Plus*. The proteins were focused in the stacking gel (4.5% polyacrylamide) for 30 min at 75 V and then separated in the resolving gel (7.5% polyacrylamide) at 90 V until good separation was achieved (see Table 16).

Table 16. Polyacrylamide gel recipe

Name	Recipe
Stacking gel (4.5%)	2.90 ml H_2O 1.25 ml stacking gel buffer 0.835 ml acrylamide 30 µl APS 15 µl TEMED
Resolving gel (7.5%)	5.03 ml H2O 2.50 ml resolving gel buffer 2.33 ml acrylamide 60 µl APS 30 µl TEMED

2.9.15 Western blotting

After separation by SDS-PAGE, the proteins were transferred electrophoretically from the gel to a polyvenylidene fluoride (PVDF) membrane by tank blotting. The negatively charged proteins in the acrylamide gel were transferred to the MeOH-activated PVDF membrane in the *Peqlab tankblotter* at 80 mA for 12-16 h.

2.9.16 Immunodetection of transferred proteins

After protein transfer, the free protein binding sites on the membrane were saturated by incubating the membrane at room temperature for 1 h in tris-buffered saline with tween (TBST) and with 5% milk powder. Thereafter, the membrane was incubated with the primary antibody in TBST with 5% milk powder in the indicated dilution (see Table 7) at room temperature for 1 h in a tube rotator. Excess primary antibody was subsequently removed by washing the membrane

three times for 10 min with TBST. The secondary antibody was then incubated for 1 h in TBST in the indicated dilution (see Table 8). Unbound antibody was washed away three times for 10 min with TBST. The antibody-labeled proteins were detected with peroxidase substrate *ECL Select* or *ECL Prime* and the emitted light was detected with the *Fusion FX7* detection system.

2.9.17 Shedding experiments with alkaline phosphatase-coupled substrates (AP-assays)

The shedding activity of ADAM17 variants was determined with an alkaline phosphatase (AP)-tagged TGF-α substrate (TGF-α AP). The TGF-α AP carries an alkaline phosphatase at its extracellular domain which is released in the supernatant after ADAM17-mediated cleavage. This substrate was transfected into eukaryotic cells as described in 2.9.11 and supernatants and lysates were collected as described in 2.9.12. The activity of the AP was determined by the hydrolysis of the colorless AP substrate p-nitrophenylphosphat (p-NPP) to the yellow p-nitrophenol (p-NP). Therefor, 100 µl of the supernatant was mixed with 100 µl of AP-substrate solution (p-NPP, 2mg/ml in AP buffer) in triplicates in a 96-well plate. 10 µl of the lysates were diluted 1:10 in AP buffer in triplicates and 100 µl of AP-substrate solution was added. The plates were incubated at 37°C and the extinction was measured repeatedly at 405 nm in a plate reader until the highest value was close to 1. The ratio between the AP-activity in the supernatant to the AP-activity in the cell lysates is directly related to the relative quantity of shed ADAM17-substrates. To calculate the relative TGF-α AP activity of ADAM17, the ratio of the AP activity in the supernatant compared to the total TGF-α AP activity of supernatant and cell lysates was determined, base-line corrected with the ADAM17 E/A control and then normalized to the stimulated ADAM17 WT.

2.9.18 Cleavage experiments with a soluble fluorogenic ADAM substrate

To measure proteolytic activity of ADAM17 proteins, COS-7 cells were transfected in 24 well plates with 0.25 µg of the respective ADAM17 plasmid and 0.5 µl Turbofect (analog to 2.9.11). 24 h after transfection, medium was replaced with serum-free medium supplemented with 5 µM fluorogenic ADAM substrate (*Enzo Life Sciences*) and the cells were incubated for 6 h at 37°C and 5% CO_2 in a humidified atmosphere. Fluorescence in the supernatant was determined at 485 nm excitation and 530 nm emission reflecting proteolysis of the fluorogenic ADAM substrate.

2.9.19 Flow cytometric analysis of ADAM17 surface expression

For analyzing the surface expression of the ADAM17 proteins, MEFs were transfected with the respective plasmid and 24 h later harvested with Accutase. To block unspecific binding sites, the cells were first incubated with 3% BSA in PBS and afterwards in FACS buffer with *Fc-Block* (1 µg per $1*10^6$ cells). Thereafter, cells were either not stained, or stained with *K133* anti-ADAM17 antibody or rabbit IgG_1 antibodies as isotype control for 1 h at 4°C. The cells were washed and incubated for 1 h with 6.6 µg/mL anti-rabbit *Alexa Fluor 488* detection antibody, washed again and analyzed by flow cytometry in FACS buffer with the *BD Fortessa* flow cytometer. The flow cytometry data were analyzed by using the *FlowJo* software.

2.9.20 Statistical analysis

Statistics were generated using *one-way analysis of variance (one-way ANOVA)* and *Bonferroni multiple comparison post-hoc test* for the shedding assays. The methylation data were tested with *Mann-Whitney-U test* corrected for multiple testing with the *Benjamini-Hochberg method*. The RNA data were tested with *paired t-test*. All tests were carried out with either *R* or *Graphpad Prism***.** *P* values < 0.05 were considered statistically significant. The different significance niveaus were defined as * $P < 0.05$, ** $P < 0.01$, *** $P < 0.001$ and **** $P < 0.0001$.

2.10 Epigenetic investigations

2.10.1 Colorectal cancer patient samples

The patient samples used for the investigation of methylation alterations in colorectal cancer originated from the national genome research project *integrated genomic investigation of colorectal carcinoma*. Prof. Dr. med. Jochen Hampe (Klinik für Innere Medizin I, Christian-Albrechts-Universität, Kiel, Germany) and Prof. Dr. med. Clemens Schafmayer (Klinik für Allgemeine Chirurgie, Viszeral-, Thorax-, Transplantations- und Kinderchirurgie, Christian-Albrechts-Universität, Kiel, Germany) kindly provided the DNA samples. Julia Kolarova (Institute of Human Genetics, Christian-Albrechts University, Kiel, Germany) conducted the methylation assay. All patient samples originated from patients suffering from colorectal carcinoma (CRC). During surgery tumor tissue and adjacent peri-tumoral non-malignant tissue were resected. The peri-tumoral non-malignant tissue was used as a control and was treated the same as the tumor tissue. All tissue samples originated from various colon locations. In total, samples from 119 patients

were derived (n=117 (ctrl), n=119 (cancer)). After resection, the tumor tissue and control tissue were investigated by a trained pathologist. Genomic DNA extraction was done using *DNeasy* kit (Qiagen, GER). All patients declared written consent.

2.10.2 Lung cancer patient samples

Matched tissue samples (tumor-free lung and tumor) were obtained from patients undergoing pneumectomy or lobectomy at the *LungenClinic Grosshansdorf* (n=40) in the course of surgical treatment of previously diagnosed lung cancer. Tissues for cryo-fixation were immediately frozen in liquid nitrogen and kept at -80°C until further use. DNA methylation analysis was performed using the *Infinium Human Methylation 450k BeadChip Kit*. The generated methylation data was kindly provided by Prof. Dr. rer. nat. Ole Ammerpohl and Prof. Dr. med. Reiner Siebert for further analysis (Institute of Human Genetics, Christian-Albrechts University, Kiel, Germany).

2.10.3 Oral squamous-cell carcinoma and *oral lichen planus* samples

Methylation data of ADAM/TS genes from patients suffering from *oral lichen planus* and/or oral squamous-cell carcinoma were kindly provided by Prof. Dr. rer. nat. Ole Ammerpohl and Prof. Dr. med. Reiner Siebert (Institute of Human Genetics, Christian-Albrechts University, Kiel, Germany) for further analysis. The sample collection was under supervision of Dr. Dr. Volker Gassling (Klinik für Mund-, Kiefer- und Gesichtschirurgie, Universitätsklinikum Schleswig-Holstein, Kiel, Germany). As control samples non-inflamed tissue from the same patient was collected. DNA methylation analysis was performed using the *Infinium Human Methylation 450k BeadChip Kit*.

2.10.4 *Non-alcoholic Steatohepatitis (NASH)* and *Non-alcoholic fatty liver disease (NAFLD)* patient samples

Liver samples were collected from patients undergoing liverbiopsy for suspected NAFLD. Control samples were obtained from patients undergoing major oncological surgery for exclusion of liver malignancy. None of the normal control individuals underwent preoperative chemotherapy and liverhistology demonstrated absence of both cirrhosis and malignancy (n_{ctrl}=19, n_{NAFLD}=18, n_{NASH}=16). All patients provided written, informed consent. The study cohort was published in Ahrens et al., 2013. DNA methylation analysis was performed using the *Infinium Human Methylation 450k BeadChip Kit*.

2.10.5 Bisulfite conversion and methylation analysis

The DNA samples were bisulfite converted with the *EZ DNA Methylation™* and afterwards measured for DNA methylation with the *Infinium Human Methylation 450k BeadChip Kit*. This was conducted by Julia Kolarova (Institute of Human Genetics, Christian-Albrechts University, Kiel, Germany) according to the manufacturer's protocol in case of the colorectal cancer samples. The measurement was done with the *iScan* methylation array scanner. The generated *IDAT* files were further processed with the *Genomestudio Software* to derive the β-values. Methylation levels in *Illumina Methylation* assays are quantified using the ratio of intensities between methylated and unmethylated alleles. The β-values are continuous and range from 0 (unmethylated) to 1 (completely methylated) (Kuan et al., 2010).

2.10.6 Acquisition and analysis of data from *The Cancer Genome Atlas* project

The Cancer Genome Atlas (TCGA) project is an extensive, worldwide and multi-laboratory project to study and characterize genetics and epigenetics of various cancers. Methylation data of *Colon adenocarcinoma & Rectum adenocarcinoma* (*COADREAD*, n=44 (ctrl), n=384 (canc)) from the *TCGA data portal* were downloaded (https://tcga-data.nci.nih.gov) and further analyzed. Additionally, mRNA data for the same cohort was downloaded and further analyzed (n=22 (ctrl), n=224 (canc)). The gene expression profile was measured experimentally using *Agilent 244K custom gene expression G4502A_07_3 microarrays* by the *University of North Carolina TCGA genomic characterization center*. The data were gene-level normalized by independently subtracting the mean of the genomic location.

2.10.7 Real-time RT-qPCR analysis

RNA samples were kindly provided by Dr. rer. nat. Christian Röder and Prof. Dr. rer. nat. Holger Kalthoff (Institute for Experimental Cancer Research, University Hospital Kiel, Germany) and were derived from the same colorectal cancer patients as the DNA for methylation analysis. 0.5 µg RNA from tumor tissue and control tissue were reverse transcribed with *PrimeScript RT Master Mix* according to the manufacturer's manual. Thereafter, the cDNA was diluted with RNAse-free water 1:5 yielding cDNA with a theoretical concentration of 10 ng/µl. A control without RNA was treated the same and used as RNA-negative control in the qPCR. For the real-time RT-qPCR reaction, 5 µl *5X SYBR Green/Rox Select Master Mix*, 1 µl cDNA in H_2O (10 ng), 1 µl primer pair (0.25 µM end

concentration of each) and 3 µl RNAse-free water were mixed in a *MicroAMP Fast 96-well Reaction Plate*. Additionally, a non template control was carried along to exclude primer dimers or unspecific amplifications. The qPCR was carried out in a *StepOnePlus Real-Time PCR System*. The qPCR protocol was performed as follows: Activation 2 min at 95°C, 40 cycles (denaturation 2 s at 95°C, annealing 30 s at the primer-specific temperature, amplification 30 s at 72°C). After the amplification, melting curves were recorded to ensure that only one amplicon species was generated. On a random basis, the amplicons were as an additional control analyzed by agarose gel electrophoreses and compared with the expected size of the amplicon. During establishment of the assay, three different house-keeping genes were tested: *hypoxanthine-guanine phosphoribosyltransferase (HPRT), glyceraldehyde 3-phosphate dehydrogenase (GAPDH), and ß-2-microglobulin (B2M)*. All house-keeping genes showed similar expression profiles. Following the guidelines in de Kok et al., 2005, *HPRT* was chosen as reference gene for all further qPCR analyses. All samples were measured in duplicates. In case that ct values differed between duplicates more than or equal to 0.5, the measurement was repeated minimum once and the average was used. The data was analyzed using the *ΔΔct-method* ($2^{-\Delta\Delta ct}$) or *Δct-method* ($2^{-\Delta ct}$) according to Yuan et al., 2006, with *HPRT* as reference gene. The intron-spanning primer for human *ADAMTS16* were generated with *GETPrime* (Gubelmann et al., 2011) and validated with *Primerblast* (Ye et al., 2012). Primer sequences are shown in Table 17. Moreover, in all samples the mRNA expression of the cancer marker *SURVIVIN/BIRC5* was measured. In 86.49% of the samples a higher expression of *BIRC5* was detected in the cancer sample. The intron-spanning primer from *SURVIVIN* were taken from Shen et al., 2008.

Table 17. qPCR primers

Name	Sequence (5'→3')	Amplicon size (bp)	Annealing temperature
ADAMTS16 forward	TGTGTAACGGGAATAACTCAG	81	60°C
ADAMTS16 reverse	TGTGATAATACTGGTTGGTGTG		
HPRT forward	TTGCTGACCTGCTGGATTAC	113	60°C
HPRT reverse	CCCTGTTGACTGGTCATTAC		
SURVIVIN forward	AGAACTGGCCCTTCTTGGAGG	170	60°C
SURVIVIN reverse	CTTTTTATGTTCCTCTATGGGGTC		

2.10.8 Data analysis and statistics

The generated β-values of the patient samples (methylation data) were further statistically analyzed with the script language *R*, *Graphpad Prism* and *Excel*. CpGs were defined as *differentially methylated* if the difference of the mean β-values ($\Delta\beta_{mean}$) was larger than 0.2 ($|\Delta\beta_{mean}| \geq 0.2$) compared to the control and significant after *Mann-Whitney-U* testing with multiple testing correction ($P < 0.05$). CpGs which did not meet these criteria, but showed an methylation difference $0.1 \leq |\Delta\beta_{mean}| < 0.2$ ($P < 0.05$) were defined as *intermediate methylated*. For further details about the statistics see 2.9.20.

3 Results

3.1 Mutations in the hydrophobic part, but not in the hydrophilic part of the alpha-helical CANDIS region abolish transmembrane sheddase activity of ADAM17

3.1.1 A two amino acid substitution in the hydrophobic part of the alpha-helical CANDIS region of ADAM17 abolishes TGF-α shedding *in vitro*

Recently, an evolutionary conserved sequence in the ADAM17 protease, located between the transmembrane domain and the membrane-proximal domain, was characterized and named *Conserved ADAM seventeeN Dynamic Interaction Sequence (CANDIS)*. It was shown that this juxtamembrane segment can bind some ADAM17 substrates such as IL-6R, but not others such as TNF-α (Düsterhöft et al., 2014). The corresponding peptide shows an alpha helical-conformation (Düsterhöft et al., 2014) with an amphipathic character (Figure 4). The hydrophobic face of CANDIS is able to interact with lipid bilayers (Düsterhöft et al., 2015) implying that an interaction between the CANDIS region and the cell membrane could have physiological relevance for the shedding activity of ADAM17. Moreover, mutated CANDIS peptides with mutations in the hydrophobic face have shown impaired lipid binding e.g., CANDIS with F652E F655E substitutions (Düsterhöft et al., 2015). These findings led to the question whether disruption of the lipid binding ability in the full-length ADAM17 would affect ADAM17-mediated substrate release. Therefore, I generated an ADAM17 mutant carrying the same mutations as the isolated CANDIS peptide. Two highly hydrophobic phenylalanines in the CANDIS region were exchanged with two negatively charged glutamic acid residues. These mutations destroyed the hydrophobic face (FLVLFVII) of CANDIS (Figure 5) and the lipid binding ability of the CANDIS peptide, as evidenced by fluorescence and circular dichroism spectroscopy analyses (Düsterhöft et al., 2015). The effect of these mutations on ADAM17 shedding activity was investigated. Two phenylalanines were substituted with two glutamic acid residues (E) and the mutant was named ADAM17 EE.

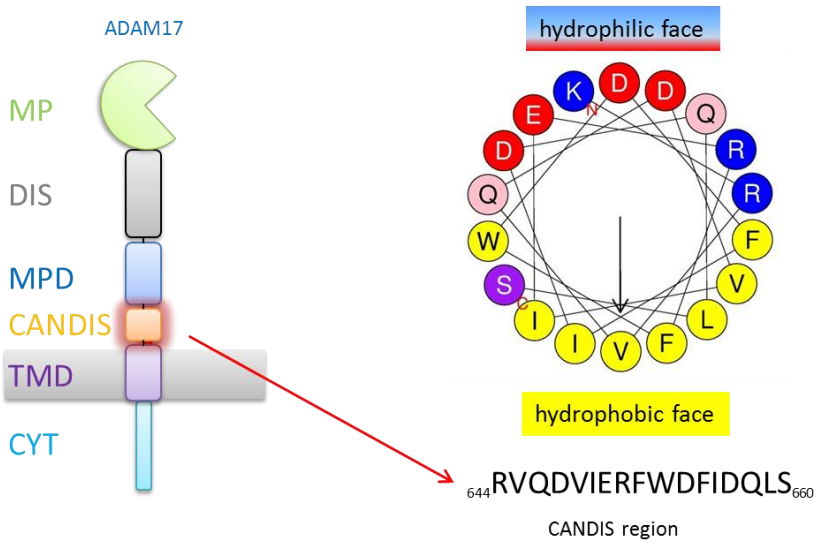

Figure 4. The Conserved ADAM seventeeN Dynamic Interaction Sequence (CANDIS) in ADAM17 forms an amphipathic alpha helix. ***(left)*** ADAM17 consists of several functional domains: metalloprotease domain (MP), disintegrin domain (DIS), membrane-proximal domain (MPD), transmembrane domain (TMD) and the cytosolic tail (CYT). Additionally, an evolutionary conserved short region in ADAM17 between the MPD and TMD was defined: CANDIS. ***(right)*** CANDIS forms an amphipathic alpha helix, with the hydrophobic face consisting of the amino acids FVLFVII. The alpha-helical wheel prediction and depiction was done with HeliQuest (Gautier et al., 2008). Lysine (K) in the helix projection is not part of the defined CANDIS region but was included in the helix prediction since it contributes to the hydrophilic face of CANDIS.

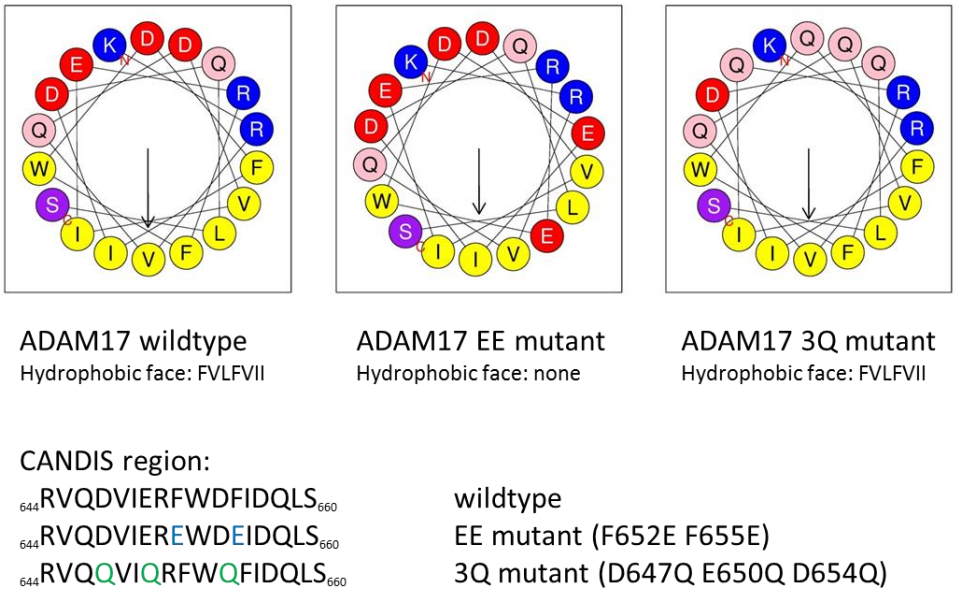

Figure 5. Two ADAM17 mutants with altered amino acid sequence in the CANDIS region were generated. Two phenylalanines were substituted with glutamic acids (F652E F655E) in the ADAM17 EE mutant. As depicted in the helix wheel projection, the hydrophobic face (FVLFVII) of the wildtype (left scheme) is destroyed in the EE mutant (middle scheme). Additionally, ADAM17 was altered in the hydrophilic face of the CANDIS region through substitution of three negatively charged amino acids with non-charged glutamines, thus retaining the hydrophobic face (right scheme). The helix wheel projection and calculation was done with HeliQuest (Gautier et al., 2008). Lysine (K) in the helix projection is not part of the defined CANDIS region but was included in the helix prediction since it contributes to the hydrophilic face of CANDIS.

The generated mutant ADAM17 EE (A17 EE), the ADAM17 wildtype (A17 WT) and the inactive ADAM17 E/A (A17 E/A) variant were retransfected in ADAM10/ADAM17-double-deficient murine embryonic fibroblasts (MEFs), together with an alkaline phosphatase (AP)-tagged TGF-α as substrate. The AP-tag permits the measurement of the ADAM17-mediated TGF-α substrate shedding (TGF-α shedding activity). The retransfected cells were stimulated for 2 h with PMA (Figure 6A) or 30 min with ionomycin (Figure 6B), and TGF-α shedding activity was measured subsequently. The shedding activity of the inactive A17 E/A mutant was subtracted from the measured activities as baseline correction. The A17 WT showed constitutive TGF-α shedding activity that was significantly increased by the ADAM17 stimuli PMA and ionomycin. In contrast, the A17 EE mutant shedding activity was completely abolished and did not increase after PMA or ionomycin treatment.

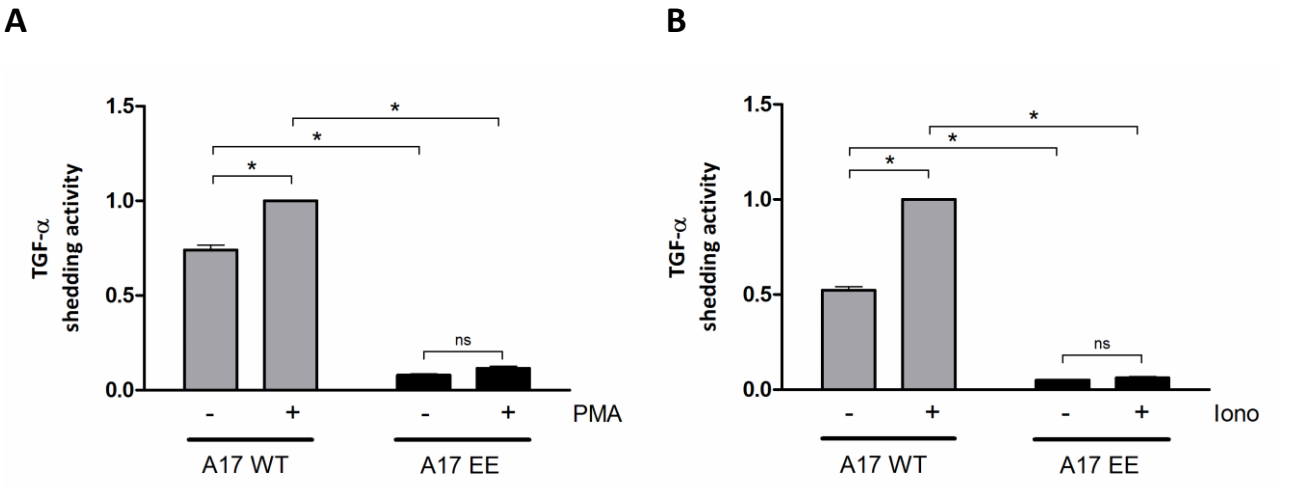

Figure 6. Two substitutions in the hydrophobic face of CANDIS completely abolish the ability of ADAM17 to shed the transmembrane substrate TGF-α. ADAM10/17-double-deficient mouse embryonic fibroblasts (MEFs) were retransfected with inactive ADAM17 E/A variant as control, murine ADAM17 wildtype (A17 WT) or the ADAM17 EE (A17 EE) mutant and plasmids containing alkaline phosphatase coupled TGF-α (TGF-α AP). 24 h after transfection, MEFs were treated or not treated with phorbol 12-myristate 13-acetate (PMA, 200 ng/ml) for 2 h ***(A)*** or ionomycin (Iono, 1 µM) for 30 min ***(B)***. Afterwards the ADAM17-mediated TGF-α shedding activity was determined. Retransfection of A17 WT rescued constitutive and stimulated TGF-α release. In contrast, retransfection of A17 EE did not rescue constitutive and stimulated TGF-α shedding. Data represent the means +SEM (standard error of mean) of three independent experiments (n=3) and were tested by one-way analysis of variance (one-way ANOVA) with Bonferroni multiple comparison post hoc test (* $P < 0.05$).

3.1.1.1 The ADAM17 EE mutant is transported to the cell surface and similarly expressed as the wildtype ADAM17

The protein expression of the ADAM17 variants was analyzed by western blotting in parallel to the TGF-α release assays. These analyses were conducted to exclude that differences in ADAM17 protein expression caused the observed differences in ADAM17-mediated TGF-α shedding. The western blot analyses showed that ADAM17 protein expression of all ADAM17 variants was similar (Figure 7A). Mutations in ADAM17 could potentially also lead to an altered transport of the protease to the cell surface, thus influencing the shedding activity. Despite that possibility, transfected A17 WT and A17 EE are similarly expressed on the cell surface of MEFs as revealed by flow cytometric analysis (Figure 7B).

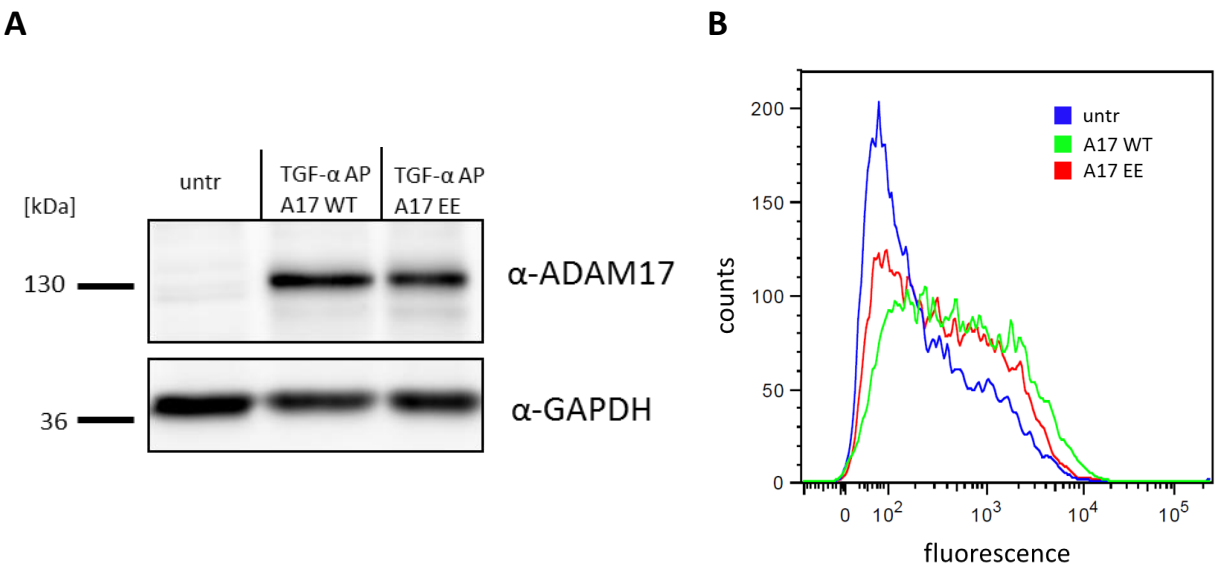

Figure 7. The ADAM17 EE mutant shows similar protein expression as the wildtype ADAM17 and is expressed on the cell surface. ***(A)*** Representative western blot analysis of ADAM10/17-deficient mouse embryonic fibroblasts (MEFs) lysates 24 h after transfection with ADAM17 wildtype (A17 WT) or ADAM17 EE (A17 EE) and TGF-α AP plasmids. The blot was stained with anti-ADAM17 antibody (α-ADAM17) and, as loading control, with anti-GAPDH antibody (α-GAPDH). The A17 EE mutant showed similar ADAM17 expression levels as the wildtype. ***(B)*** Flow cytometric analysis of MEFs transfected with A17 WT and A17 EE mutant showed similar expression levels on the cell surface. untr=untransfected.

3.1.1.2 The ADAM17 EE mutant is still able to cleave soluble ADAM17 substrate

To investigate whether the EE mutations interfere with the proteolytic activity of the catalytic center of ADAM17, a fluorogenic peptide cleavage assay was performed. Overexpression of the EE mutant and the A17 WT in COS-7 cells lead to a comparable increase in fluorescence (Figure 8).

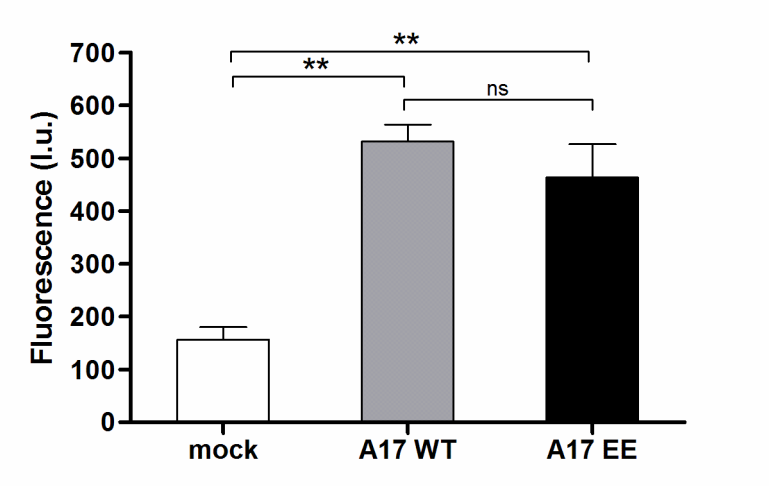

Figure 8. The ADAM17 EE mutant is able to cleave a soluble fluorogenic ADAM peptide substrate despite its abrogated TGF-α shedding activity. COS-7 cells were transfected with murine ADAM17 wildtype (A17 WT) or ADAM17 EE (A17 EE) mutant or proteolytically inactive ADAM17 E/A variant (mock) as control. 24 h after transfection, the cells were cultured in fresh medium with fluorogenic ADAM substrate peptide (5 µM). After 6 hours fluorescence was measured in the supernatants. Overexpression of the EE mutant in COS-7 cells lead to comparable increase in fluorescence as the wildtype did. Shown are the light units (l.u.) measured. Data represent the means +SEM (standard error of mean) of three independent experiments (n=3) and were tested by one-way analysis of variance (one-way ANOVA) with Bonferroni multiple comparison post hoc test (** $P < 0.01$). ns=non-significant.

3.1.2 Amino acid substitutions in the hydrophilic part of the alpha-helical CANDIS region of ADAM17 do not interfere with TGF-α shedding

The EE mutation in the hydrophobic site completely abolished the ADAM17 shedding activity. To answer the question, if also alterations in the hydrophilic face of the CANDIS region would have an effect on the shedding activity, another mutant was generated. Three negatively charged amino acids in the hydrophilic face of the CANDIS region were substituted with non-charged, but still polar amino acids (Figure 5). The generated ADAM17 3Q mutant was tested for its TGF-α shedding activity analog to the A17 EE mutant (Figure 9A-B).

There was no significant difference detected between the wildtype ADAM17 and the 3Q mutant regarding the TGF-α shedding activity and the response to PMA (Figure 9A) and ionomycin (Figure 9B). The mutant was similarly expressed as the wildtype ADAM17 as confirmed by western blot analyses and flow cytometric analysis (Figure 10A-B).

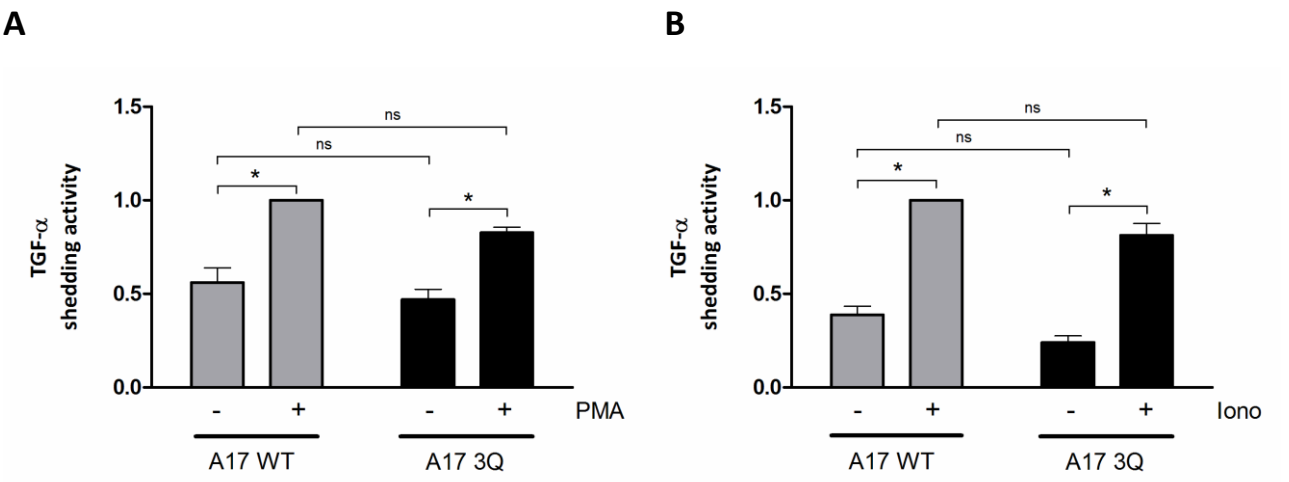

Figure 9. Substitutions in the hydrophilic face of CANDIS do not interfere with the ability of ADAM17 to shed the transmembrane substrate TGF-α. ADAM10/17-double-deficient mouse embryonic fibroblasts (MEFs) were retransfected with the inactive ADAM17 E/A variant as control, the murine ADAM17 wildtype (A17 WT) or the ADAM17 3Q mutant (A17 3Q) and plasmids containing alkaline phosphatase coupled TGF-α (TGF-α AP). 24 h after transfection, MEFs were treated or not treated with phorbol 12-myristate 13-acetate (PMA, 200 ng/ml) for 2 h ***(A)*** or ionomycin (Iono, 1 µM) for 30 min ***(B)***. Afterwards the ADAM17-mediated TGF-α shedding activity was determined. The TGF-α release was not significantly altered in the cells retransfected with A17 3Q compared to the cells retransfected with wildtype ADAM17. Data represent the means +SEM (standard error of mean) of three independent experiments (n=3) and were tested by one-way analysis of variance (one-way ANOVA) with Bonferroni multiple comparison post hoc test (* $P < 0.05$). AP=alkaline phosphatase; ns=non-significant.

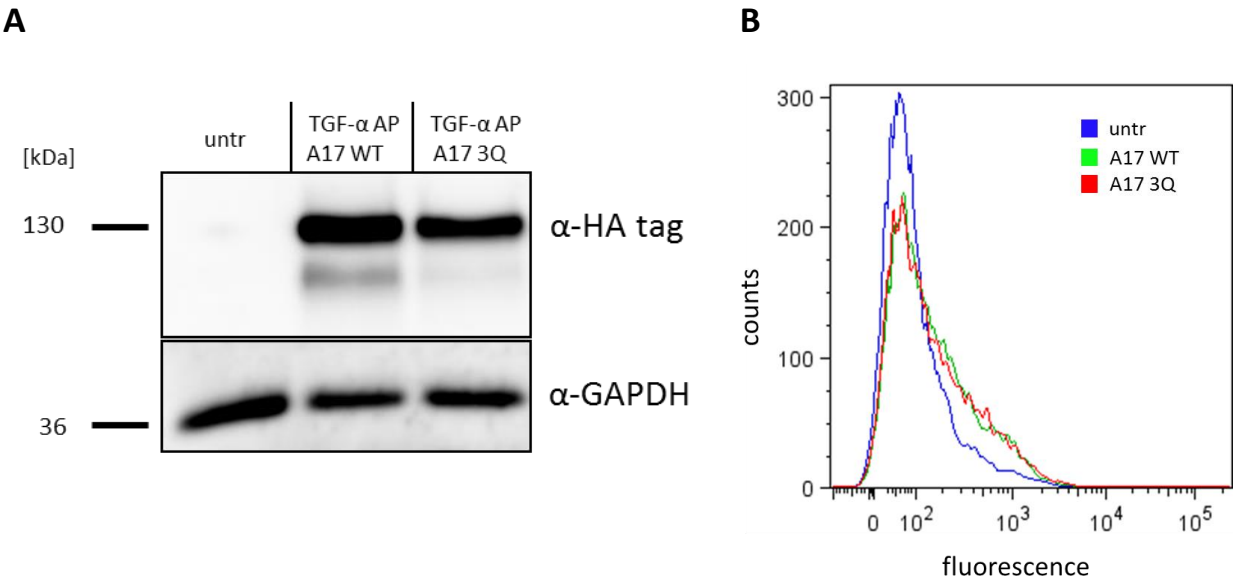

Figure 10. The ADAM17 3Q mutant shows similar protein expression as the wildtype A17. ***(A)*** Representative western blot analysis of ADAM10/17-double-deficient mouse embryonic fibroblasts (MEFs) lysates 24 h after transfection with ADAM17 wildtype (A17 WT) or ADAM17 3Q mutant (A17 3Q) and TGF-α AP plasmids. The blot was stained with anti-HA tag antibody (α-HA tag) and, as loading control, with anti-GAPDH antibody (α-GAPDH). The A17 3Q mutant showed similar expression levels of ADAM17 as the wildtype. ***(B)*** Flow cytometric analysis of MEFs transfected with A17 WT and A17 3Q mutant showed similar expression levels on the cell surface. untr=untransfected.

3.1.3 Exchange of the CANDIS region in ADAM17 with the corresponding segment of ADAM10 reduces ADAM17-mediated TGF-α shedding

ADAM10 comprises a corresponding region to the ADAM17 CANDIS segment which is highly conserved among diverse species. However, this region has no sequence similarity to the ADAM17 CANDIS sequence. Furthermore, the corresponding peptide of that ADAM10 region shows less alpha-helical character (Düsterhöft et al., 2014). To investigate whether this region of ADAM10 could functionally substitute the CANDIS region of ADAM17, an ADAM17 chimera was tested for its TGF-α shedding activity. This chimera consisted of ADAM17 with CANDIS substituted by the corresponding amino acids of ADAM10 and was named ADAM17p10.

The chimera showed about 50% reduction of PMA-stimulated TGF-α shedding activity compared to the wildtype. The shedding was significantly increased compared to the background activity. The PMA-induction could be inhibited by the matrix metalloprotease inhibitor marimastat (MM) in both cases (Figure 11). The mutant was similarly expressed as the wildtype ADAM17 confirmed by western blotting and flow cytometric analyses (Figure 12A-B).

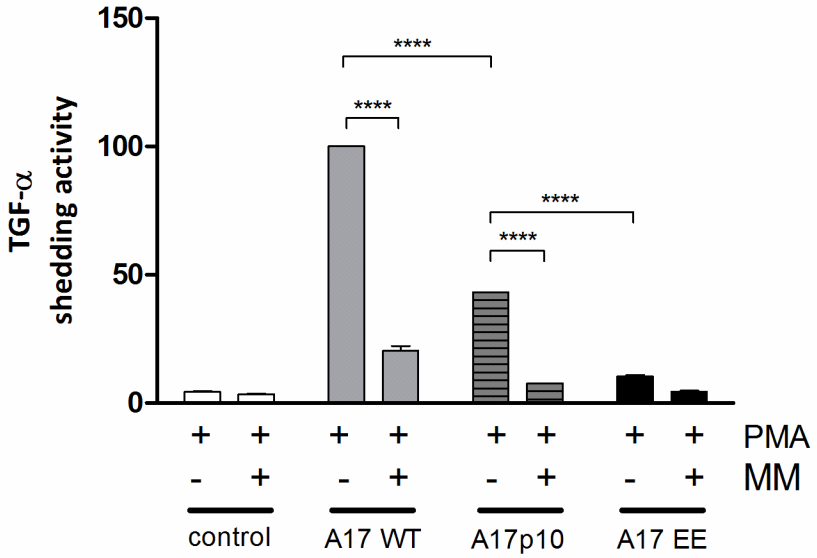

Figure 11. Exchange of the CANDIS region in ADAM17 with the corresponding region of ADAM10 (ADAM17p10) reduces ADAM17-mediated TGF-α shedding. ADAM10/17-double-deficient mouse embryonic fibroblasts (MEFs) were transfected with the inactive ADAM17 E/A variant (control), the murine ADAM17 WT (A17 WT), the ADAM17 chimera (A17p10) or the ADAM17 EE (A17 EE) mutant and plasmids containing alkaline phosphatase coupled TGF-α (TGF-α AP). 24 h after transfection, MEFs were treated with phorbol 12-myristate 13-acetate (PMA, 200 ng/ml) for 2 h. The metalloprotease inhibitor marimastat (MM) was used to block protease activity. Afterwards, the ADAM17-mediated TGF-α shedding activity was determined. The PMA-stimulated TGF-α shedding of the A17p10 chimera was significantly reduced compared to the A17 WT, but still significantly higher compared to the A17 EE mutant. Data represent the means +SEM (standard error of mean) of three independent experiments (n=3) and were tested by one-way analysis of variance (one-way ANOVA) with Bonferroni multiple comparison post hoc test (**** $P < 0.0001$).

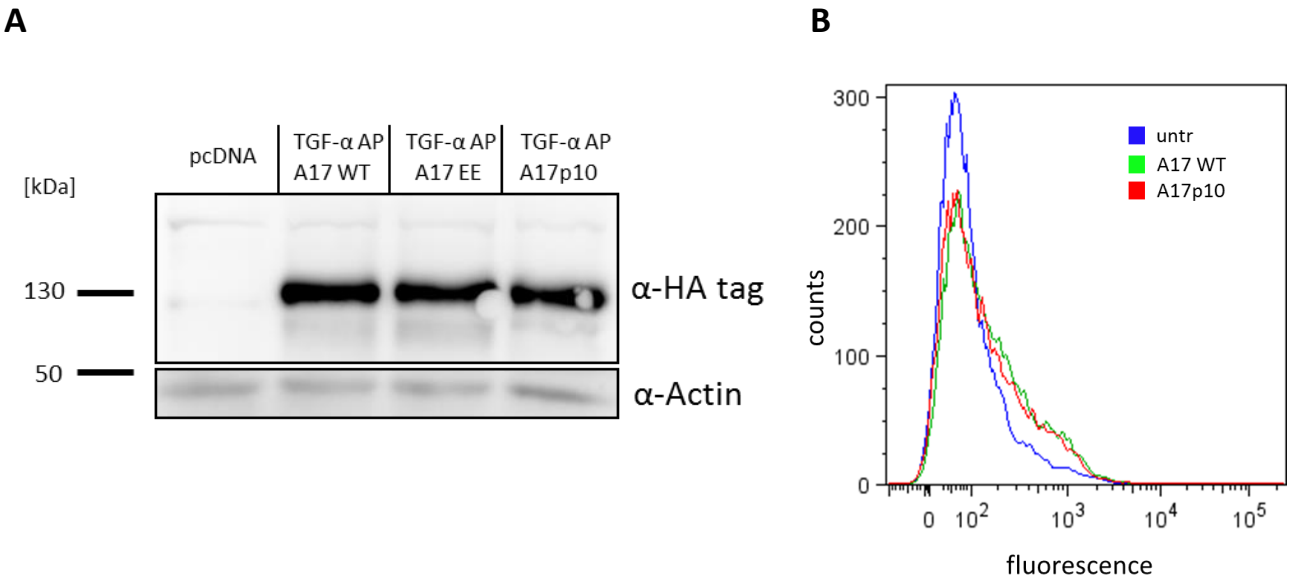

Figure 12. ADAM17p10 shows similar protein expression as the wildtype and the ADAM17 EE mutant. ***(A)*** Representative western blot analysis of ADAM10/17-double-deficient mouse embryonic fibroblasts (MEFs) lysates 24 h after transfection with ADAM17 wildtype (A17 WT), ADAM17 (A17 EE), ADAM17p10 (A17p10) or the empty vector (pcDNA) and TGF-α AP plasmids. The blot was stained with anti-HA tag antibody (α-HA tag) and, as a loading control, with anti-Actin antibody (α-Actin). All three ADAM17 variants showed similar expression levels of ADAM17. ***(B)*** Flow cytometric analysis of MEFs transfected with A17 WT and A17p10 chimera showed similar expression levels on the cell surface.

3.2 Epigenetic regulation of ADAM and ADAMTS genes

The posttranslational regulation of ADAM-related proteases, especially the ADAM family itself, is currently intensively investigated and was also under the scope of the first part of this thesis. Surprisingly, regulation mechanisms such as epigenetic modifications are poorly investigated. To delineate the role of epigenetic regulation mechanisms of ADAM and ADAMTS proteases in various inflammatory diseases and cancerous diseases, the methylation pattern of patients suffering from these diseases were investigated. In first analyses the methylation status of 1145 CpGs in 51 ADAM and ADAMTS genes was measured with the *HumanMethylation450 BeadChip Array* in tissue samples from patients suffering from the inflammatory diseases *Non-alcoholic fatty liver disease*, *Non-alcoholic Steatohepatitis* and *oral lichen planus*. In further studies, the investigated diseases were expanded to cancerous diseases. In all conducted analyses, only the methylation of CpGs in genes which are related to ADAM and ADAMTS were included. CpGs were defined as *differentially methylated* if the difference of the mean β-values ($\Delta\beta_{mean}$) was larger than 0.2 ($|\Delta\beta_{mean}| \geq 0.2$) compared to the control and significant after *Mann-Whitney-U testing* with multiple testing correction ($P < 0.05$).

3.2.1 ADAM/TS genes show no epigenetic methylation alterations in the preinflammatory disease *Non-alcoholic fatty liver disease* and the inflammatory disease *Non-alcoholic Steatohepatitis*

Non-alcoholic fatty liver disease (NAFLD) is a form of fatty liver disease, in which abnormal lipid accumulation in the liver takes place due to causes other than excessive alcohol abuse. DNA of liver samples from control (ctrl) and NAFLD-patients was extracted and the CpG methylation was measured (n_{ctrl}=19, n_{NAFLD}=18). The methylation data were filtered for ADAM and ADAMTS genes. All measured CpGs in these proteases showed no significant differences greater than 10% in the mean methylation status (mean β-values) of control and NAFLD-samples.

Since no relevant changes in NAFLD were observed, DNA of patients suffering from the more severe inflammatory form, *Non-alcoholic Steatohepatitis (NASH)*, was investigated for methylation changes (n_{ctrl}=19, n_{NASH}=16). Similarly to NAFLD, differences in the mean methylation between control tissue and the tissue from NASH patients were, with one exception, smaller than 10%. The CpG cg04815959 in the *ADAM19* gene showed a mean methylation difference higher than 0.1. The $\Delta\beta_{mean}$ of cg04815959 in *ADAM19* was 0.12, reflecting 12% more methylation in the tissue from patients suffering from NASH than in the control tissue in this CpG.

3.2.2 ADAM/TS genes show moderate methylation alterations in the precancerous disease *oral lichen planus*

The investigated inflammatory diseases showed no differentially methylated CpG-dinucleotides in ADAM/TS genes. Since inflammation is one of the two "*enabling characteristics*" of the 8 hallmarks of cancer pathogenesis (Hanahan and Weinberg, 2011), the analyses were extended from plain inflammatory diseases to the precancerous, inflammatory *oral lichen planus* and further to cancerous diseases. In *oral lichen planus* patients, a moderate number of differentially methylated CpGs was found compared to NASH and NAFLD. In total, 7 CpGs in *ADAMTS1*, *ADAMTS2*, *ADAM12*, *ADAMTS18*, *ADAMTSL5* and *ADAMTS17* were increased or decreased in their methylation by more than 20% ($|\Delta\beta_{mean}| \geq 0.2$) (Figure 13). All of these CpGs were hypermethylated ($\Delta\beta_{mean} \geq 0.2$, $P < 0.05$) compared to the control, except cg04834770 which showed hypomethylation ($\Delta\beta_{mean} \leq -0.2$, $P < 0.05$).

CpG	gene symbol	β_{mean} (ctrl)	β_{mean} (infl)	$\Delta\beta_{mean}$	$\lvert\Delta\beta_{mean}\rvert$	p-value	adjusted p-value	significance
cg04834770	ADAM12	0,682	0,443	-0,239	0,239	0,01455	0,03867	*
cg00952789	ADAMTS1	0,428	0,67	0,242	0,242	0,00013	0,00175	**
cg01231141	ADAMTS2	0,181	0,386	0,205	0,205	0,00052	0,00361	**
cg09918751	ADAMTS17	0,475	0,748	0,273	0,273	0,00003	0,00147	**
cg25357666	ADAMTS17	0,418	0,653	0,235	0,235	0,00003	0,00147	**
cg05485250	ADAMTS18	0,639	0,839	0,2	0,2	0,00003	0,00147	**
cg09791746	ADAMTSL5	0,423	0,665	0,242	0,242	0,00003	0,00147	**

Figure 13. The precancerous, inflammatory disease oral lichen planus shows moderate genomic methylation alterations in ADAM/TS genes in the inflamed tissue. Biopsies of inflamed and non-inflamed (ctrl) tissue from the same patient suffering from oral lichen planus were immediately frozen with liquid nitrogen (n=18 (ctrl), n=9 (infl)). Afterwards, genomic DNA was analyzed with the HumanMethylation450 BeadChip Array for the methylation of 450k CpG sites. From 1145 CpGs located in ADAM/TS genes, 6 CpGs were significantly hypermethylated and 1 hypomethylated compared to the control. The depicted β-value represents a quantitation of the methylation level of the respective CpG-locus. Data were statistically analyzed with Mann-Whitney-U test and corrected for multiple testing with the Benjamini-Hochberg method (* $P < 0.05$, ** $P < 0.01$). Hypermethylation was defined as $\Delta\beta_{mean} \geq 0.2$ ($P < 0.05$) and hypomethylation as $\Delta\beta_{mean} \leq -0.2$ ($P < 0.05$) compared to the control. Only hyper- or hypomethylated CpGs are presented. ctrl=control, non-inflamed tissue; infl=inflamed tissue.

3.2.3 ADAM/TS genes show major epigenetic alterations in cancerous diseases, especially in the *ADAMTS16* gene

3.2.3.1 Major genomic DNA methylation changes in ADAM and ADAMTS genes take place in the tumor of colorectal cancer patients

While differentially methylated genes were observed in *oral lichen planus*, no differentially methylated genes were observed in NASH and NAFLD. *Oral lichen planus* is not only an inflammatory disease, but also regarded as a precancerous condition. This fact, together with our results therefore suggested to investigate cancerous diseases for methylation alterations. In first analyses, tissues from 119 colorectal cancer (CRC) patients were studied. Resected samples of the tumor tissue and, as control, peri-tumoral non-malignant tissue of the same patient were analysed for methylation differences. In contrast to samples from inflammatory diseases, many CpGs showed significant differences in the mean methylation between tumor and control tissue with more than 20% difference. The 72 CpGs are listed in Figure 14. Most of the CpGs affected by methylation alterations were located in the *ADAMTS16* or *ADAMTS2* genes. A visualization of the methylation changes in the colorectal cancer patiens is depicted in Figure 15 in form of a heatmap. The color code reflects the level of methylation by a color transition from blue (low methylation) to red (high methylation). Visible is the change of the uniform pattern in the peri-tumoral non-malignant tissue (ctrl) to a more diffuse pattern in the tumor tissue (cancer), reflecting major methylation changes in the tumor tissue in colorectal cancer patients.

CpG	gene symbol	β_{mean} (ctrl)	β_{mean} (canc)	$\Delta\beta_{mean}$	$\lvert\Delta\beta_{mean}\rvert$	p-value	adjusted p-value	significance
cg24166018	ADAM12	0,756	0,464	-0,292	0,292	0,00001	0,00001	****
cg11580615	ADAM12	0,881	0,599	-0,282	0,282	0,00001	0,00001	****
cg13488201	ADAM12	0,191	0,393	0,202	0,202	0,00001	0,00001	****
cg05237641	ADAM12	0,204	0,433	0,229	0,229	0,00001	0,00001	****
cg10084554	ADAM12	0,517	0,305	-0,212	0,212	0,00001	0,00001	****
cg14621053	ADAM12	0,136	0,349	0,213	0,213	0,00001	0,00001	****
cg02235497	ADAM12	0,762	0,514	-0,248	0,248	0,00001	0,00001	****
cg20667008	ADAM12	0,765	0,544	-0,221	0,221	0,00001	0,00001	****
cg14594063	ADAM12	0,687	0,461	-0,226	0,226	0,00001	0,00001	****
cg04834770	ADAM12	0,696	0,479	-0,217	0,217	0,00001	0,00001	****
cg25077558	ADAM19	0,657	0,437	-0,22	0,22	0,00001	0,00001	****
cg04371413	ADAM23	0,717	0,399	-0,318	0,318	0,00001	0,00001	****
cg25097705	ADAM29	0,675	0,448	-0,227	0,227	0,00001	0,00001	****
cg00472814	ADAMTS1	0,084	0,313	0,229	0,229	0,00001	0,00001	****
cg24262066	ADAMTS1	0,062	0,322	0,26	0,26	0,00001	0,00001	****
cg04590718	ADAMTS10	0,613	0,372	-0,241	0,241	0,00001	0,00001	****
cg07700393	ADAMTS12	0,775	0,459	-0,316	0,316	0,00001	0,00001	****
cg04578894	ADAMTS12	0,764	0,469	-0,295	0,295	0,00001	0,00001	****
cg08768395	ADAMTS12	0,602	0,365	-0,237	0,237	0,00001	0,00001	****
cg23359363	ADAMTS12	0,699	0,468	-0,231	0,231	0,00001	0,00001	****
cg01881590	ADAMTS16	0,823	0,488	-0,335	0,335	0,00001	0,00001	****
cg17627328	ADAMTS16	0,787	0,442	-0,345	0,345	0,00001	0,00001	****
cg09588888	ADAMTS16	0,784	0,534	-0,25	0,25	0,00001	0,00001	****
cg25973534	ADAMTS16	0,263	0,516	0,253	0,253	0,00001	0,00001	****
cg06758605	ADAMTS16	0,781	0,534	-0,247	0,247	0,00001	0,00001	****
cg04136610	ADAMTS16	0,276	0,534	0,258	0,258	0,00001	0,00001	****
cg16508480	ADAMTS16	0,29	0,517	0,227	0,227	0,00001	0,00001	****
cg15409013	ADAMTS16	0,23	0,451	0,221	0,221	0,00001	0,00001	****
cg15048991	ADAMTS16	0,235	0,499	0,264	0,264	0,00001	0,00001	****
cg02109699	ADAMTS16	0,616	0,372	-0,244	0,244	0,00001	0,00001	****
cg24030232	ADAMTS16	0,589	0,37	-0,219	0,219	0,00001	0,00001	****
cg22562853	ADAMTS16	0,757	0,552	-0,205	0,205	0,00001	0,00001	****
cg22954449	ADAMTS16	0,336	0,556	0,22	0,22	0,00001	0,00001	****
cg06434454	ADAMTS16	0,895	0,661	-0,234	0,234	0,00001	0,00001	****
cg24863552	ADAMTS17	0,621	0,392	-0,229	0,229	0,00001	0,00001	****
cg21314318	ADAMTS17	0,52	0,259	-0,261	0,261	0,00001	0,00001	****
cg03300787	ADAMTS17	0,735	0,485	-0,25	0,25	0,00001	0,00001	****
cg05884870	ADAMTS17	0,773	0,558	-0,215	0,215	0,00001	0,00001	****
cg05178576	ADAMTS18	0,112	0,338	0,226	0,226	0,00001	0,00001	****
cg19489885	ADAMTS2	0,774	0,548	-0,226	0,226	0,00001	0,00001	****
cg25550425	ADAMTS2	0,632	0,402	-0,23	0,23	0,00001	0,00001	****
cg14409941	ADAMTS2	0,1	0,385	0,285	0,285	0,00001	0,00001	****
cg07124832	ADAMTS2	0,883	0,667	-0,216	0,216	0,00001	0,00001	****
cg15870576	ADAMTS2	0,739	0,504	-0,235	0,235	0,00001	0,00001	****
cg03703637	ADAMTS2	0,192	0,441	0,249	0,249	0,00001	0,00001	****
cg26429655	ADAMTS2	0,12	0,337	0,217	0,217	0,00001	0,00001	****
cg18331515	ADAMTS2	0,097	0,355	0,258	0,258	0,00001	0,00001	****
cg13909534	ADAMTS2	0,074	0,295	0,221	0,221	0,00001	0,00001	****
cg20422099	ADAMTS2	0,224	0,431	0,207	0,207	0,00001	0,00001	****
cg09046370	ADAMTS2	0,573	0,36	-0,213	0,213	0,00001	0,00001	****
cg05214690	ADAMTS2	0,119	0,37	0,251	0,251	0,00001	0,00001	****
cg00532157	ADAMTS2	0,191	0,429	0,238	0,238	0,00001	0,00001	****
cg06002305	ADAMTS2	0,729	0,507	-0,222	0,222	0,00001	0,00001	****
cg24643381	ADAMTS20	0,724	0,432	-0,292	0,292	0,00001	0,00001	****
cg07974833	ADAMTS3	0,746	0,435	-0,311	0,311	0,00001	0,00001	****
cg04812351	ADAMTS3	0,625	0,343	-0,282	0,282	0,00001	0,00001	****
cg05797623	ADAMTS3	0,667	0,382	-0,285	0,285	0,00001	0,00001	****
cg11243196	ADAMTS3	0,058	0,266	0,208	0,208	0,00001	0,00001	****
cg19523085	ADAMTS5	0,072	0,304	0,232	0,232	0,00001	0,00001	****
cg13601496	ADAMTS5	0,098	0,317	0,219	0,219	0,00001	0,00001	****
cg07771160	ADAMTS5	0,512	0,31	-0,202	0,202	0,00001	0,00001	****
cg03202077	ADAMTS5	0,151	0,39	0,239	0,239	0,00001	0,00001	****
cg15237494	ADAMTS5	0,221	0,473	0,252	0,252	0,00001	0,00001	****
cg23986671	ADAMTS5	0,12	0,387	0,267	0,267	0,00001	0,00001	****
cg08190291	ADAMTS5	0,107	0,391	0,284	0,284	0,00001	0,00001	****
cg21646598	ADAMTS5	0,146	0,457	0,311	0,311	0,00001	0,00001	****
cg02147292	ADAMTS8	0,633	0,425	-0,208	0,208	0,00001	0,00001	****
cg06476693	ADAMTS8	0,781	0,573	-0,208	0,208	0,00001	0,00001	****
cg14502847	ADAMTSL1	0,678	0,413	-0,265	0,265	0,00001	0,00001	****
cg16714091	ADAMTSL1	0,225	0,439	0,214	0,214	0,00001	0,00001	****
cg13748845	ADAMTSL2	0,795	0,573	-0,222	0,222	0,00001	0,00001	****
cg04138185	ADAMTSL3	0,128	0,338	0,21	0,21	0,00001	0,00001	****

Figure 14. 72 CpGs are differentially methylated in tumor tissue compared to non-tumor tissue in patients suffering from colorectal cancer. Tumor resectats (canc) and peri-tumoral non-malignant resectats (ctrl) from the same patient were immediately frozen (n=117 (ctrl), n=119 (canc)). Afterwards, genomic DNA was analyzed with the HumanMethylation450 BeadChip Array for the methylation of 450k CpG sites. 72 of 1145 CpGs located in ADAM/TS genes were differentially methylated. The depicted β-value represents a quantitation of the methylation level of the respective CpG-locus. Data were statistically analyzed with Mann-Whitney-U test and corrected for multiple testing with Benjamini-Hochberg method (**** $P < 0.0001$). Hypermethylation was defined as $\Delta\beta_{mean} \geq 0.2$ ($P < 0.05$) and hypomethylation as $\Delta\beta_{mean} \leq -0.2$ ($P < 0.05$) compared to the control. Only hyper- or hypomethylated CpGs are presented.

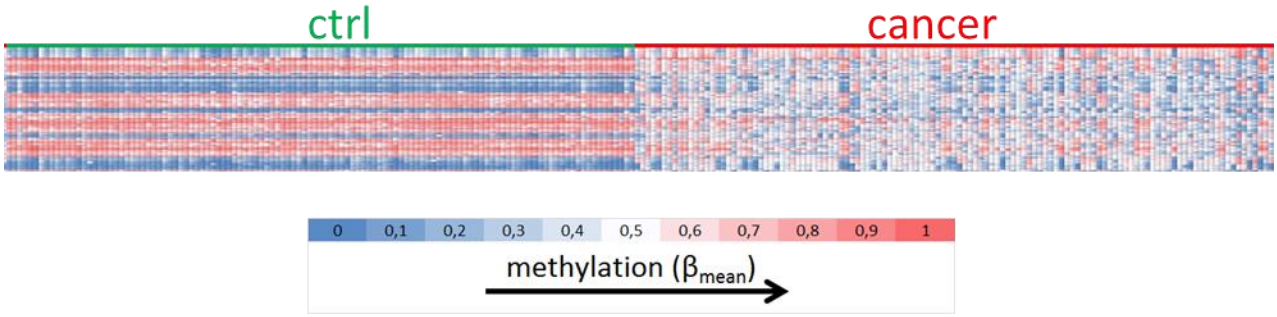

Figure 15. The heatmap of all differentially methylated CpGs in colorectal cancer patients visualizes that major genomic methylation changes take place in the tumor tissue. Each column of the matrix represents a patient and each row a differentially methylated CpG. The color represents the methylation level. Major changes in the methylation status of the cancer tissue compared to the control tissue are visible. ctrl=control, peri-tumoral non-malignant tissue; cancer=cancerous tissue.

3.2.3.2 *ADAMTS16* and *ADAMTS2* are the most frequently differentially methylated ADAM/TS genes in colorectal cancer patients

In total 72 CpGs in 18 genes were affected by hyper- or hypomethylation compared to the control. 39% of these CpGs were CpG-dinucleotides in *ADAMTS16* (14 CpGs) and *ADAMTS2* (14 CpGs) (Figure 14). In case of *ADAMTS16*, the heatmap of all *ADAMTS16* CpGs (Figure 16) which were significantly altered in their methylation by more than 20%, showed a bimodal distribution in the control. In the cancer tissue this bimodal distribution was resolved and tendentially inverted.

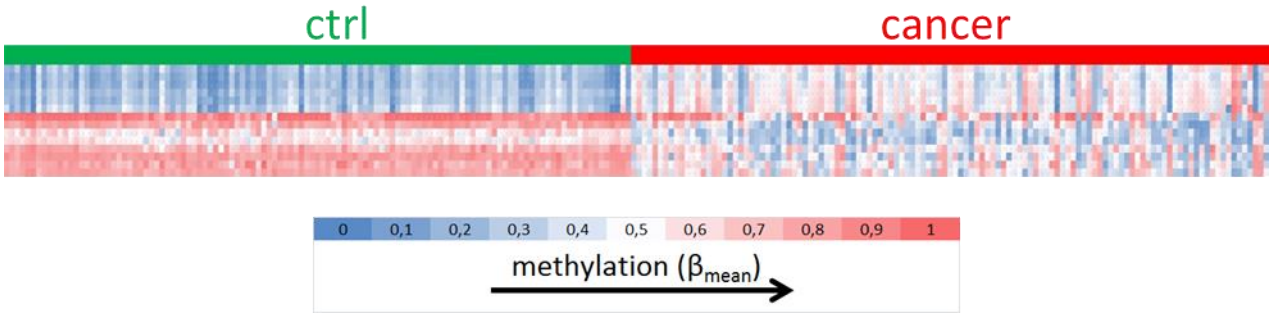

Figure 16. The Heatmap of the 14 differentially methylated *ADAMTS16* CpGs in colorectal cancer patients visualizes the methylation changes. Each column of the matrix represents a patient and each row a differentially methylated CpG. The color represents the methylation level. In the control tissue a bimodal-distribution is visible which is absent in the cancerous tissue. ctrl=control, peri-tumoral non-malignant tissue; cancer=cancerous tissue.

The methylation profile of the cancer tissue (red line) and the non-malignant tissue (blue line) for all 53 measured CpGs in the *ADAMTS16* gene is presented in Figure 17. 14 CpGs were found to be differentially methylated ($|\Delta\beta_{mean}| \geq 0.2$, $P < 0.05$) and 11 CpGs (together 47,17% of all CpGs) showed an intermediate methylation difference of more than 0.1 ($0.1 \leq |\Delta\beta_{mean}| < 0.2$, $P < 0.05$).

The methylation profile of the cancer tissue showed major differences compared to the control tissue. In the region between chromosome position 5139853 and 5140646, 6 CpGs were hypermethylated in the tumor tissue compared to the control tissue. This region lies within the promoter region of *ADAMTS16*. In contrast, in the gene body (between the chromosome position 5146320 and 5313892) 8 CpGs were hypomethylated in the tumor tissue. The one CpG on chromosome position 5140646 which is located in the first exon, showed an intermediate methylation alteration with an enhancement in the methylation ($\Delta\beta_{mean}$ = 0.13). The measured CpGs in *ADAMTS16* are outlined in Figure 18.

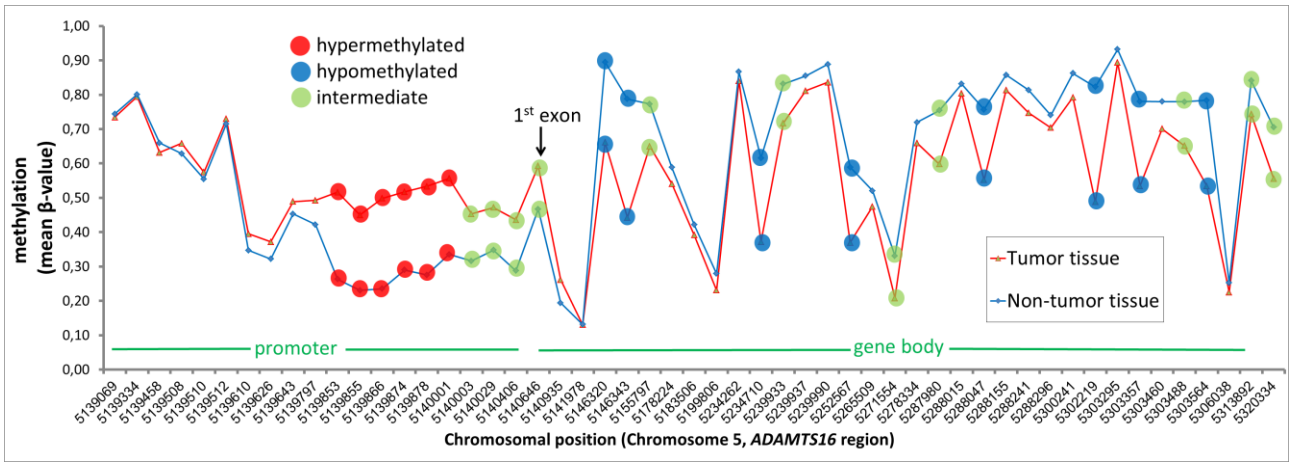

Figure 17. The methylation in the *ADAMTS16* gene is extensively altered in cancer tissue resectats of colorectal cancer patients compared to peri-tumoral non-malignant tissue. Shown is the average methylation (mean β-value) of 53 different CpG sites of 119 patients. The red line indicates tumor tissue and the blue line indicates matched peri-tumoral non-malignant tissue (control). 6 CpGs were hypermethylated (red spots), 11 CpGs showed intermediate methylation (green spots) and 8 CpGs showed hypomethylation (blue spots). Hypermethylation was defined as $\Delta\beta_{mean} \geq 0.2$ ($P < 0.05$), hypomethylation as $\Delta\beta_{mean} \leq -0.2$ ($P < 0.05$) and intermediate methylation as $0.1 \leq |\Delta\beta_{mean}| < 0.2$ compared to the control.

CpG	β_{mean} (ctrl)	β_{mean} (canc)	$\Delta\beta_{mean}$	$\lvert\Delta\beta_{mean}\rvert$	p-value	adjusted p-value	significance	mapinfo	region
cg13603589	0,75	0,73	-0,01	0,01	0,185483	0,214118	ns	5139069	promoter
cg16068490	0,80	0,80	-0,01	0,01	0,607244	0,637496	ns	5139334	promoter
cg25536014	0,66	0,63	-0,03	0,03	0,096148	0,118297	ns	5139458	promoter
cg19452011	0,63	0,66	0,03	0,03	0,007251	0,010719	*	5139508	promoter
cg10881764	0,56	0,58	0,02	0,02	0,131243	0,156331	ns	5139510	promoter
cg18503643	0,72	0,73	0,02	0,02	0,082914	0,103219	ns	5139512	promoter
cg07834743	0,35	0,40	0,05	0,05	0,009213	0,013381	*	5139610	promoter
cg01085224	0,32	0,37	0,05	0,05	0,002678	0,004184	**	5139626	promoter
cg19813025	0,45	0,49	0,04	0,04	0,033426	0,044169	*	5139643	promoter
cg16670809	0,42	0,49	0,07	0,07	0,000224	0,000399	***	5139797	promoter
cg25973534	0,26	0,52	0,25	0,25	0,000001	0,000001	****	5139853	promoter
cg15409013	0,23	0,45	0,22	0,22	0,000001	0,000001	****	5139855	promoter
cg15048991	0,24	0,50	0,26	0,26	0,000001	0,000001	****	5139866	promoter
cg16508480	0,29	0,52	0,23	0,23	0,000001	0,000001	****	5139874	promoter
cg04136610	0,28	0,53	0,26	0,26	0,000001	0,000001	****	5139878	promoter
cg22954449	0,34	0,56	0,22	0,22	0,000001	0,000001	****	5140001	promoter
cg03209854	0,32	0,45	0,14	0,14	0,000001	0,000001	****	5140003	promoter
cg00127167	0,35	0,47	0,13	0,13	0,000001	0,000001	****	5140029	promoter
cg01717727	0,29	0,44	0,15	0,15	0,000001	0,000001	****	5140406	promoter
cg22784954	0,47	0,59	0,13	0,13	0,000001	0,000001	****	5140646	1st Exon
cg22983903	0,19	0,26	0,07	0,07	0,000103	0,000191	***	5140935	gene body
cg06843687	0,13	0,13	0,00	0,00	0,791305	0,812331	ns	5141978	gene body
cg06434454	0,90	0,66	-0,23	0,23	0,000001	0,000001	****	5146320	gene body
cg17627328	0,79	0,44	-0,35	0,35	0,000001	0,000001	****	5146343	gene body
cg26892415	0,77	0,65	-0,12	0,12	0,000001	0,000001	****	5155797	gene body
cg26868514	0,59	0,54	-0,05	0,05	0,027440	0,037067	*	5178224	gene body
cg16163140	0,42	0,39	-0,03	0,03	0,004615	0,006983	**	5183506	gene body
cg15411554	0,28	0,23	-0,05	0,05	0,000001	0,000001	****	5199806	gene body
cg25386699	0,87	0,84	-0,03	0,03	0,030645	0,040918	*	5234262	gene body
cg02109699	0,62	0,37	-0,24	0,24	0,000001	0,000001	****	5234710	gene body
cg10561103	0,83	0,72	-0,11	0,11	0,000001	0,000001	****	5239933	gene body
cg18308985	0,86	0,81	-0,04	0,04	0,000569	0,000963	***	5239937	gene body
cg07567767	0,89	0,84	-0,05	0,05	0,000091	0,000171	***	5239990	gene body
cg24030232	0,59	0,37	-0,22	0,22	0,000001	0,000001	****	5252567	gene body
cg00087067	0,52	0,48	-0,05	0,05	0,000999	0,001642	**	5265509	gene body
cg25485055	0,33	0,21	-0,12	0,12	0,000001	0,000001	****	5271554	gene body
cg24164257	0,72	0,66	-0,06	0,06	0,001074	0,001763	**	5278334	gene body
cg14521614	0,75	0,60	-0,16	0,16	0,000001	0,000001	****	5287980	gene body
cg26908818	0,83	0,80	-0,03	0,03	0,107637	0,130904	ns	5288015	gene body
cg22562853	0,76	0,55	-0,21	0,21	0,000001	0,000001	****	5288047	gene body
cg12660315	0,86	0,81	-0,04	0,04	0,001601	0,002552	**	5288155	gene body
cg21926451	0,81	0,75	-0,07	0,07	0,000057	0,000107	***	5288241	gene body
cg09456340	0,74	0,70	-0,04	0,04	0,015457	0,021715	*	5288296	gene body
cg21514291	0,86	0,79	-0,07	0,07	0,000001	0,000001	****	5300241	gene body
cg01881590	0,82	0,49	-0,34	0,34	0,000001	0,000001	****	5302219	gene body
cg08546589	0,93	0,89	-0,04	0,04	0,000637	0,001070	**	5303295	gene body
cg06758605	0,78	0,53	-0,25	0,25	0,000001	0,000001	****	5303357	gene body
cg17760878	0,78	0,70	-0,08	0,08	0,000001	0,000001	****	5303460	gene body
cg24573724	0,78	0,65	-0,13	0,13	0,000001	0,000001	****	5303488	gene body
cg09588888	0,78	0,53	-0,25	0,25	0,000001	0,000001	****	5303564	gene body
cg06623930	0,25	0,23	-0,03	0,03	0,032167	0,042803	*	5306038	gene body
cg12858370	0,84	0,74	-0,10	0,10	0,000001	0,000001	****	5313892	gene body
cg03824768	0,71	0,56	-0,15	0,15	0,000001	0,000001	****	5320334	3'UTR

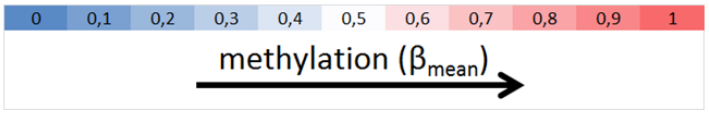

Figure 18. Methylation status of all *ADAMTS16* CpGs in patients suffering from colorectal cancer. Tumor resectats and peri-tumoral non-malignant (ctrl) resectats from the same patient were immediately frozen with liquid nitrogen (n=117 (ctrl), n=119 (canc)). Afterwards, genomic DNA was analyzed with the HumanMethylation450 BeadChip Array for the methylation of 450k CpG sites. From 53 CpGs located in *ADAMTS16*, 14 CpGs were differentially methylated and 11 CpGs showed intermediate methylation alterations ($0.1 \leq |\Delta\beta_{mean}| < 0.2$). The depicted β-value represents a quantitation of the methylation level of the respective CpG-locus. Data were statistically analyzed with Mann-Whitney-U test and corrected for multiple testing with Benjamini-Hochberg method (* $P < 0.05$, ** $P < 0.01$, *** $P < 0.001$, **** $P < 0.0001$). Hypermethylation was defined as $\Delta\beta_{mean} \geq 0.2$ ($P < 0.05$) and hypomethylation as $\Delta\beta_{mean} \leq -0.2$ ($P < 0.05$) compared to the control. ctrl=control, peri-tumoral non-malignant tissue; canc=cancerous tissue.

3.2.3.3 8 CpGs in *ADAMTS16* are commonly altered in their methylation in three different epithelial cancers

To delineate whether the observed epigenetic alterations in the *ADAMTS16* gene in colorectal cancer were cancer type specific, two other cancer entities were investigated. Resectats from 40 lung cancer (LC) and 15 oral squamous-cell carcinoma (SCC) patients were analyzed for methylation changes. 78 differentially methylated CpGs were found in LC and 29 in SCC. In a first step, all differentially methylated CpGs in these cancers were filtered for commonly differentially methylated CpGs. Strikingly, 8 CpGs in all three cancer entities were commonly differentially methylated (Figure 19). All of them are located in the *ADAMTS16* gene. The methylation profiles of the three cancer entities for *ADAMTS16* are depicted in Figure 20. The overall methylation profiles and methylation changes were very similar in all three cancer entities. All three cancer tissues shared the hypermethylated region in the promoter (between chromosome position 5139853 and 5140001), the increased methylation in the exon1 CpG (cg22784954) and the region in the gene body (between 5234710 and 5303564) where many CpGs were hypomethylated in the cancer tissue compared to the control. Furthermore, the overall course of the graphs was very similar reflecting a similar methylation profile in the three cancer entities.

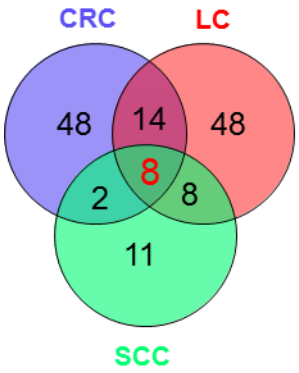

Figure 19. Venn diagram showing the overlap of differentially methylated CpGs between lung cancer (LC), colorectal cancer (CRC) and oral squamous-cell carcinoma (SCC). 8 CpGs are commonly differentially methylated in the three cancer entities. All are located in the *ADAMTS16* gene. The venn diagram was generated with VENNY 2.0 (Oliveros, 2007).

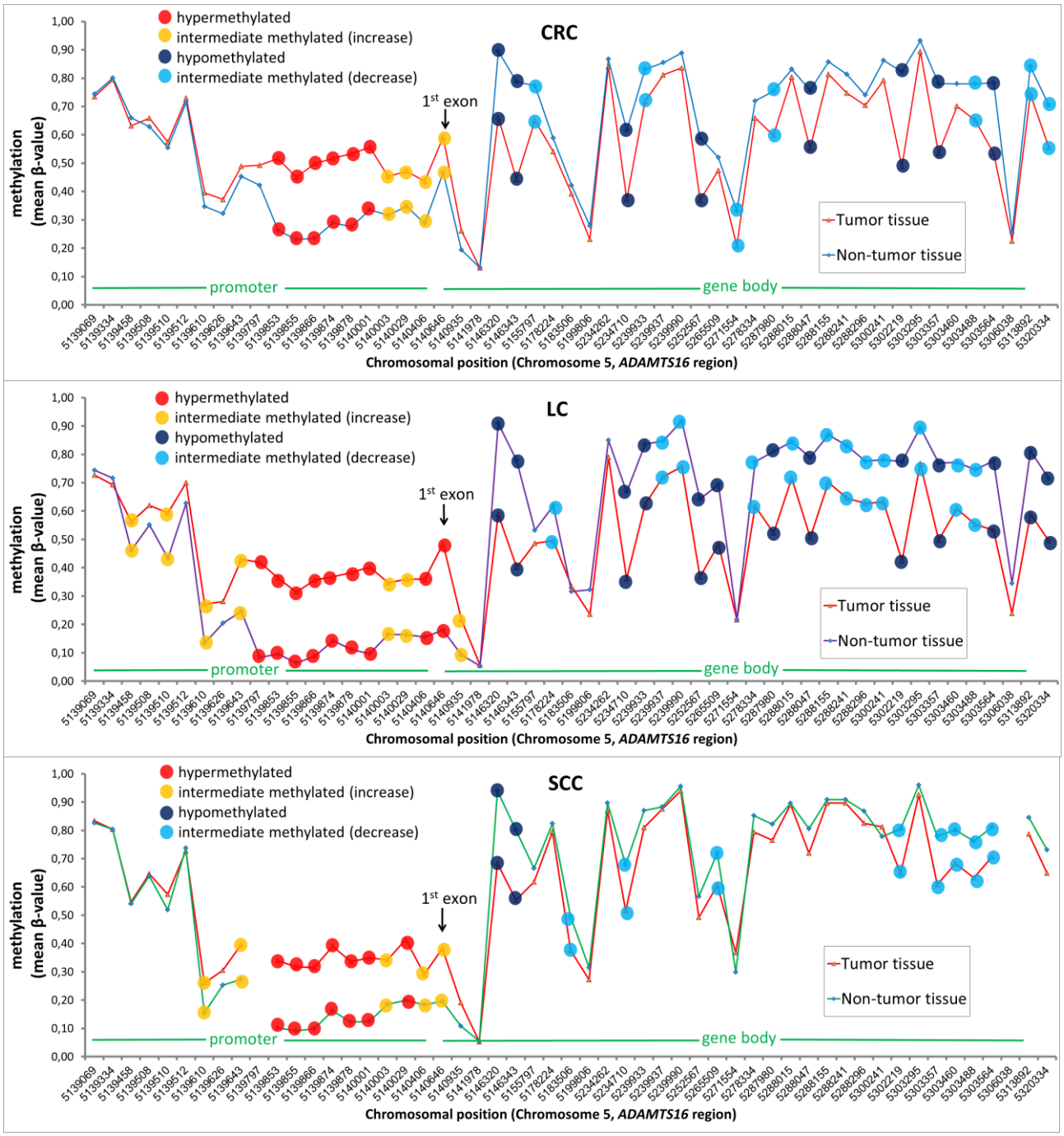

Figure 20. Methylation profile of the *ADAMTS16* gene in colorectal cancer (CRC), lung cancer (LC) and oral squamous-cell carcinoma (SCC) patients. Shown is the average methylation (mean β-value) of 53 different CpG sites in *ADAMTS16*. All three cancer entities show very similar methylations profiles. Hypermethylation was defined as $\Delta\beta_{mean} \geq 0.2$ ($P < 0.05$), hypomethylation as $\Delta\beta_{mean} \leq -0.2$ ($P < 0.05$) and intermediate methylation as $0.1 \leq |\Delta\beta_{mean}| < 0.2$ compared to the control (n=117 $(ctrl)_{CRC}$, n=119 $(canc)_{CRC}$, n=40 $(ctrl)_{LC}$, n=40 $(canc)_{LC}$, n=18 $(ctrl)_{SCC}$, n=15 $(canc)_{SCC}$).

More profound analyses of the 8 commonly differentially methylated CpGs (Figure 21 and Figure 22) revealed that the change in direction of these CpGs was in all three cancer entities the same. The 6 CpGs in the promoter region were all hypermethylated, whereas the 2 CpGs in the gene body of *ADAMTS16* were hypomethylated compared to the control. Regarding the mean methylation of these CpGs, the lung cancer and the oral squamous-cell carcinoma patients showed nearly the same mean values, in contrast to the colorectal cancer patients. Noticeable, the colorectal cancer tissues had in most cases a higher mean methylation than the LC and SCC in these CpGs.

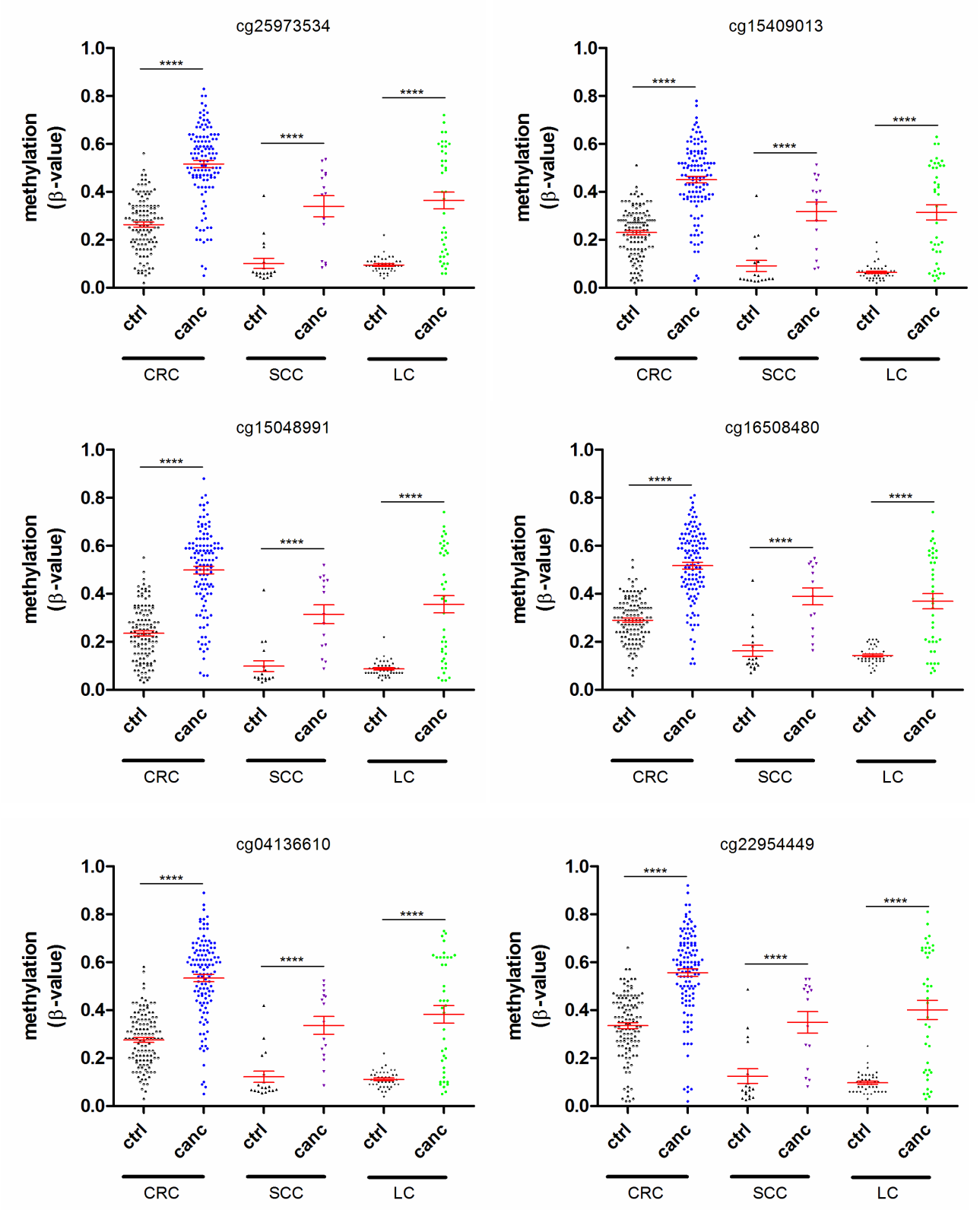

Figure 21. 6 hypermethylated *ADAMTS16* CpGs in colorectal cancer (CRC) patients were also hypermethylated in lung cancer (LC) and oral squamous-cell carcinoma (SCC) patients. Data represent the methylation (β-value) for individual patients (spots) with the mean ±SEM (red lines). Data were statistically analyzed with Mann-Whitney-U test and corrected for multiple testing with Benjamini-Hochberg method (**** $P < 0.0001$, n=117 $(ctrl)_{CRC}$, n=119 $(canc)_{CRC}$, n=40 $(ctrl)_{LC}$, n=40 $(canc)_{LC}$, n=18 $(ctrl)_{SCC}$, n=15 $(canc)_{SCC}$). ctrl=peri-tumoral non-malignant tissue; canc=cancer tissue; SEM=standard error of mean.

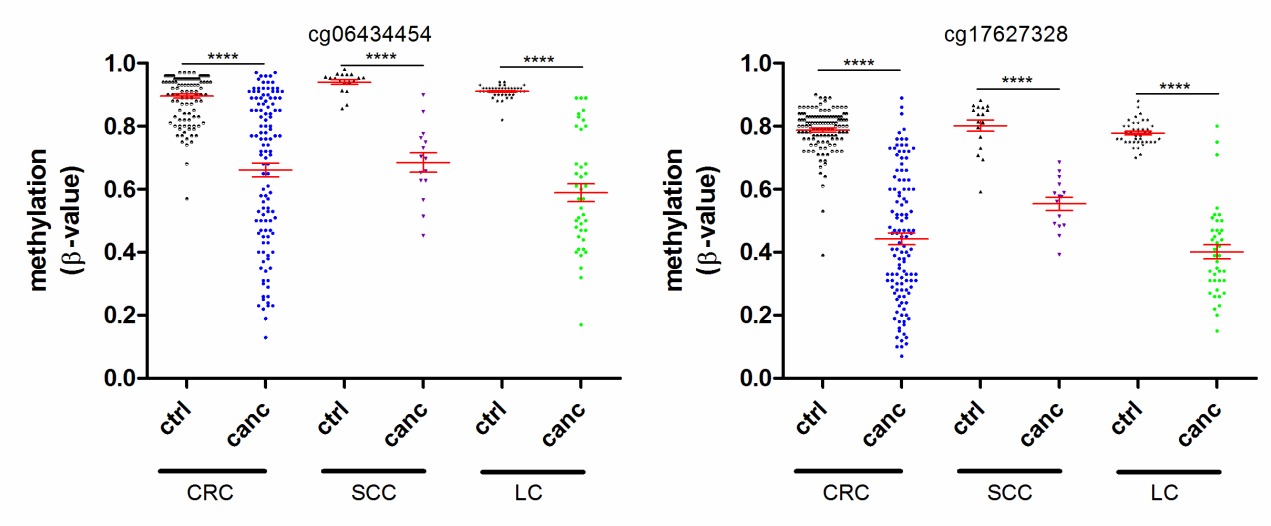

Figure 22. 2 hypomethylated *ADAMTS16 CpGs* in colorectal cancer (CRC) patients are also hypomethylated in lung cancer (LC) and oral squamous-cell carcinoma (SCC) patients. Data represent the methylation (β-value) for individual patients (spots) with the mean ±SEM (red lines). Data were statistically analyzed with Mann-Whitney-U test and corrected for multiple testing with Benjamini-Hochberg method (**** $P < 0.0001$, n=117 $(ctrl)_{CRC}$, n=119 $(canc)_{CRC}$, n=40 $(ctrl)_{LC}$, n=40 $(canc)_{LC}$, n=18 $(ctrl)_{SCC}$, n=15 $(canc)_{SCC}$). ctrl=peri-tumoral non-malignant tissue; canc=cancer tissue; SEM=standard error of mean.

The 8 CpGs can be classified in two groups: *Group I-CpGs* (cg25973534, cg15409013, cg15048991, cg16508480, cg04136610, cg22954449,) were hypermethylated and located in the promoter region, while *Group II-CpGs* (cg06434454, cg17627328) were hypomethylated and located in the gene body (Figure 23). Additionally, many intermediate methylated CpGs showed an increase in the promoter and a decrease in methylation in the gene body.

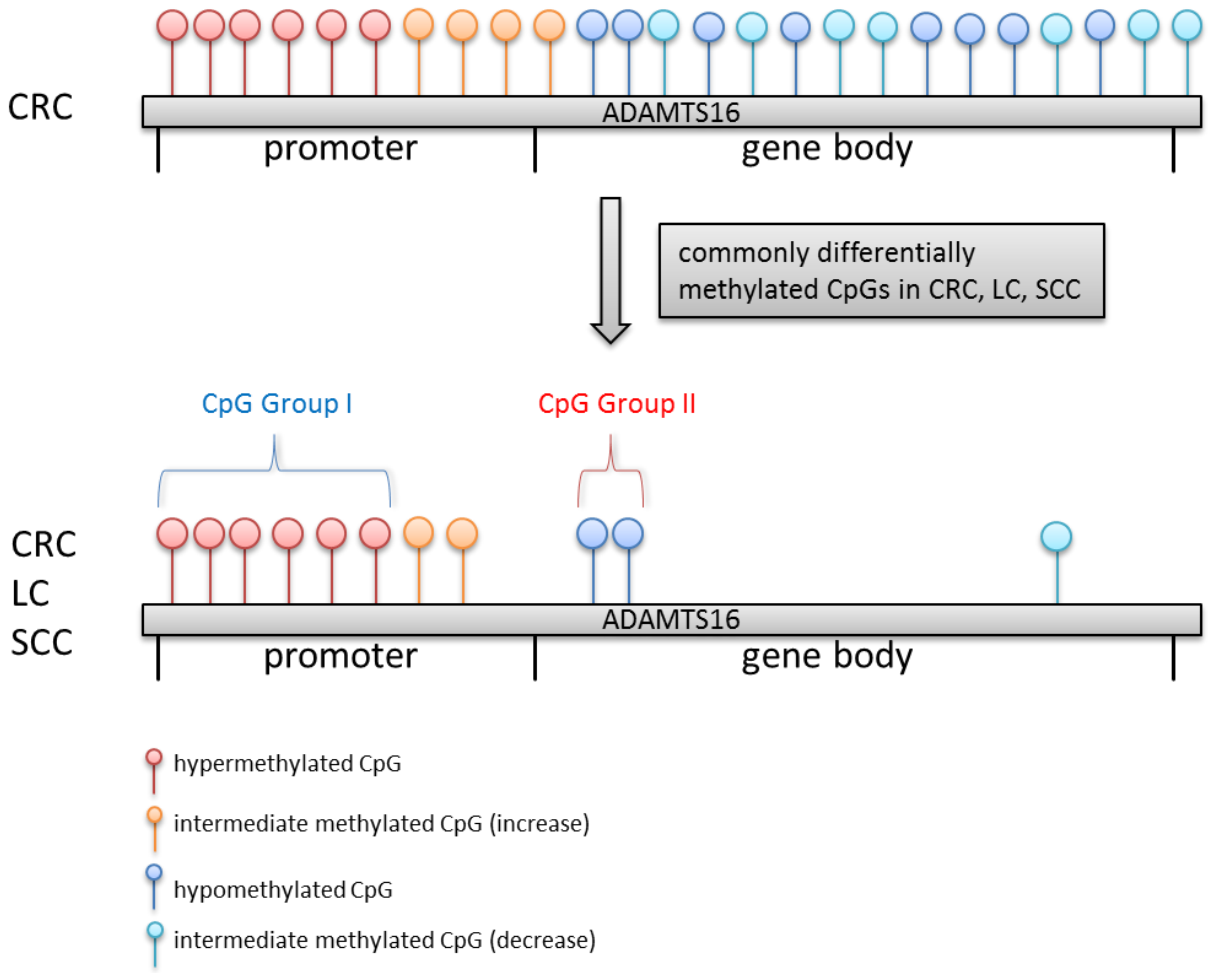

Figure 23. Classification and location of the commonly differentially methylated CpGs between the 3 cancer entities. The 6 CpGs commonly hypermethylated are located in the promoter region and classified as CpG-Group-I, whereas the 2 commonly hypomethylated CpGs are located in the gene body and classified as CpG-Group-II.

3.2.3.4 The *Colon adenocarcinoma & Rectum adenocarcinoma* cohort of *The Cancer Genome Atlas* project shows the same methylation changes in *ADAMTS16*

The Cancer Genome Atlas (TCGA) project is an extensive worldwide, multi-laboratory project to study and characterize genetics and epigenetics of various cancers. Most of the acquired data are freely available for download (https://tcga-data.nci.nih.gov). To validate our finding that 8 CpGs were differentially methylated in colorectal cancer patients, methylation data of *Colon adenocarcinoma & Rectum adenocarcinoma* (*COADREAD*, n=44 (ctrl), n=384 (canc)) from the *TCGA data portal* were downloaded and analyzed for the methylation status of these 8 CpGs (Figure 24 and Figure 25). Indeed, all 8 CpGs showed the same hyper- or hypomethylation. However, the differences in the TCGA COADREAD cohort were generally higher than in our CRC cohort (> 0.2 compared to 0.3).

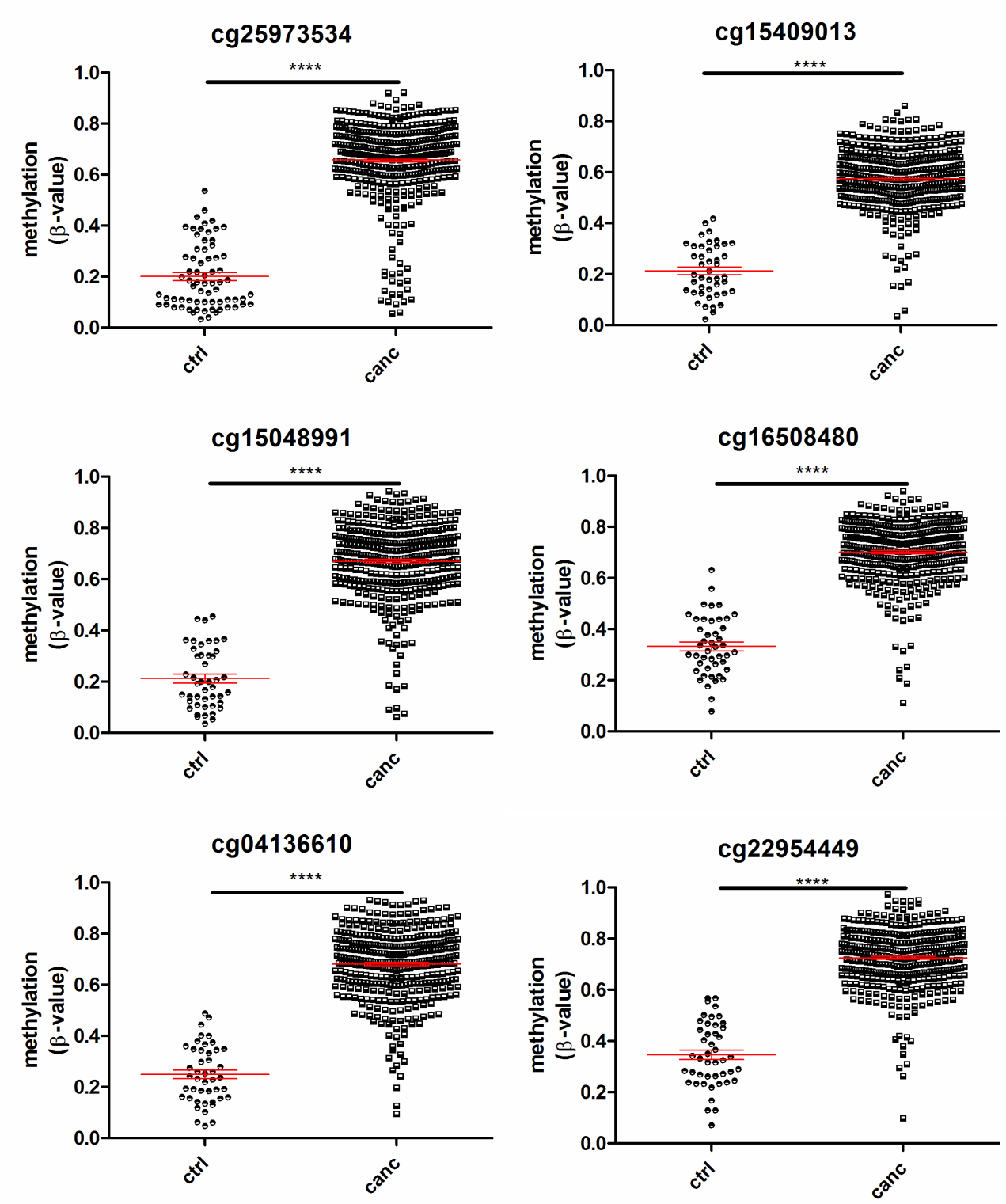

Figure 24. Methylation data from The Cancer Genome Atlas (TCGA) Colon adenocarcinoma & Rectum adenocarcinoma cohort (COADREAD, n=44 (ctrl), n=384 (canc)) show the same methylation changes in the 8 commonly differentially methylated CpGs as colorectal cancer (CRC), lung cancer (LC) and oral squamous-cell carcinoma (SCC). Shown are the 6 in CRC, LC and SCC commonly hypermethylated CpGs for the COADREAD cohort. Data represent the methylation (β-value) for individual patients (spots) with the mean ±SEM (red lines). Data were statistically analyzed with Mann-Whitney-U test and corrected for multiple testing with Benjamini-Hochberg method (**** $P < 0.0001$). ctrl=peri-tumoral non-malignant tissue; canc=cancer tissue; SEM=standard error of mean. The results shown here are based upon data generated by the TCGA Research Network: http://cancergenome.nih.gov/.

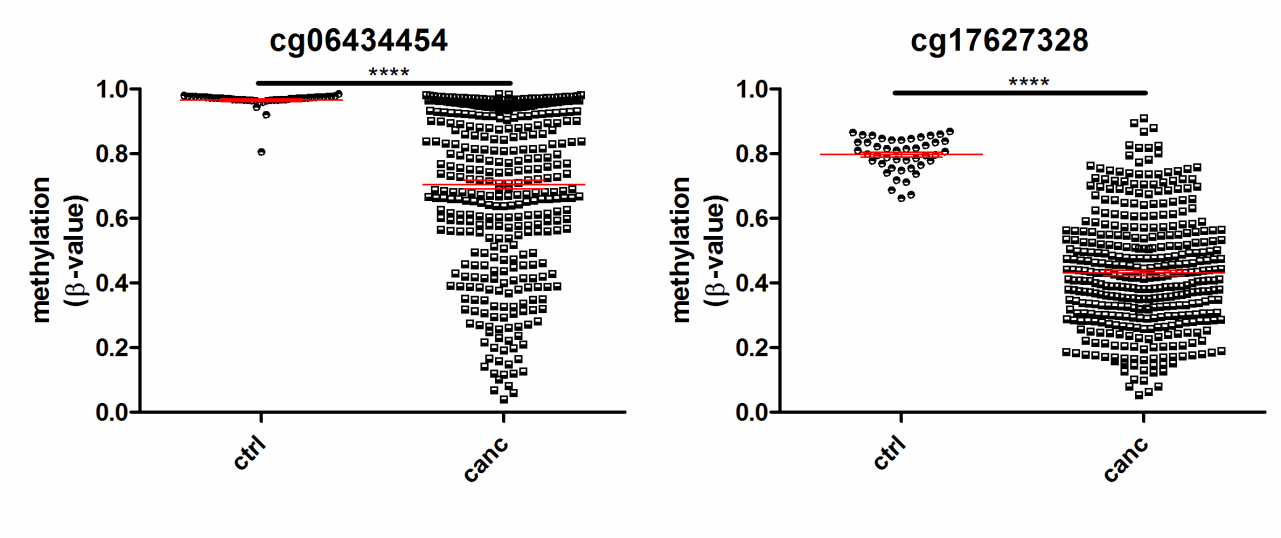

Figure 25. Methylation data from The Cancer Genome Atlas (TCGA) Colon adenocarcinoma & Rectum adenocarcinoma cohort (COADREAD, n=44 (ctrl), n=384 (canc)) show the same methylation changes in the 8 commonly differentially methylated CpGs as colorectal cancer (CRC), lung cancer (LC) and oral squamous-cell carcinoma (SCC). Shown are the 2 in CRC, LC and SCC commonly hypomethylated CpGs for the COADREAD cohort. Data represent the methylation (β-value) for individual patients (spots) with the mean ±SEM (red lines). Data were statistically analyzed with Mann-Whitney-U test and corrected for multiple testing with Benjamini-Hochberg method (**** $P < 0.0001$). ctrl=peri-tumoral non-malignant tissue; canc=cancer tissue; SEM=standard error of mean. The results shown here are based upon data generated by the TCGA Research Network: http://cancergenome.nih.gov/.

3.2.3.5 *ADAMTS16* is silenced in the TCGA COADREAD cohort in cancer

Methylation alterations are one of the major epigenetic modifications to alter and regulate gene expression. To delineate, whether the observed methylation changes could lead to an altered *ADAMTS16* gene expression in the colorectal cancer patients, gene expression data for the same TCGA COADREAD cohort were downloaded from the *TCGA data portal* and analyzed (n=22 (ctrl), n=224 (canc)). The *ADAMTS16* mRNA expression was significantly decreased from 0.29 in the control (ctrl) to 0.04 in the cancer tissue (canc). This decrease reflects a reduction of the *ADAMTS16* mRNA expression of 86.3% and indicates therefore an *ADAMTS16* gene silencing in colorectal cancer patients (Figure 26).

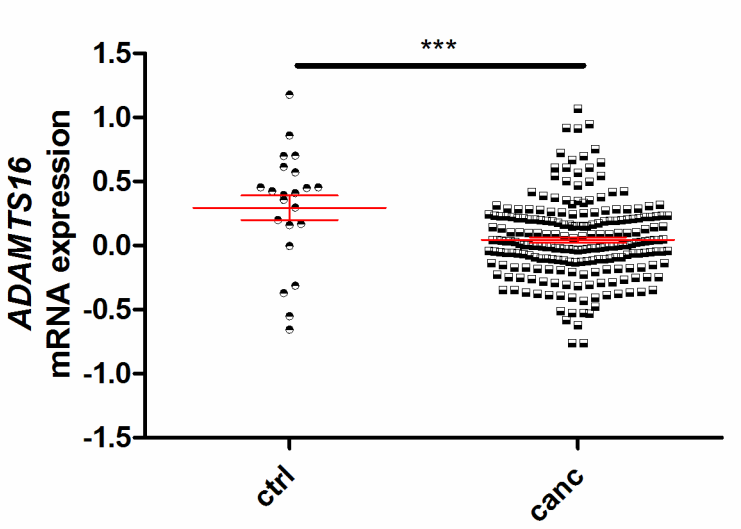

Figure 26. Methylation data of The Cancer Genome Atlas project show that *ADAMTS16* gene expression is lower in Colon adenocarcinoma & Rectum adenocarcinoma compared to control tissue. Analysis of gene expression data from The Cancer Genome Atlas project (TCGA, Colon adenocarcinoma & Rectum adenocarcinoma (COADREAD)) showed a significant reduction of *ADAMTS16* mRNA in cancer tissues. Data represent the relative *ADAMTS16* mRNA expression for individual patients (spots) with the mean ±SEM (red lines). Data were statistically analyzed with Mann-Whitney-U test and corrected for multiple testing with Benjamini-Hochberg method (*** $P < 0.001$, n=22 (ctrl), n=224 (canc)). ctrl=control; canc=cancerous tissue; SEM=standard error of mean. The results shown here are based upon data generated by the TCGA Research Network: http://cancergenome.nih.gov/.

3.2.3.6 The gene expression of matched pairs of tumor and non-tumoral tissue of the CRC patients shows no tendency towards up- or downregulation of *ADAMTS16* in contrast to the TCGA COADREAD cohort

Matched pairs of cancer and control tissue from 35 patients of our CRC cohort were analyzed for *ADAMTS16* mRNA expression by real-time RT-qPCR. As depicted in Figure 27, no clear tendency regarding up or downregulation was found. 14 patients had lower *ADAMTS16* expression in the cancer tissue compared to the control tissue, 8 patients had no change, and 9 patients had a higher *ADAMTS16* expression in the cancer tissue. In contrast to the TCGA COADREAD cohort, relative mRNA expression analyses in our CRC cohort revealed no significant difference in the two tissues (Figure 28).

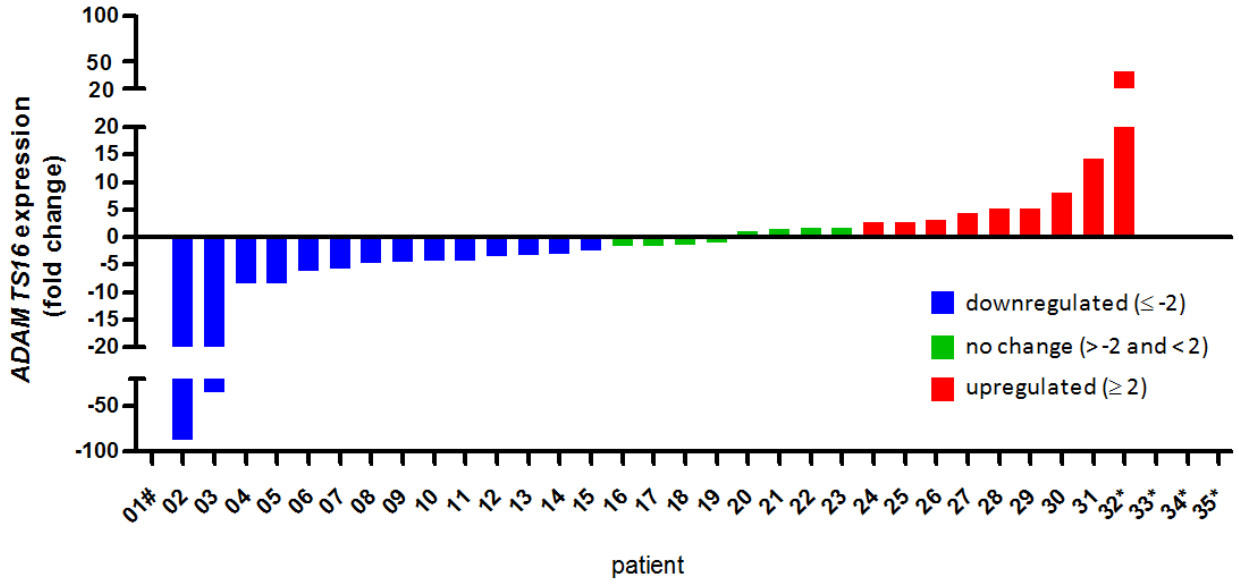

Figure 27. Matched pairs of the studied colorectal cancer cohort show a balanced up- and downregulation of *ADAMTS16* throughout the patients. RNA of the previously analyzed patient samples was isolated and measured for *ADAMTS16* and *HPRT* (house keeping gene) mRNA expression by real-time RT-qPCR. The data were analyzed by $2^{-\Delta\Delta CT}$-method for fold change up- or downregulation. *ADAMTS16* regulation showed no tendency towards up- or downregulation (n=35 patients). #=no *ADAMTS16* detected in tumor; *=no *ADAMTS16* detected in control tissue.

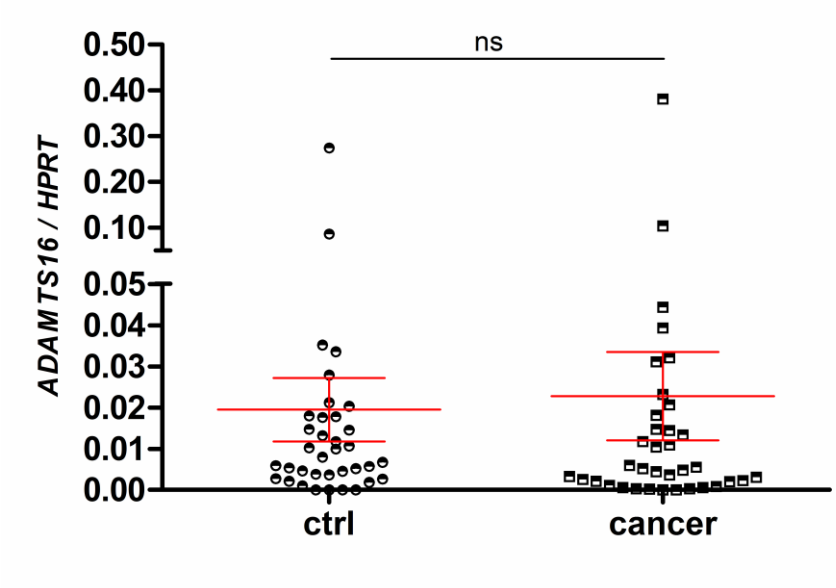

Figure 28. There is no significant difference in gene expression of *ADAMTS16* between the cancer tissue and the peri-tumoral non-malignant tissue in the studied CRC cohort in contrast to the TCGA COADREAD cohort. RNA of the previously analyzed patient samples was isolated and measured for *ADAMTS16* and *HPRT* (housekeeping gene) mRNA expression by real-time RT-qPCR. The data were analyzed by $2^{-\Delta CT}$-method for the relative expression of *ADAMTS16* compared to *HPRT*. There was no significant difference in the relative gene expression of *ADAMTS16* between the control (ctrl) and the tumor tissue in matched pairs. Data represent the relative *ADAMTS16* mRNA expression for individual patients (spots) with the mean ±SEM (red lines). Data were statistically analyzed with paired t-test and Bonferroni multiple comparison post hoc test (* $P < 0.05$, n=35 (ctrl), n=35 (tumor)). ns=non-significant; SEM=standard error of mean.

4 Discussion

4.1 The extracellular juxtamembrane segment CANDIS is able to interact with membranes and this interaction is essential for ADAM17-mediated shedding

In the first part of this thesis, posttranslational regulation of ADAM17-mediated shedding was investigated. The metalloprotease ADAM17 plays a crucial role in various biological processes, since its shedding of a plethora of substrates can alter the responsiveness of cells to their environment and release potent soluble mediators from the cell surface. Interestingly, this process can be rapidly enhanced by various stimuli. Importantly, this fast regulation of the ADAM17 shedding activity seems to be mostly dependent on other regulatory mechanisms than alteration of the biochemical proteolytic activity of ADAM17. Previous research has shown that, *inter alia*, substrate availability, localization and membrane fluidity have major impact on the ADAM17-mediated shedding activity. However, our understanding of how these different factors are tightly regulated, is still very limited.

Recently, we found evidence that the distinctive step in the activation of stimulated ADAM17-mediated shedding might be phosphatidylserine (PS)-exposure. PS is located normally in the inner leaflet of the cell membrane supporting the membrane asymmetry. Strikingly, PS-exposure to the outer leaflet occurs after various physiological and unphysiological stimuli that activate ADAM17-mediated shedding. We identified a polybasic PS-binding motif in the membrane-proximal domain that interacts with the exposed PS after stimulation, and might thereby position ADAM17 in the right orientation for enabling the shedding of its substrates (Sommer et al., 2015, in revision).

Interestingly, another functional sequence in ADAM17, which might contribute to this mechanism, is CANDIS. Previous studies have revealed that the corresponding CANDIS peptide is alpha-helical (Düsterhöft et al., 2014) and that it can bind certain substrates of ADAM17 (Düsterhöft et al., 2014; Lorenzen et al., 2012). We found recently another interesting feature of the CANDIS peptide: It can bind to lipid bilayers (Düsterhöft et al., 2015). We assumed that this lipid binding property might be an important feature of CANDIS and might be of functional relevance for the ADAM17-mediated shedding mechanism. Interestingly, some substitutions in the CANDIS peptide abolished the alpha-helical structure of the CANDIS peptide and destroyed its lipid binding ability as shown by our collaboration partners (AG Grötzinger, Biochemistry Department) by fluorescence and circular dichroism spectroscopy. However, whether these *in vitro* findings would have functional consequences for the ADAM17-mediated substrate release in cells, remained unclear.

Therefore, I generated similar mutations in the full-length ADAM17 and tested the shedding activity of these different mutants in a cell based system.

4.1.1 An intact hydrophobic side of CANDIS is essential for ADAM17 shedding activity

Modeling of the CANDIS sequence revealed that this alpha helix has amphipathic character and the hydrophobic face consists of the following residues: FLVLFVII. In experiments conducted in this thesis, this hydrophobic face was altered by the substitution of the two hydrophobic phenylalanine residues with two charged glutamic acid residues in the full-length ADAM17 (EE mutations). As a consequence, the introduced negatively charged amino acids destroyed the hydrophobic face. Remarkably, these mutations completely abolished the constitutive and the PMA- and ionomycin-stimulated TGF-α shedding activity of ADAM17.

In principle, protein mutations in ADAM17 could lead to impaired protein trafficking and could hinder ADAM17 to reach the cell surface, where it sheds TGF-α. However, flow cytometric analyses supported that the EE mutations did not interfere with the transport of ADAM17 to the cell surface and the ADAM17 EE mutant is similarly expressed on the cell surface as the wildtype. However, it should be noted that the transfection efficiency in MEFs is very low. Moreover, only a small amount of transfected ADAM17 is expressed on the cell surface making flow cytometric analyses difficult with the currently available antibodies. Nonetheless, further evidence that ADAM17 EE mutant is expressed on the cell surface derives from the findings that ADAM17 EE was able to cleave soluble peptide substrate in similar amounts as the wildtype protease. Most importantly, these data show that the biochemical proteolytic activity of ADAM17 is not affected by these mutations in contrast to the shedding activity.

Mutations of the hydrophilic side of CANDIS did not show any effect on the ADAM17-mediated TGF-α shedding activity. Based on these data, the intact hydrophobic face of ADAM17 is essential for the ADAM17-mediated TGF-α shedding activity.

4.1.2 The ADAM17 EE mutations may abolish the ADAM17-mediated shedding by preventing interaction of CANDIS with the plasma membrane

Membrane and protein interactions are often mediated by alpha-helical protein structures (Drin and Antonny, 2010; Elazar et al., 2004; Gerlach et al., 2010). CANDIS is an alpha-helical peptide and it was shown that it can interact with lipid bilayers. Therefore, it is logical to assume that

CANDIS can potentially also interact with cellular membranes. Mutations in the hydrophobic face of the CANDIS peptide, including the EE mutations, destroyed the alpha-helical structure and this was accompanied with the loss of the ability to interact with lipid bilayers (Düsterhöft et al., 2015). Remarkably, the same mutations in the full-length molecule abolished the ADAM17-mediated shedding activity completely. By contrast, mutations in the hydrophilic face of CANDIS had no effect on lipid binding nor on the shedding activity. Based on these data it is reasonable to assume that the loss of the lipid binding ability is responsible for the abolished ADAM17-mediated shedding activity. Accordingly, an interaction between CANDIS and the cell membrane may be an essential prerequisite in the shedding mechanism. This conclusion is further substantiated by reports that show an involvement of the cell membrane in ADAM17 regulation. The cholesterol content of the plasma membrane affects ADAM17-mediated shedding, since cholesterol depletion of cells leads to enhanced ADAM17 shedding activity of the IL-6R (Matthews et al., 2003). In line with this, the CANDIS interaction with lipid bilayers is inhibited by an increase in cholesterol content in lipid bilayers (Düsterhöft et al., 2015), indicating that the CANDIS membrane interaction could potentially contribute to this phenomenon. Additionally, it has also been reported that changes in the membrane fluidity modulate ADAM17 shedding activity (Reiss et al., 2011). It is reasonable to speculate, that different membrane fluidities would influence the CANDIS membrane interaction, since increase of cholesterol enhances membrane rigidity.

4.1.3 Other potential effects of the mutations in the hydrophobic face of CANDIS

Another important property of CANDIS, besides the lipid binding ability, needs to be considered when drawing conclusions from the experimental data in this thesis. CANDIS has been shown to bind certain ADAM17 substrates, such as IL-6R and IL-1RII, but not others such as TNF-α (Düsterhöft et al., 2014; Lorenzen et al., 2012). Whether CANDIS can actually bind TGF-α or not, has not been reported, although it might be the case. Therefore, the TGF-α shedding could be abolished due to an impairment of a potential binding of CANDIS to TGF-α and not due to impairment of its ability to interact with the membrane. However, this possibility is strongly challenged by the observation that the EE mutations also abolished the shedding of TNF-α, although TNF-α cannot bind to CANDIS (Düsterhöft et al., 2015).

Based on the findings, it cannot be completely ruled out that the observed abrogation of ADAM17-mediated shedding and the destruction of the alpha-helical structure of CANDIS is rather a

correlation than causation. Alternative explanations could be that the introduced mutations could affect the interaction of ADAM17 with other molecules, for instance *inactive Rhomboids (iRhoms)*. IRhoms have recently been reported to interact with ADAM17 and to regulate its maturation and substrate selectivity (Christova et al., 2013; Issuree et al., 2013; Li et al., 2015; McIlwain et al., 2012). However, specific interactions between CANDIS and proteins other than some ADAM17 substrates have not been reported so far. Additionally, the region comprised of the MPD and CANDIS have been also suggested to mediate multimerization of ADAM17 (Lorenzen et al., 2011). Although the relevance of multimerization of ADAM17 has not been clarified, the introduced EE mutations may interfere with this process.

4.1.4 The function of the CANDIS sequence can be partially substituted by the corresponding region of ADAM10

An interesting conclusion can be drawn from the experiments using the ADAM17p10 chimera. In this chimera the CANDIS region of ADAM17 was exchanged with the corresponding segment of ADAM10. This segment is neither structurally nor sequentially similar to the CANDIS sequence of ADAM17. Notably, the TGF-α shedding was clearly impaired but not completely abolished. From this observation one could hypothesize that the ADAM10 sequence harbors a functional substitute for the absent alpha-helical CANDIS. The peptide of the ADAM10 segment shows slight alpha-helical tendencies (Düsterhöft et al., 2015), but presumably not enough to explain the partial rescue. However, it contains a polybasic motif (RLKK), similar to the polybasic motif in the MPD (RKGK). In the MPD, the motif is responsible for interactions with PS. Therefore, it is plausible to state that the similar motif in the ADAM10 segment could substitute the normally alpha-helical interaction between the membrane and CANDIS, with an interaction between the polybasic motif and the PS.

4.1.5 ADAM17 requires distinct membrane interactions for its shedding activity: anchorage via its transmembrane domain, attraction via a polybasic motif in the MPD towards PS, and a hydrophobic interaction between the alpha-helical CANDIS and the membrane

ADAM17-mediated shedding depends on the anchorage of ADAM17 to the cell membrane via a transmembrane domain. Importantly, this transmembrane domain cannot be substituted with a simple membrane anchor, since a GPI-anchored ADAM17 is not able to shed TGF-α, TNF-α and L-selectin anymore (Li et al., 2007).

The anchorage of ADAM17 is not the only essential membrane interaction. Just recently, we made important progress to decipher the enigmatic molecular mechanism how diverse stimuli enhance ADAM17-mediated shedding. Functional analyses of another interesting ADAM17 mutant (ADAM17 3x) helped proposing a new model of how these diverse stimuli could mechanistically lead to an enhancement of ADAM17-mediated shedding. In this mutant, a polybasic motif in the MPD, upstream from the CANDIS sequence, was mutated to a non-charged motif. Importantly, these mutations had the same consequences for the ADAM17 shedding activity as the EE mutations in the CANDIS region: The constitutive and PMA- and ionomycin stimulated shedding was completely abolished (Supplemental Figure 1). On the basis of this evidence, we showed in further experiments (Sommer et al., 2015, in revision) that the polybasic motif in the MPD is a phosphatidylserine interaction sequence that can bind to PS. Phosphatidylserine is under normal conditions not exposed to the extracellular side, but remains intracellular and supports the asymmetry of the membrane. Strikingly, several ADAM17 stimuli induce a phosphatidylserine flip from the inner to the outer membrane layer. These results have provided evidence that the exposed negative phosphatidylserine attracts the polybasic motif and orientates ADAM17 in the proper position inducing the shedding event.

Notably, each of the mutations — the mutations in the hydrophobic face of CANDIS and the destruction of the polybasic motif in the MPD — are sufficient to completely abolish ADAM17 substrate shedding. This observation implies that two membrane interactions, in two distinct regions — one in the CANDIS and one in the MPD — are involved and required for the shedding mechanism. A plausible mechanistic model could be a two-step process in the activation of ADAM17: The MPD is attracted electrostatically to the negatively charged exposed phosphatidylserine and thereby pulled towards the membrane. This could orientate the CANDIS sequence in an advantageous position that facilitates the interaction of the hydrophobic CANDIS face with the membrane, further stabilizing its helical content and intensifying the membrane

interaction. In a synergistic way, this could ultimately orient ADAM17 in the proper position enabling substrate shedding (Figure 29).

Proteins which interact with membranes through amphipathic helices have been widely reported (Drin and Antonny, 2010; Elazar et al., 2004; Gerlach et al., 2010). Newer reports have additionally shown that in some proteins polybasic motifs interact with membranes and these interactions can have regulatory functions (Murray et al., 1997; Segrest et al., 1992; Xu et al., 2008). One of these studies is particularly interesting, since it has demonstrated that the *Negative Regulatory Factor (Nef)* uses both types of motifs, a polybasic and an alpha-helical motif, in a consecutive way to interact and associate to membranes (Gerlach et al., 2010). The proposed ADAM17-activation model has similarities with the kinetic binding model of Nef. In case of Nef, the cytosolic Nef is attracted to the membrane by electrostatic interactions between a polybasic motif and the acidic lipids in the membrane. Then hydrophobic residues and myristate insert into the lipid bilayer and the binding is concluded by the formation of an N-terminal amphipathic helix stabilizing the interaction. It should be noted that the purpose of the described mechanism in case of Nef differs from that in case of ADAM17. Nef is associated and then anchored to the membrane via this mechanism. ADAM17, by contrast, is already anchored via its transmembrane domain, but potentially positioned correctly for the shedding of substrates by this mechanism. Taken together, three membrane interactions in concert are needed for proper ADAM17 shedding activity: The transmembrane domain, the polybasic motif in the MPD and the alpha-helical CANDIS.

The research carried out in this thesis helped to further delineate a novel model of ADAM17 activation. Nevertheless, this model still provides a limited understanding of ADAM17-mediated shedding and its regulation. Many aspects are not understood yet and need to be further investigated. For instance, we cannot explain how the constitutive shedding activity of ADAM17 might fit into this model. Furthermore, we are still missing a complete picture how all these different aspects of ADAM17-mediating shedding, such as membrane interactions, localization, substrate accessibility and substrate selectivity come together and provide a complex system of regulatory mechanisms. Additionally, the levels of regulation may vary for each substrate. For instance, it is not known, whether other substrates than TGF-α and TNF-α are also depending on the CANDIS membrane interaction. This could be further clarified by testing other substrates with the ADAM17 EE mutant. Whether the proposed model can be applied to the *in vivo* situation remains to be investigated. An important next step would be the generation of transgenic mice

that carry the above described mutations in the CANDIS region and the MPD. The resulting phenotypes might give further important insights into ADAM17-mediated shedding under physiological conditions.

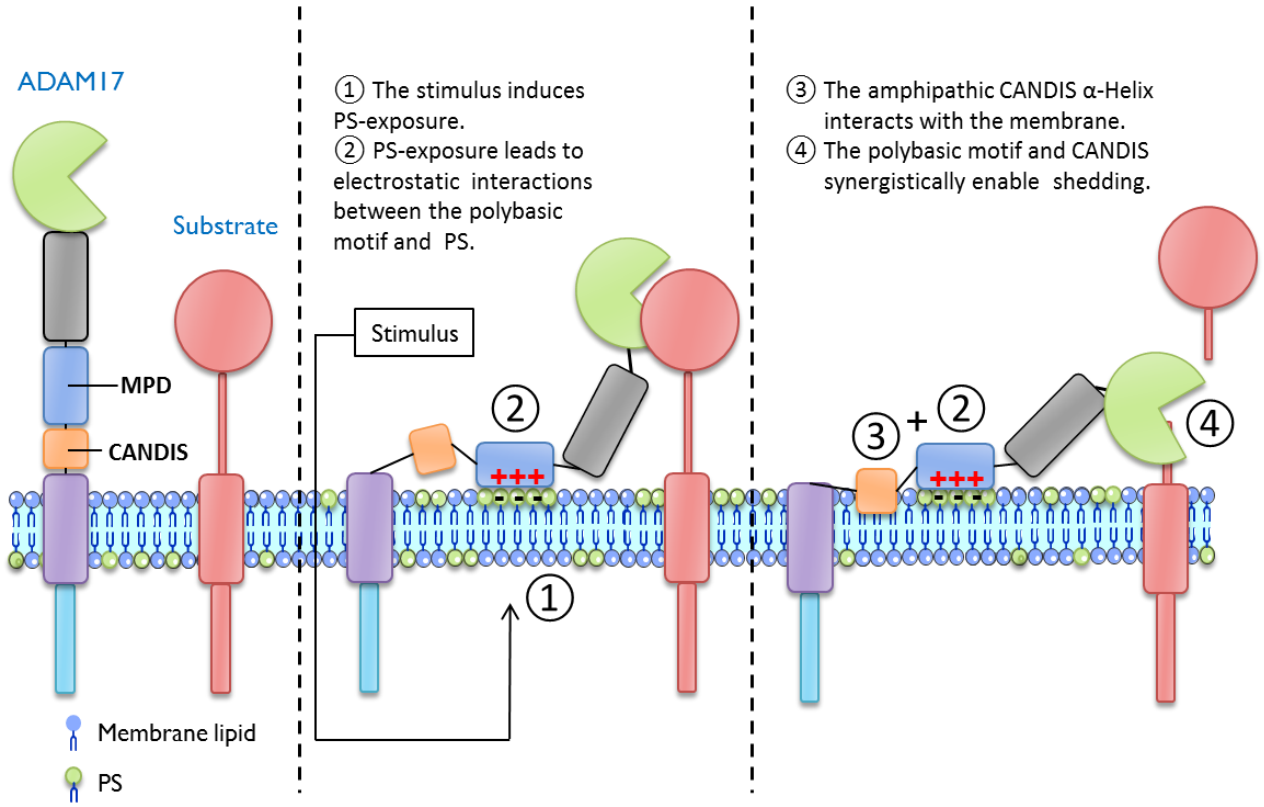

Figure 29. Refined model of ADAM17-mediated shedding. Activation of ADAM17-mediated shedding follows a two-step membrane interaction. Various stimuli lead to a transient exposure of phosphatidylserine (PS) to the extracellular side of the membrane. The polybasic motif in the membrane-proximal domain (MPD) of ADAM17 interacts with the exposed, negatively charged PS, thereby pulling ADAM17 towards the membrane. Subsequently, the amphipathic alpha-helical CANDIS interacts with the membrane. Together, both interactions orientate ADAM17 in the proper position towards its substrate, thereby enabling shedding. Model according to (Sommer et al., 2015, in revision).

4.2 Epigenetic methylation changes of ADAM/TS genes in disease

In the second part of this thesis, tissues from patients suffering from preinflammatory, inflammatory, precancerous and cancerous diseases were investigated for methylation alterations in ADAM/TS genes. Most strikingly, major epigenetic changes were identified in one of the ADAMTS members, *ADAMTS16*, in colorectal cancers and two other cancer entities. In these cancers, hypermethylation in the promoter region of *ADAMTS16* and hypomethylation in the gene body compared to the peri-tumoral non-malignant tissue was observed, suggesting that the *ADAMTS16* gene is silenced in these cancers. Surprisingly, no methylation alterations in *ADAM10* and *ADAM17* were observed in inflammatory or cancerous diseases.

4.2.1 Epigenetic methylation changes do not occur in ADAM/TS genes in the preinflammatory *Non-alcoholic fatty liver disease (NAFLD)* and the inflammatory *Non-alcoholic Steatohepatitis (NASH)*

Neither in patients suffering from NAFLD, nor NASH, any differentially methylated CpGs in ADAM or ADAMTS genes were observed. The general term NAFLD comprises a range of liver conditions: the mildest, hepatic steatosis or fatty liver, the more severe form, NASH and the severest condition, liver cirrhosis. It should be noted that NAFLD is used in the literature as a collective name for all three conditions as well as only for the hepatic steatosis in distinction to the other two conditions. In this thesis, it will be used to refer to hepatic steatosis in distinction to NASH. Moreover, the distinction between these conditions was many times redefined over the years and is found inconsistently used in the literature (Okazaki et al., 2014). Since NAFLD is mostly characterized by pathological retention of lipids in hepatocytes without inflammation and fibrotic processes, major epigenetic changes in ADAMs and ADAMTS which are involved in these processes, were not expected. NAFLD is a preinflammatory condition, since it can evolve to the more severe form, NASH. The latter is characterized by inflammatory processes and remodeling of the extracellular matrix accompanied by fibrotic processes (Farrell et al., 2012). TNF-α plays a pivotal role in inflammation and matrix metalloproteases are the major players in remodeling the extracellular matrix, therefore they are intensively studied and discussed for the pathogenesis of NASH (Farrell et al., 2012; Okazaki et al., 2014). Surprisingly, also in NASH, ADAM and ADAMTS genes did not show any methylation alterations, although they are key regulators of these processes. This result indicates that epigenetic regulation of ADAM/TS genes by DNA methylation

does not play a major role in these diseases. Interestingly, diabetes mellitus is a major risk factor for the development of NAFLD and particularly for the progression from NAFLD to the severe form, NASH. Advanced glycation endproducts accumulate in patients with diabetes and are suggested as the link between diabetes and progression to NASH by activating ADAM17 posttranslationally. ADAM17 is then thought to mediate the inflammatory processes in the progression to NASH (Jiang et al., 2013). This report of posttranslational ADAM17 regulation together with the lack of methylation changes indicates that posttranslational regulation rather than epigenetic regulation of ADAM17 may play a role in NASH.

Moreover, it has been reported that overexpression of ADAM17 in mice is neither leading to increased TNF-α shedding nor an elevated inflammatory response (Yoda et al., 2013). Based on these data and the fact that no epigenetic changes for ADAM17 were found in all investigated diseases, it seems reasonable to assume that epigenetic regulation of ADAM17 is not of major importance for its functions in inflammatory diseases.

4.2.2 Methylation changes in the *ADAMTS16* gene are prominent in the investigated cancerous diseases

In contrast to NASH and NAFLD, in the inflammatory disease *oral lichen planus*, a few genes showed differentially methylated CpGs. In theory, even one or two differentially methylated CpGs per gene could alter the transcription activity of these genes, but it is hard to make any assumption without gene expression profiling. Nevertheless, seeing more differentially methylated CpGs in an inflammatory disease which is regarded as a precancerous condition, suggests that more methylation changes in these genes could occur in cancerous diseases rather than solely inflammatory diseases. Indeed, 72 CpGs were differentially methylated in colorectal cancer tissues compared to the non-malignant adjacent tissue. The most numerous and interesting methylation alterations were observed in the *ADAMTS16* gene.

4.2.3 Characteristic methylation changes in the *ADAMTS16* gene region were found in three different cancer entities

The methylation profile of *ADAMTS16* was extensively altered and showed hypermethylated CpGs in the promoter region and hypomethylated CpGs in the gene body. Additionally, many intermediate methylated CpGs were observed whose methylation changes were also directed

towards hypermethylation in the promoter and hypomethylation in the gene body. This methylation profile clearly implicates an epigenetic downregulation of this gene in tumor tissue. It is widely reported that promoter methylation and gene body demethylation correlates with reduction of transcription. A very profound demonstration of this correlation was reported recently. The mean methylation profile of all actively transcribed genes in a DAUDI cell line showed a reduced methylation status in the promoter region and exon 1 region, and an enhanced methylation status in the gene body compared to the not transcribed genes (Kreck et al., 2013). Similarly, the methylation profile of *ADAMTS16* in the cancer tissue corresponds to the methylation profile of an inactive gene, and the profile in normal tissue of an active gene. Moreover, a genome-wide methylation study reported that the correlation between methylation in the first exon is even more tightly linked to transcriptional silencing than the methylation in the upstream promoter region (Brenet et al., 2011). In line with that, the CpG covered by the methylation chip shows intermediate methylation in the exon 1 towards hypermethylation in the investigated CRC, also supporting a silencing of *ADAMTS16*. Strikingly, two other epithelial cancers showed similar overall methylation profile changes and 8 CpGs commonly showed the exact same behavior in regard to hyper- or hypomethylation. This suggests a general epigenetic alteration in epithelial cancers for *ADAMTS16*, but comparative studies for other epithelial and non-epithelial cancers are needed to evaluate this theory. Methylation measurements in an independent colorectal cancer cohort which was conducted by another lab in the frame of the TCGA project further confirm that the methylation alteration in these 8 CpGs are a general event in colorectal cancers.

4.2.4 *ADAMTS16* is transcriptionally silenced in the TCGA COADREAD cohort, but not in the studied CRC cohort, potentially due to discrepancies in transcript variant detection

Gene expression data generated by the *TCGA consortium* show that *ADAMTS16* is indeed silenced in colorectal tumors. This further supports the hypothesis that the observed methylation changes could effectively lead to the silencing of *ADAMTS16* in these tumors. Contradictory to the observed silencing of *ADAMTS16* in the TCGA cohort, there was no reduction in the average *ADAMTS16* gene expression in the investigated CRC cohort that was reported in this thesis and no trend in the gene regulation in matched pairs of this cohort. One possible explanation could be that the different methods used for detecting *ADAMTS16* mRNA levels detect different transcript variants. Currently, there are 4 transcript variants listed in the *ensemble genome browser*

database encoding for 3 different ADAMTS-16 protein isoforms. This complicates the investigation of *ADAMTS16* expression levels, especially that functional differences between the 3 isoforms have not been reported. The TCGA expression was measured with the *Agilent 244K Custom Gene Expression G4502A-07-3* platform which detects 3 transcript variants (ENST00000388896, ENST00000388898, ENST00000274181) of *ADAMTS16*. Unfortunately, 2 of the 3 transcripts that this platform detects are now marked as *retired,* which means that they are obsolete due to a dramatic change in the used gene or transcript model in the *ensemble database*. Attempts to match them to transcript IDs, which are marked as *current*, were unsuccessful and could not clarify if they are the same as for the qPCR measurements. Clearly, both systems commonly detect the canonical transcript variant (ENST00000274181). Additionally, the qPCR system also detects a second transcript variant, but not all known variants due to limitation in primer design. In conclusion, it cannot be excluded that differences in both gene expression analyses differ due to detection of different transcript variants and that the qPCR system may have missed to detect a transcript variant of importance.

Moreover, the epigenetic methylation changes could also affect the expression of these different transcript variants in different ways, influencing for instance only the expression of one transcription variant leaving the others unchanged. A similar effect was reported where site-specific methylation changes regulated the expression of different transcripts in a different way (Salami et al., 2015). Additionally, exon methylation can effect alternative splicing (Maunakea et al., 2013). To delineate whether the methylation changes could have this effect on the *ADAMTS16* transcripts, transcript specific primers for each different transcript could be designed and used to detect transcript-specific expression changes in the colorectal cancer samples. Taken together, the TCGA gene expression data and the methylation profiling implicate a silencing of *ADAMTS16* in colorectal cancer. However, no conclusive statement can be made whether *ADAMTS16* is silenced or not, due to the lack of a silencing effect on gene expression in the studied CRC cohort. There is compelling reason to assume that the absent silencing effect in the studied CRC cohort in contrast to the TCGA cohort is based on the potential detection of different transcript variants and that therefore a silencing of *ADAMTS16* in CRC takes place. Nevertheless, the discrepancy could also be due to fact that in the CRC cohort, control and cancer tissues are matched pairs from the same patient, whereas the COADREAD cohort contains non-matched control and cancer samples.

To further clarify the impact of the observed *ADAMTS16* methylation changes, most important are analyses of the resulting protein levels. Unfortunately, the limited time frame of this thesis did not

allow such analyses. However, further studies are planned to address this question. Particularly, western blot analyses and immunohistochemistry of cryosections of matched samples from the CRC cohort will provide deeper insights into the ADAMTS-16 regulation.

4.2.5 ADAMTS-16 is a potential tumor suppressor

Epigenetic silencing of genes is a common feature in human cancers (Jones and Baylin, 2007). Although epigenetic changes also affect genes which are probably not involved in promoting cancerous development, many genes affected are critical in cancer development (Esteller, 2007; Toyota and Issa, 2005). Epigenetic silencing of genes is involved in critical pathways of cancer development, such as DNA repair genes, apoptosis mediators, cell adhesion molecules and many other genes. Strikingly, often the epigenetic silencing of genes by promoter hypermethylation has the same effect as genetic mutations in these genes: Retinoblastoma protein, the first discovered tumor suppressor protein, can be inactivated either through genetic mutations or promoter methylation, thus causing cancer (Sakai et al., 1991). Based on the observed methylation changes in *ADAMTS16*, one could speculate that *ADAMTS16* expression may also be unbeneficial for tumor development or could even be a tumor suppressor gene which is therefore silenced by promoter hypermethylation. Supporting this hypothesis, ADAMTS-18, the closest relative of ADAMTS-16 (with overall identity of 57%, (Porter et al., 2005)) is discussed as an tumor suppressor gene, since it is generally silenced in various cancers by promoter hypermethylation (Xu et al., 2015). Furthermore, functional analysis revealed that overexpression of ADAMTS-18 has an inhibitory effect on anchorage-dependent and -independent cell growth, further supporting a function as tumor suppressor protein (Jin et al., 2007). Interestingly, the only reported involvement of ADAMTS-16 in cancer is the aberrant expression in esophageal squamous-cell carcinoma. ADAMTS-16 has been shown to be overexpressed in this cancer and siRNA-mediated knock-down of *ADAMTS16* inhibited invasiveness and proliferation in esophageal cancer cell lines. Unfortunately, methylation changes were not investigated in this study. The reported overexpression and tumor promoting functions of ADAMTS-16 in esophageal squamous-cell carcinoma seem to be in conflict to the proposed role of *ADAMTS16* as a tumor suppressor gene in epithelial cancers. But this does not necessary need to be a contradiction: *ADAMTS16* has been reported to show genetic mutations in 90% of esophageal squamous-cell carcinoma patients (*International Cancer Genome Consortium data portal*, https://dcc.icgc.org/). This is very high. In comparison only 15% of the patients suffering from lung cancer and 10% of the patients suffering

from colorectal cancers have mutations in *ADAMTS16*. The mutations in esophageal squamous-cell carcinoma, in contrast to the other cancers, could alter the functions of ADAMTS-16 to be tumor promoting instead of their normal anti-tumorigenic function. While not being investigated, the probability that the esophageal carcinoma cell lines have these mutated *ADAMTS16* too, is high and could thus explain the inhibited cell proliferation after siRNA knock-down. This theory is further supported by a report that have shown that overexpression of wildtype ADAMTS-16 is anti-proliferative in a chondrosarcoma cell line (Surridge et al., 2009). Nevertheless, despite these major epigenetic changes found in *ADAMTS16* gene, only further functional studies, such as siRNA and overexpression experiments in colorectal cancer cell lines, will clarify and narrow down the biological importance and the functions of ADAMTS-16 in malignancy.

4.2.6 *ADAMTS16* as a potential epigenetic biomarker

Strikingly, the observed methylation changes in the *ADAMTS16* gene were found in three different cancer entities, namely colorectal cancer, oral squamous-cell carcinoma and lung cancer, and were additionally validated in an independent colorectal cancer TCGA cohort. Besides the potential functional relevance of these methylation alterations, they pose a possible diagnostic biomarker. Additionally, if functionally relevant for the pathology or the treatment strategy, it could be also a possible predictive biomarker (treatment) or prognostic biomarker (disease course). Epigenetic biomarker such as promoter hypermethylation promise great benefits in early prediction, diagnosis of disease and prediction of therapeutic success towards personalized medicine. The obstacles until a potential biomarker becomes a proven clinical biomarker are similarly high and complex as for any other clinical trial (Mikeska et al., 2012). Major requirements are high reproducibility, validation with a different methodology, high specificity and sensitivity, and better or different clinical value then the current gold standard. So far, considerable progress was made in the advance of DNA methylation as epigenetic biomarkers, but most potential biomarkers have not yet made it to the clinical bedside. The first proposed biomarker *O^6-methylguanine-DNA methyltransferase (MGMT)* which predicts response to chemotherapeutic treatment (Mineura et al., 1996) took a long way with many challenges until finally validated and accepted (Wick et al., 2014), and feasible diagnostic methods reached the clinics. Many other candidate biomarkers are still in one of the many development stages before becoming a proven clinical biomarker. In case of *ADAMTS16*, the three investigated cohorts showed strong methylation alterations in specific CpG sites in the averaged methylation levels of cancerous tissue in the whole cohort. In contrast,

single patient analyses showed that some patients did not show these changes in the same amplitude as the overall cohort or not even at all (data not shown). Therefore, the potential of *ADAMTS16* as a novel biomarker needs to be further investigated for the overall specificity and sensitivity, also in different populations, and needs additionally to be validated by an alternative method such as pyrosequencing.

4.2.7 Limitations of methylation analyses in tissue samples due to cell heterogeneity

One limitation of conducting comparative DNA methylation analyses between the tissue of interest and the control tissue is that they typically differ in cell composition. Therefore, measurement of all the cell types in those tissue samples can lead to discovery of methylation differences that reflect differences in cell type composition rather than differences in methylation changes in the cell type of interest. This is in principle also true for the methylation analyses conducted in this thesis. For instance, tumor tissue is often infiltrated by immune cells which can have a different methylation pattern than the tissue-specific cells. The observed methylation changes could be therefore biased by the differences in heterogeneity of the compared tissues. Solutions to this problem such as accurately obtaining the cell composition of each sample and correcting the observed methylation pattern for heterogeneity are complex and often not feasible for every single sample. To circumvent this bottleneck, more alternatives such as high-throughput singe-cell DNA methylation analyses (Kantlehner et al., 2011) or statistical approaches without knowledge of cell composition (Zou et al., 2014) are developed. Nevertheless, the bias introduced in the methylation analyses conducted in this thesis, should not be overestimated. Prior to the methylation analyses, the lung cancer samples were further enriched in their tumor cell content by micro-dissection, and showed just the same methylation alterations as the other cancer entities.

Taken together, the profound methylation changes in the *ADAMTS16* gene in three different cancer entities demand the functional investigation of ADAMTS-16 in the context of cancerous diseases, hopefully also narrowing down its functions in normal cellular processes.

5 Summary

Zinc-dependent metalloproteases are important in many physiological processes such as releasing signaling molecules, inactivating receptors and degrading adhesion molecules. Two major families of these metalloproteases are the *(A) Disintegrin And Metalloproteases (ADAMs)* and the *ADAMs with Thrombospondin motif (ADAMTSs)*. Both families are strongly related with a similar domain structure, but distinct functions. While the ADAM family comprises mostly transmembrane proteases with very important functions as sheddases, the ADAMTSs lack the transmembrane domain and are therefore secreted proteases with major functions in the remodeling of the extracellular matrix.

ADAM17 is the best characterized member of the ADAM family. However, how the ADAM17-mediated substrate release is regulated is not understood so far. Recently, we found evidence that phosphatidylserine (PS)-exposure might be the distinctive step in the stimulated ADAM17-mediated shedding. While PS is normally located in the inner membrane leaflet, it is transiently exposed upon stimulation with diverse stimuli. A PS-binding motif in the membrane-proximal domain of ADAM17 has been identified that binds to the exposed PS, enabling substrate shedding. Interestingly, another potential extracellular membrane interaction motif has been described and named *Conserved ADAM seventeeN Dynamic Interaction Sequence (CANDIS)*. This sequence resembles an amphipathic alpha helix which has been shown to bind to lipid bilayers. This lipid binding property suggests a second putative membrane interaction between ADAM17 and the plasma membrane. One aim of this thesis was to evaluate whether the lipid binding ability of the CANDIS region contributes to the ADAM17 shedding activity. Strikingly, mutations in the hydrophobic site, that destroyed the hydrophobic face of the helix, completely abolished ADAM17-mediated shedding of *transforming growth factor alpha (TGF-α)*. By contrast, mutations in the hydrophilic site of CANDIS had no impact on TGF-α shedding. The abolishment of TGF-α shedding correlated with the loss of the lipid binding ability. Therefore, the hydrophobic site of the CANDIS region is essential for ADAM17-mediated shedding and may modulate the shedding mechanism by interacting with the plasma membrane.

In the second part of this thesis, epigenetic regulation mechanisms of ADAM/TS proteases were investigated. Interestingly, epigenetic methylation patterns of neither *ADAM10* nor *ADAM17* were altered in patients suffering from inflammatory or cancerous diseases, although both proteases play a critical role in shedding of inflammatory cytokines and cell adhesion molecules. By contrast,

a member of the related ADAMTS family, *ADAMTS16*, showed major epigenetic changes in cancers. Several CpGs in the *ADAMTS16* gene locus of colorectal cancer (CRC) patients showed altered methylation compared to the control. Furthermore, the same methylation changes were observed in two other cancer entities, namely oral squamous-cell carcinoma and lung cancer. Many CpGs in the promoter region were hypermethylated in the cancer tissue compared to the peri-tumoral non-malignant tissue and hypomethylated in the gene body. These methylation alterations implicate an epigenetic downregulation of ADAMTS-16 in epithelial cancers. Indeed, analysis of gene expression data of *ADAMTS16* in patients suffering from *Colon adenocarcinomas & Rectum adenocarcinomas (COADREAD)* measured by the *TCGA consortium*, showed a silencing of *ADAMTS16* in these patients. Moreover, analyses of available methylation data of these patients further validated the observed methylation changes in CRC also for the COADREAD cohort. However, qPCR analyses of the expression of *ADAMTS16* in matched pairs in the CRC cohort did not show a clear tendency towards up- or downregulation of *ADAMTS16* and no reduction in the average *ADAMTS16* gene expression. Unfortunately, ADAMTS-16 is one of the least studied ADAMTSs and its functions remain widely enigmatic, since the only known substrate is α2-macroglobulin, a general protease inhibitor. The observed major methylation changes in *ADAMTS16* in cancers indicate an important function of ADAMTS-16 e.g., as a tumor suppressor – yet this function remains to be found. Therefore, functional studies are needed to delineate the role of ADAMTS-16 in cancerous diseases. Besides a potential functional relevance, the epigenetic alterations found here, might represent a novel epigenetic biomarker in epithelial cancers.

6 Zusammenfassung

Zink-abhängige Metalloproteasen spielen in vielen physiologischen Prozessen eine wichtige Rolle, unter anderem durch die Freisetzung von Signalmolekülen, der Inaktivierung von Rezeptoren und der Degradierung von Adhäsionsmolekülen. Zwei Hauptfamilien dieser Metalloproteasen sind die *Disintegrin und Metalloproteasen (ADAMs)* und die *ADAMs mit Thrombospondin-Motiv (ADAMTSs)*. Beide Familien ähneln sich in ihrer Domänenstruktur, haben aber unterschiedliche biologische Funktionen. Während die ADAM-Familie hauptsächlich aus transmembranen Proteasen besteht, welche sehr wichtige Funktionen als sogenannte Sheddasen ausüben, fehlt den ADAMTSs die Transmembrandomäne. Sie sind daher sekretierte Proteasen, die eine Hauptfunktion bei dem Umbau der extrazellulären Matrix einnehmen. Wie die ADAM17-vermittelte Substratfreisetzung reguliert wird, ist bisher kaum verstanden. Vor Kurzem haben wir Hinweise gefunden, dass Phosphatidylserin (PS)-Exposition der entscheidende Schritt in der Aktivierung der stimulierten ADAM17-vermittelten Substratfreisetzung sein könnte. PS ist normalerweise in der inneren Lipiddoppelschicht der Membran lokalisiert, wird aber durch verschiedene Stimuli transient nach außen exponiert. Ein potenzielles PS-Bindungsmotiv in der membranproximalen Domäne von ADAM17 wurde identifiziert, welches das extrazellulär exponierte PS bindet und dadurch Substrat-Shedding ermöglicht.

Interessanterweise wurde ein weiteres potenzielles, extrazelluläres Membraninteraktionsmotiv beschrieben und *Conserved ADAM seventeeN Dynamic Interaction Sequence (CANDIS)* genannt. Es wurde gezeigt, dass diese Sequenz eine amphipathische Alpha-Helix Struktur besitzt und Lipiddoppelschichten binden kann. Diese Lipidbindungseigenschaft weist darauf hin, dass möglicherweise eine zweite Membraninteraktion zwischen ADAM17 und der Plasmamembran von entscheidender Bedeutung für das ADAM17-vermittelte Shedding sein könnte. Ein Ziel dieser Arbeit war es zu untersuchen, ob die Lipidbindungsfähigkeit der CANDIS Region zum ADAM17-vermittelten Substrat-Shedding beiträgt. Interessanterweise führten Mutationen in der hydrophoben Seite der amphipathischen Helix zum vollständigen Erliegen des ADAM17-vermittelten *Transformierender Wachstumsfaktor Alpha (TGF-α)* Sheddings. Mutationen in der hydrophilen Seite hingegen hatten keine Auswirkungen auf das TGF-α Shedding. Der Verlust der Fähigkeit von ADAM17 TGF-α zu prozessieren, korrelierte dabei mit dem Verlust der Fähigkeit von CANDIS, Lipide zu binden. Die hydrophobe Seite der CANDIS Region ist daher wichtig für das ADAM17-vermittelte Shedding und könnte den Sheddingmechanismus durch eine Interaktion mit der Plasmamembran modulieren.

Im zweiten Teil dieser Arbeit wurden epigenetische Regulationsmechanismen von ADAM/TS Proteasen untersucht. Erstaunlicherweise wurden weder in *ADAM10* noch in *ADAM17* veränderte epigenetische Methylierungsmuster bei Patienten mit entzündlichen Erkrankungen oder Krebs gefunden, obwohl beide Proteasen eine kritische Rolle bei der Freisetzung von proinflammatorischen Zytokinen und dem Abbau von Zelladhäsionsmolekülen spielen. Ein Mitglied der verwandten ADAMTS-Familie, *ADAMTS16,* zeigte hingegen weitreichende epigenetische Veränderungen bei Krebserkrankungen. Mehrere CpGs im *ADAMTS16* Genlocus von Patienten mit kolorektalem Karzinom (CRC) zeigten im Vergleich zur Kontrolle eine veränderte Methylierung. Erstaunlicherweise wurden die gleichen Methylierungveränderungen in zwei anderen Tumorarten beobachtet, nämlich im Plattenepithelkarzinom und im Lungenkrebs. Viele CpGs im Promotorbereich von *ADAMTS16* waren im Tumor, im Vergleich zum peri-tumoralem nicht-malignem Gewebe, hypermethyliert und im *gene body* hypomethyliert. Diese Methylierungsveränderungen implizieren eine epigenetische Herunterregulation von *ADAMTS16* in epithelialen Tumoren. Tatsächlich zeigte eine Analyse von Genexpressionsdaten von Patienten mit *Kolonadenokarzinomen & Rektumadenokarzinomen (COADREAD)*, deren Daten vom *TCGA Konsortium* erhoben wurden, dass *ADAMTS16* bei diesen Patienten stark herunterreguliert war. Darüber hinaus bestätigte eine weitere Analyse der verfügbaren Methylierungsdaten zu diesen Patienten, dass sie die gleichen Methylierungsänderungen zeigten wie die CRC Kohorte. Allerdings zeigten Genexpressionsanalysen mittels qPCR von *ADAMTS16* in den gepaarten Proben der CRC-Kohorte keine klare Tendenz in Richtung Herauf- oder Herunterregulation von *ADAMTS16* und auch keine Verringerung der durchschnittlichen *ADAMTS16* Genexpression bei diesen Patienten. ADAMTS-16 ist eines der am wenigsten untersuchten ADAMTSs und seine Funktionen bleiben weitgehend rätselhaft, da das einzige bekannte Substrat der allgemeine Proteaseinhibitor α2-Makroglobulin ist. Die beobachteten starken Methylierungsänderungen in *ADAMTS16* in den verschiedenen Krebsarten weisen auf eine wichtige Funktion von ADAMTS-16 hin, beispielsweise als Tumorsuppressor. Dennoch bleibt diese Funktion von ADAMTS-16 vorerst ungeklärt. Daher sind funktionelle Studien im Hinblick auf die Rolle von ADAMTS-16 in Krebserkrankungen dringend nötig. Zusätzlich zu einer potenziellen funktionellen Bedeutung könnten die gefunden epigenetischen Veränderungen einen neuen epigenetischen Biomarker für epitheliale Tumore darstellen.

7 Abbreviations

°C	degree Celsius
A17	ADAM17
ADAM/TS	ADAM and ADAMTS
ADAMs	A Disintegrin And Metalloproteases
ADAMTS16	*ADAMTS16* (human gene or transcript)
ADAMTS-16	ADAMTS-16 (protein)
ADAMTSLs	ADAMTS-like proteases
ADAMTSs	ADAMs with thrombospondin motifs
ANOVA	analysis of variance
AP	alkaline phosphatase
ATP	adenosine triphosphate
B2M	β-2-microglobulin
BSA	bovine serum albumin
CANDIS	Conserved ADAM seventeeN Dynamic Interaction Sequence
COADREAD	Colon adenocarcinomas & Rectum adenocarcinomas
CpG	cytosine and guanine connected through a phosphate
ctrl	control
DMEM	Dulbecco´s Modified Eagle Medium
ECM	extracellular matrix
EGF	epidermal growth factor
EGFR	epidermal growth factor-receptor
FACS	Fluorescence-activated cell sorting
FCS	fetal calf serum
FSH	follicle-stimulating hormone
GAPDH	glyceraldehyde 3-phosphate dehydrogenase
GER	Germany
GPI	glycosylphosphatidylinositol
h	hour(s)
HA	hemagglutinin
HPRT	hypoxanthine-guanine phosphoribosyltransferase
HRP	horseradish peroxidase

IL-1RII	interleukin-1 receptor type 2
IL-6R	interleukin-6 receptor
infl	inflamed tissue
Iono or IO	ionomycin
iRhoms	inactive Rhomboids
JPN	Japan
l	liters
LB	Luria-Bertani
LC	lung cancer
m	meter(s)
M	molar
MEFs	ADAM10/17-double deficient knockout murine embryonic fibroblasts
MGMT	O^6-methylguanine-DNA methyltransferase
min	minute(s)
MM	marimastat
MMP13	matrix metalloprotease-13
MPD	membrane-proximal domain
MT1-MMP	matrix metallopeptidase 14
NAFLD	Non-alcoholic fatty liver disease
NASH	Non-alcoholic Steatohepatitis
Nef	Negative Regulatory Factor
NF-κ-B	nuclear factor kappa-light-chain-enhancer of activated B cells
NL	Netherlands
ns	non-significant
PBS	phosphate-buffered saline
PDI	protein-disulfide isomerase
Pen/Strep	Penicillin / Streptomycin
PLAC	protease and lacunin
PMA	phorbol 12-myristate 13-acetate
p-NP	p-nitrophenol
p-NPP	p-nitrophenylphosphat
PS	phosphatidylserine

PVDF	polyvenylidene fluoride
rcf	relative centrifugal force
real-time RT-qPCR	real-time reverse-transcriptase quantitative polymerase chain reaction
rpm	rounds per minute
s	second(s)
SCC	oral squamous-cell carcinoma
SD	spacer domain
SDS-PAGE	sodium dodecyl sulfate polyacrylamide gel electrophoresis
SVMPs	Snake venom metalloproteinases
TACE	tumor necrosis factor converting enzyme
TBS	tris-buffered saline
TBST	tris-buffered saline with tween
TCGA	The Cancer Genome Atlas
TGF-α AP	alkaline phosphatase-tagged transforming growth factor alpha
TGF-α shedding activity	ADAM17-mediated TGF-α substrate shedding
TGF-α	transforming growth factor alpha
TGF-β	transforming growth factor beta
TNFR	tumor necrosis factor receptor
TNF-α	tumor necrosis factor alpha
TSP-1	thrombospondin type 1
UK	United Kingdom
USA	United States of America
v/v	volume/volume
VEGF	vascular endothelial growth factor
vWFCP	Von Willebrand factor-cleaving protease
w/v	weight/volume
WB	western blot
WT	wildtype

8 References

Abdul-Majeed, S., Mell, B., Nauli, S.M., and Joe, B. (2014). Cryptorchidism and infertility in rats with targeted disruption of the Adamts16 locus. PLoS One *9*, e100967.

Ahrens, M., Ammerpohl, O., Von Schönfels, W., Kolarova, J., Bens, S., Itzel, T., Teufel, A., Herrmann, A., Brosch, M., Hinrichsen, H., et al. (2013). DNA methylation analysis in nonalcoholic fatty liver disease suggests distinct disease-specific and remodeling signatures after bariatric surgery. Cell Metab. *18*, 296–302.

Anders, A., Gilbert, S., Garten, W., Postina, R., and Fahrenholz, F. (2001). Regulation of the alpha-secretase ADAM10 by its prodomain and proprotein convertases. FASEB J. *15*, 1837–1839.

Apte, S.S. (2004). A disintegrin-like and metalloprotease (reprolysin type) with thrombospondin type 1 motifs: the ADAMTS family. Int. J. Biochem. Cell Biol. *36*, 981–985.

Arribas, J., and Esselens, C. (2009). ADAM17 as a therapeutic target in multiple diseases. Curr. Pharm. Des. *15*, 2319–2335.

Bandsma, R.H.J., van Goor, H., Yourshaw, M., Horlings, R.K., Jonkman, M.F., Schölvinck, E.H., Karrenbeld, A., Scheenstra, R., Kömhoff, M., Rump, P., et al. (2015). Loss of ADAM17 is associated with severe multi-organ dysfunction. Hum. Pathol. *46*, 923–928.

Bax, D. V., Messent, A.J., Tart, J., Van Hoang, M., Kott, J., Maciewicz, R.A., and Humphries, M.J. (2004). Integrin α5β1 and ADAM-17 interact in vitro and co-localize in migrating HeLa cells. J. Biol. Chem. *279*, 22377–22386.

Bennett, T.A., Edwards, B.S., Sklar, L.A., and Rogelj, S. (2000). Sulfhydryl regulation of L-selectin shedding: phenylarsine oxide promotes activation-independent L-selectin shedding from leukocytes. J. Immunol. *164*, 4120–4129.

Bevitt, D.J., Li, Z., Lindrop, J.L., Barker, M.D., Clarke, M.P., and McKie, N. (2005). Analysis of full length ADAMTS6 transcript reveals alternative splicing and a role for the 5' untranslated region in translational control. Gene *359*, 99–110.

Black, R.A., Rauch, C.T., Kozlosky, C.J., Peschon, J.J., Slack, J.L., Wolfson, M.F., Castner, B.J., Stocking, K.L., Reddy, P., Srinivasan, S., et al. (1997). A metalloproteinase disintegrin that releases tumour-necrosis factor-alpha from cells. Nature *385*, 729–733.

Bode, W., Gomis-Ruth, F.X., and Stockler, W. (1993). Astacins, serralysins, snake venom and matrix metalloproteinases exhibit identical zinc-binding environments (HEXXHXXGXXH and Met-turn) and topologies and should be grouped into a common family, the "metzincins." FEBS Lett. *331*, 134–140.

Bradford, M.M. (1976). A rapid and sensitive method for the quantitation of microgram quantities of protein utilizing the principle of protein-dye binding. Anal. Biochem. *72*, 248–254.

Brenet, F., Moh, M., Funk, P., Feierstein, E., Viale, A.J., Socci, N.D., and Scandura, J.M. (2011). DNA methylation of the first exon is tightly linked to transcriptional silencing. PLoS One *6*.

Brocker, C.N., Vasiliou, V., and Nebert, D.W. (2009). Evolutionary divergence and functions of the ADAM and ADAMTS gene families. Hum. Genomics *4*, 43–55.

Cal, S., and López-Otín, C. (2015). ADAMTS proteases and cancer. Matrix Biol. 1–9.

Cal, S., Obaya, A.J., Llamazares, M., Garabaya, C., Quesada, V., and López-Otín, C. (2002). Cloning, expression analysis, and structural characterization of seven novel human ADAMTSs, a family of metalloproteinases with disintegrin and thrombospondin-1 domains. Gene *283*, 49–62.

Charbonneau, M., Harper, K., Grondin, F., Pelmus, M., McDonald, P.P., and Dubois, C.M. (2007). Hypoxia-inducible factor mediates hypoxic and tumor necrosis factor alpha-induced increases in tumor necrosis factor-alpha converting enzyme/ADAM17 expression by synovial cells. J. Biol. Chem. *282*, 33714–33724.

Christova, Y., Adrain, C., Bambrough, P., Ibrahim, A., and Freeman, M. (2013). Mammalian iRhoms have distinct physiological functions including an essential role in TACE regulation. EMBO Rep. *14*, 884–890.

Demircan, K., Cömertoglu, I., Akyol, S., Yigitoglu, B.N., and Sarikaya, E. (2014). A new biological marker candidate in female reproductive system diseases: Matrix metalloproteinase with thrombospondin motifs (ADAMTS). J. Turkish Ger. Gynecol. Assoc. *15*, 250–255.

Doberstein, K., Steinmeyer, N., Hartmetz, A., Eberhardt, W., Mittelbronn, M., Harter, P.N., Juengel, E., Blaheta, R., Pfeilschifter, J., and Gutwein, P. (2013). MicroRNA-145 targets the metalloprotease ADAM17 and is suppressed in renal cell carcinoma patients. Neoplasia *15*, 218–230.

Drin, G., and Antonny, B. (2010). Amphipathic helices and membrane curvature. FEBS Lett. *584*, 1840–1847.

Du, W., Wang, S., Zhou, Q., Li, X., Chu, J., Chang, Z., Tao, Q., Ng, E.K.O., Fang, J., Sung, J.J.Y., et al. (2012). ADAMTS9 is a functional tumor suppressor through inhibiting AKT/mTOR pathway and associated with poor survival in gastric cancer. Oncogene 1–10.

Düsterhöft, S., Jung, S., Hung, C.-W., Tholey, A., Sönnichsen, F.D., Grötzinger, J., and Lorenzen, I. (2013). Membrane-Proximal Domain of a Disintegrin and Metalloprotease-17 Represents the Putative Molecular Switch of Its Shedding Activity Operated by Protein-disulfide Isomerase. J. Am. Chem. Soc. *135*, 5776–5781.

Düsterhöft, S., Höbel, K., Oldefest, M., Lokau, J., Waetzig, G.H., Chalaris, A., Garbers, C., Scheller, J., Rose-John, S., Lorenzen, I., et al. (2014). A disintegrin and metalloprotease 17 dynamic interaction sequence, the sweet tooth for the human interleukin 6 receptor. J. Biol. Chem. *289*, 16336–16348.

Düsterhöft, S., Michalek, M., Kordowski, F., Oldefest, M., Sommer, A., Röseler, J., Reiss, K., Grötzinger, J., and Lorenzen, I. (2015). Extracellular Juxtamembrane Segment of ADAM17 Interacts with Membranes and Is Essential for Its Shedding Activity. Biochemistry 150908133814005.

Edwards, D.R., Handsley, M.M., and Pennington, C.J. (2008). The ADAM metalloproteinases. Mol. Aspects Med. *29*, 258–289.

Elazar, M., Liu, P., Rice, C.M., and Glenn, J.S. (2004). An N-Terminal Amphipathic Helix in Hepatitis C Virus (HCV) NS4B Mediates Membrane Association, Correct Localization of Replication Complex Proteins, and HCV RNA Replication. J. Virol. *78*, 11393–11400.

Esteller, M. (2002). CpG island hypermethylation and tumor suppressor genes: a booming present, a brighter future. Oncogene *21*, 5427–5440.

Esteller, M. (2007). Cancer epigenomics: DNA methylomes and histone-modification maps. Nat. Rev. Genet. *8*, 286–298.

Farrell, G.C., Van Rooyen, D., Gan, L., and Chitturi, S. (2012). NASH is an inflammatory disorder: Pathogenic, prognostic and therapeutic implications. Gut Liver *6*, 149–171.

Le Gall, S.M., Bobé, P., Reiss, K., Horiuchi, K., Niu, X.-D., Lundell, D., Gibb, D.R., Conrad, D., Saftig, P., and Blobel, C.P. (2009). ADAMs 10 and 17 represent differentially regulated components of a general shedding machinery for membrane proteins such as transforming growth factor alpha, L-selectin, and tumor necrosis factor alpha. Mol. Biol. Cell *20*, 1785–1794.

Le Gall, S.M., Maretzky, T., Issuree, P.D.A., Niu, X.-D., Reiss, K., Saftig, P., Khokha, R., Lundell, D., and Blobel, C.P. (2010). ADAM17 is regulated by a rapid and reversible mechanism that controls access to its catalytic site. J. Cell Sci. *123*, 3913–3922.

Gao, G., Westling, J., Thompson, V.P., Howell, T.D., Gottschall, P.E., and Sandy, J.D. (2002). Activation of the proteolytic activity of ADAMTS4 (aggrecanase-1) by C-terminal truncation. J. Biol. Chem. *277*, 11034–11041.

Gao, S., De Geyter, C., Kossowska, K., and Zhang, H. (2007). FSH stimulates the expression of the ADAMTS-16 protease in mature human ovarian follicles. Mol. Hum. Reprod. *13*, 465–471.

Gautier, R., Douguet, D., Antonny, B., and Drin, G. (2008). HELIQUEST: A web server to screen sequences with specific alpha-helical properties. Bioinformatics *24*, 2101–2102.

Gerlach, H., Laumann, V., Martens, S., Becker, C.F.W., Goody, R.S., and Geyer, M. (2010). HIV-1 Nef membrane association depends on charge, curvature, composition and sequence. Nat. Chem. Biol. *6*, 46–53.

Le Goff, C., and Cormier-Daire, V. (2011). The ADAMTS(L) family and human genetic disorders. Hum. Mol. Genet. *20*, R163–R167.

Gopalakrishnan, K., Kumarasamy, S., Abdul-Majeed, S., Kalinoski, A.L., Morgan, E.E., Gohara, A.F., Nauli, S.M., Filipiak, W.E., Saunders, T.L., and Joe, B. (2012). Targeted disruption of Adamts16 gene in a rat genetic model of hypertension. Proc. Natl. Acad. Sci. U. S. A. *109*, 20555–20559.

De Groot, R., Bardhan, A., Ramroop, N., Lane, D.A., and Crawley, J.T.B. (2009). Essential role of the disintegrin-like domain in ADAMTS13 function. Blood *113*, 5609–5616.

Gruemmer, R., Klein-Hitpass, L., and Neulen, J. (2005). Regulation of gene expression in endothelial cells: the role of human follicular fluid. J. Mol. Endocrinol. *34*, 37–46.

Gubelmann, C., Gattiker, A., Massouras, A., Hens, K., David, F., Decouttere, F., Rougemont, J., and Deplancke, B. (2011). GETPrime: A gene- or transcript-specific primer database for quantitative real-time PCR. Database *2011*, 1–12.

Guo, N.H., Krutzsch, H.C., Inman, J.K., and Roberts, D.D. (1997). Thrombospondin 1 and type I repeat peptides of thrombospondin 1 specifically induce apoptosis of endothelial cells. Cancer Res. *57*, 1735–1742.

Gutwein, P., Mechtersheimer, S., Riedle, S., Stoeck, A., Gast, D., Joumaa, S., Zentgraf, H., Fogel, M., and Altevogt, D.P. (2003). ADAM10-mediated cleavage of L1 adhesion molecule at the cell surface and in released membrane vesicles. FASEB J. *17*, 292–294.

Hanahan, D., and Weinberg, R.A. (2011). Hallmarks of cancer: The next generation. Cell *144*, 646–674.

Hartmann, D., de Strooper, B., Serneels, L., Craessaerts, K., Herreman, A., Annaert, W., Umans, L., Lübke, T., Lena Illert, A., von Figura, K., et al. (2002). The disintegrin/metalloprotease ADAM 10 is essential for Notch signalling but not for alpha-secretase activity in fibroblasts. Hum. Mol. Genet. *11*, 2615–2624.

Herman, J.G., and Baylin, S.B. (2003). Gene silencing in cancer in association with promoter hypermethylation. N. Engl. J. Med. *349*, 2042–2054.

Horiuchi, K., Le Gall, S., Schulte, M., Yamaguchi, T., Reiss, K., Murphy, G., Toyama, Y., Hartmann, D., Saftig, P., and Blobel, C.P. (2007). Substrate selectivity of epidermal growth factor-receptor ligand sheddases and their regulation by phorbol esters and calcium influx. Mol. Biol. Cell *18*, 176–188.

Hubmacher, D., and Apte, S.S. (2015). ADAMTS proteins as modulators of microfibril formation and function. Matrix Biol.

Iruela-Arispe, M.L., Lombardo, M., Krutzsch, H.C., Lawler, J., and Roberts, D.D. (1999). Inhibition of angiogenesis by thrombospondin-1 is mediated by 2 independent regions within the type 1 repeats. Circulation *100*, 1423–1431.

Issuree, P.D.A., Maretzky, T., McIlwain, D.R., Monette, S., Qing, X., Lang, P.A., Swendeman, S.L., Park-Min, K.-H., Binder, N., Kalliolias, G.D., et al. (2013). iRHOM2 is a critical pathogenic mediator of inflammatory arthritis. J. Clin. Invest. 1–5.

Jacobi, C.L.J., Rudigier, L.J., Scholz, H., and Kirschner, K.M. (2013). Transcriptional regulation by the Wilms tumor protein, Wt1, suggests a role of the metalloproteinase Adamts16 in murine genitourinary development. J. Biol. Chem. *288*, 18811–18824.

Jiang, J.X., Chen, X., Fukada, H., Serizawa, N., Devaraj, S., and Török, N.J. (2013). Advanced glycation endproducts induce fibrogenic activity in nonalcoholic steatohepatitis by modulating TNF-α-converting enzyme activity in mice. Hepatology *58*, 1339–1348.

Jin, H., Wang, X., Ying, J., Wong, A.H.Y., Li, H., Lee, K.Y., Srivastava, G., Chan, A.T.C., Yeo, W., Ma, B.B.Y., et al. (2007). Epigenetic identification of ADAMTS18 as a novel 16q23.1 tumor suppressor frequently silenced in esophageal, nasopharyngeal and multiple other carcinomas. Oncogene *26*, 7490–7498.

Joe, B., Saad, Y., Dhindaw, S., Lee, N.H., Frank, B.C., Achinike, O.H., Luu, T. V, Gopalakrishnan, K., Toland, E.J., Farms, P., et al. (2009). Positional identification of variants of Adamts16 linked to inherited hypertension. Hum. Mol. Genet. *18*, 2825–2838.

Jones, G.C., and Riley, G.P. (2005). ADAMTS proteinases: a multi-domain, multi-functional family with roles in extracellular matrix turnover and arthritis. Arthritis Res. Ther. *7*, 160–169.

Jones, P.A., and Baylin, S.B. (2007). The Epigenomics of Cancer. Cell *128*, 683–692.

Kantlehner, M., Kirchner, R., Hartmann, P., Ellwart, J.W., Alunni-Fabbroni, M., and Schumacher, A. (2011). A high-throughput DNA methylation analysis of a single cell. Nucleic Acids Res. *39*, 1–9.

Kevorkian, L., Young, D.A., Darrah, C., Donell, S.T., Shepstone, L., Porter, S., Brockbank, S.M. V, Edwards, D.R., Parker, A.E., and Clark, I.M. (2004). Expression profiling of metalloproteinases and their inhibitors in cartilage. Arthritis Rheum. *50*, 131–141.

De Kok, J.B., Roelofs, R.W., Giesendorf, B.A., Pennings, J.L., Waas, E.T., Feuth, T., Swinkels, D.W., and Span, P.N. (2005). Normalization of gene expression measurements in tumor tissues: comparison of 13 endogenous control genes. Lab. Invest. *85*, 154–159.

Kreck, B., Richter, J., Ammerpohl, O., Barann, M., Esser, D., Petersen, B.S., Vater, I., Murga Penas, E.M., Bormann Chung, C.A., Seisenberger, S., et al. (2013). Base-pair resolution DNA methylome of the EBV-positive Endemic Burkitt lymphoma cell line DAUDI determined by SOLiD bisulfite-sequencing. Leukemia *27*, 1751–1753.

Kuan, P.F., Wang, S., Zhou, X., and Chu, H. (2010). A statistical framework for Illumina DNA methylation arrays. Bioinformatics *26*, 2849–2855.

Kumar, S., Rao, N., and Ge, R. (2012). Emerging Roles of ADAMTSs in Angiogenesis and Cancer. Cancers (Basel). *4*, 1252–1299.

Kuno, K., and Matsushima, K. (1998). ADAMTS-1 protein anchors at the extracellular matrix through the thrombospondin type I motifs and its spacing region. J. Biol. Chem. *273*, 13912–13917.

Lammich, S., Kojro, E., Postina, R., Gilbert, S., Pfeiffer, R., Jasionowski, M., Haass, C., and Fahrenholz, F. (1999). Constitutive and regulated alpha-secretase cleavage of Alzheimer's amyloid precursor protein by a disintegrin metalloprotease. Proc. Natl. Acad. Sci. U. S. A. *96*, 3922–3927.

Li, X., Pérez, L., Pan, Z., and Fan, H. (2007). The transmembrane domain of TACE regulates protein ectodomain shedding. Cell Res. *17*, 985–998.

Li, X., Maretzky, T., Weskamp, G., Monette, S., Qing, X., Issuree, P.D.A., Crawford, H.C., McIlwain, D.R., Mak, T.W., Salmon, J.E., et al. (2015). iRhoms 1 and 2 are essential upstream regulators of ADAM17-dependent EGFR signaling. Proc. Natl. Acad. Sci. 201505649.

Lorenzen, I., Trad, A., and Grötzinger, J. (2011). Multimerisation of A disintegrin and metalloprotease protein-17 (ADAM17) is mediated by its EGF-like domain. Biochem. Biophys. Res. Commun. *415*, 330–336.

Lorenzen, I., Lokau, J., Düsterhöft, S., Trad, A., Garbers, C., Scheller, J., Rose-John, S., and Grötzinger, J. (2012). The membrane-proximal domain of A Disintegrin and Metalloprotease 17 (ADAM17) is responsible for recognition of the interleukin-6 receptor and interleukin-1 receptor II. FEBS Lett. *586*, 1093–1100.

Majerus, E.M., Zheng, X., Tuley, E.A., and Sadler, J.E. (2003). Cleavage of the ADAMTS13 Propeptide Is Not Required for Protease Activity. J. Biol. Chem. *278*, 46643–46648.

Malfait, A.M., Liu, R.Q., Ijiri, K., Komiya, S., and Tortorella, M.D. (2002). Inhibition of ADAM-TS4 and ADAM-TS5 prevents aggrecan degradation in osteoarthritic cartilage. J. Biol. Chem. *277*, 22201–22208.

Maskos, K., Fernandez-Catalan, C., Huber, R., Bourenkov, G.P., Bartunik, H., Ellestad, G.A., Reddy, P., Wolfson, M.F., Rauch, C.T., Castner, B.J., et al. (1998). Crystal structure of the catalytic domain of human tumor necrosis factor-alpha-converting enzyme. Proc. Natl. Acad. Sci. U. S. A. *95*, 3408–3412.

Matthews, V., Schuster, B., Schütze, S., Bussmeyer, I., Ludwig, A., Hundhausen, C., Sadowski, T., Saftig, P., Hartmann, D., Kallen, K.J., et al. (2003). Cellular cholesterol depletion triggers shedding of the human interleukin-6 receptor by ADAM10 and ADAM17 (TACE). J. Biol. Chem. *278*, 38829–38839.

Maunakea, A.K., Chepelev, I., Cui, K., and Zhao, K. (2013). Intragenic DNA methylation modulates alternative splicing by recruiting MeCP2 to promote exon recognition. Cell Res. *23*, 1256–1269.

McIlwain, D.R., Lang, P.A., Maretzky, T., Hamada, K., Ohishi, K., Maney, S.K., Berger, T., Murthy, A., Duncan, G., Xu, H.C., et al. (2012). iRhom2 regulation of TACE controls TNF-mediated protection against Listeria and responses to LPS. Science *335*, 229–232.

Miettinen, P.J., Berger, J.E., Meneses, J., Phung, Y., Pedersen, R.A., Werb, Z., and Derynck, R. (1995). Epithelial immaturity and multiorgan failure in mice lacking epidermal growth factor receptor. Nature *376*, 337–341.

Mikeska, T., Bock, C., Do, H., and Dobrovic, A. (2012). DNA methylation biomarkers in cancer: progress towards clinical implementation. Expert Rev. Mol. Diagn. *12*, 473–487.

Milla, M.E., Leesnitzer, M.A., Moss, M.L., Clay, W.C., Carter, H.L., Miller, a B., Su, J.L., Lambert, M.H., Willard, D.H., Sheeley, D.M., et al. (1999). Specific sequence elements are required for the expression of functional tumor necrosis factor-alpha-converting enzyme (TACE). J. Biol. Chem. *274*, 30563–30570.

Mineura, K., Yanagisawa, T., Watanabe, K., Kowada, M., and Yasui, N. (1996). Human brain tumor O6-methylguanine-DNA methyltransferase mRNA and its significance as an indicator of selective chloroethylnitrosourea chemotherapy. Int. J. Cancer *69*, 420–425.

Murray, D., Ben-Tal, N., Honig, B., and McLaughlin, S. (1997). Electrostatic interaction of myristoylated proteins with membranes: simple physics, complicated biology. Structure *5*, 985–989.

Oda, K., Matsuoka, Y., Funahashi, A., and Kitano, H. (2005). A comprehensive pathway map of epidermal growth factor receptor signaling. Mol. Syst. Biol. *1*, 2005.0010.

Okazaki, I., Noro, T., Tsutsui, N., Yamanouchi, E., Kuroda, H., Nakano, M., Yokomori, H., and Inagaki, Y. (2014). Fibrogenesis and carcinogenesis in nonalcoholic steatohepatitis (NASH): Involvement of matrix metalloproteinases (MMPs) and tissue inhibitors of metalloproteinase (TIMPs). Cancers (Basel). *6*, 1220–1255.

Oliveros, J.C. (2007). VENNY. An interactive tool for comparing lists with Venn Diagrams. http://bioinfogp.cnb.csic.es/tools/venny/index.html.

Peschon, J.J. (1998). An Essential Role for Ectodomain Shedding in Mammalian Development. Science (80-.). *282*, 1281–1284.

Porter, S., Clark, I.M., Kevorkian, L., and Edwards, D.R. (2005). The ADAMTS metalloproteinases. Biochem. J. *386*, 15–27.

Pratta, M.A., Yao, W., Decicco, C., Tortorella, M.D., Liu, R.Q., Copeland, R.A., Magolda, R., Newton, R.C., Trzaskos, J.M., and Arner, E.C. (2003). Aggrecan Protects Cartilage Collagen from Proteolytic Cleavage. J. Biol. Chem. *278*, 45539–45545.

Puente, X.S., and Lo, C. (2004). A Genomic Analysis of Rat Proteases and Protease Inhibitors. Genome Res. *14*, 609–622.

Pyun, J.-A., Kim, S., and Kwack, K. (2014). Interaction between thyroglobulin and ADAMTS16 in premature ovarian failure. Clin. Exp. Reprod. Med. *41*, 120–124.

Reiss, K., and Saftig, P. (2009). The “a disintegrin and metalloprotease” (ADAM) family of sheddases: physiological and cellular functions. Semin. Cell Dev. Biol. *20*, 126–137.

Reiss, K., Cornelsen, I., Husmann, M., Gimpl, G., and Bhakdi, S. (2011). Unsaturated fatty acids drive disintegrin and metalloproteinase (ADAM)-dependent cell adhesion, proliferation, and migration by modulating membrane fluidity. J. Biol. Chem. *286*, 26931–26942.

Rocks, N., Paulissen, G., El Hour, M., Quesada, F., Crahay, C., Gueders, M., Foidart, J.M., Noel, A., and Cataldo, D. (2008). Emerging roles of ADAM and ADAMTS metalloproteinases in cancer. Biochimie *90*, 369–379.

Rodríguez-Manzaneque, J.C., Milchanowski, A.B., Dufour, E.K., Leduc, R., and Iruela-Arispe, M.L. (2000). Characterization of METH-1/ADAMTS1 processing reveals two distinct active forms. J. Biol. Chem. *275*, 33471–33479.

Sakai, T., Toguchida, J., Ohtani, N., Yandell, D.W., Rapaport, J.M., and Dryja, T.P. (1991). Allele-specific hypermethylation of the retinoblastoma tumor-suppressor gene. Am. J. Hum. Genet. *48*, 880–888.

Sakamoto, N., Oue, N., Noguchi, T., Sentani, K., Anami, K., Sanada, Y., Yoshida, K., and Yasui, W. (2010). Serial analysis of gene expression of esophageal squamous cell carcinoma: ADAMTS16 is upregulated in esophageal squamous cell carcinoma. Cancer Sci. *101*, 1038–1044.

Salami, F., Qiao, S., and Homayouni, R. (2015). Expression of mouse Dab2ip transcript variants and gene methylation during brain development. Gene *568*, 19–24.

Santiago-Josefat, B., Esselens, C., Bech-Serra, J.J., and Arribas, J. (2007). Post-transcriptional up-regulation of ADAM17 upon epidermal growth factor receptor activation and in breast tumors. J. Biol. Chem. *282*, 8325–8331.

Scheller, J., Chalaris, A., Garbers, C., and Rose-John, S. (2011). ADAM17: a molecular switch to control inflammation and tissue regeneration. Trends Immunol. *32*, 380–387.

Schlöndorff, J., Becherer, J.D., and Blobel, C.P. (2000). Intracellular maturation and localization of the tumour necrosis factor alpha convertase (TACE). Biochem. J. *347 Pt 1*, 131–138.

Schwarz, J., Schmidt, S., Will, O., Koudelka, T., Köhler, K., Boss, M., Rabe, B., Tholey, A., Scheller, J., Schmidt-Arras, D., et al. (2014). Polo-like kinase 2, a novel ADAM17 signaling component, regulates tumor necrosis factor α ectodomain shedding. J. Biol. Chem. *289*, 3080–3093.

Seals, D.F., and Courtneidge, S.A. (2003). The ADAMs family of metalloproteases: Multidomain proteins with multiple functions. Genes Dev. *17*, 7–30.

Segrest, J.P., Jones, M.K., De Loof, H., Brouillette, C.G., Venkatachalapathi, Y. V, and Anantharamaiah, G.M. (1992). The amphipathic helix in the exchangeable apolipoproteins: a review of secondary structure and function. J. Lipid Res. *33*, 141–166.

Seniski, G.G., Camargo, A.A., Ierardi, D.F., Ramos, E.A.S., Grochoski, M., Ribeiro, E.S.F., Cavalli, I.J., Pedrosa, F.O., de Souza, E.M., Zanata, S.M., et al. (2009). ADAM33 gene silencing by promoter hypermethylation as a molecular marker in breast invasive lobular carcinoma. BMC Cancer *9*, 80.

Shen, C., Hu, L., Xia, L., and Li, Y. (2008). Quantitative real-time RT-PCR detection for survivin, CK20 and CEA in peripheral blood of colorectal cancer patients. Jpn. J. Clin. Oncol. *38*, 770–776.

Skovronsky, D.M., Moore, D.B., Milla, M.E., Doms, R.W., and Lee, V.M. (2000). Protein kinase C-dependent alpha-secretase competes with beta-secretase for cleavage of amyloid-beta precursor protein in the trans-golgi network. J. Biol. Chem. *275*, 2568–2575.

Soker, S., Svahn, C.M., and Neufeld, G. (1993). Vascular endothelial growth factor (VEGF) binds to alpha-2-macroglobulin and the binding is inhibited by heparin. J.Biol.Chem. *268*, 7685–7691.

Sommer, A., Kordowski, F., Büch, J., Evers, A., Maretzky, T., Michalek, M., Andrä, J., B., C.P., Jung, S., Schirmeister, T., Kunzelmann, K., Nagata, S., Düsterhöft, S., Nehls, C., H., and L., Gutsmann, T., Grötzinger, J., Bhakdi, S., Reiss, K. (2015). Phosphatidylserine exposure represents the decisive step of ADAM17-mediated proteolysis. IN REVISION.

Surridge, A.K., Rodgers, U.R., Swingler, T.E., Davidson, R.K., Kevorkian, L., Norton, R., Waters, J.G., Goldring, M.B., Parker, A.E., and Clark, I.M. (2009). Characterization and regulation of ADAMTS-16. Matrix Biol. *28*, 416–424.

Takeda, S. (2009). Three-dimensional domain architecture of the ADAM family proteinases. Semin. Cell Dev. Biol. *20*, 146–152.

Tan, I.D.A., Ricciardelli, C., and Russell, D.L. (2013). The metalloproteinase ADAMTS1: a comprehensive review of its role in tumorigenic and metastatic pathways. Int. J. Cancer *133*, 2263–2276.

Tang, B.L. (2001). ADAMTS: a novel family of extracellular matrix proteases. Int. J. Biochem. Cell Biol. *33*, 33–44.

Teif, V.B., Beshnova, D.A., Vainshtein, Y., Marth, C., Mallm, J.P., and Rippe, T.H. (2014). Nucleosome repositioning links DNA (de)methylation and differential CTCF binding during stem cell development. Genome Res. *24*, 1285–1295.

Tellier, E., Canault, M., Rebsomen, L., Bonardo, B., Juhan-Vague, I., Nalbone, G., and Peiretti, F. (2006). The shedding activity of ADAM17 is sequestered in lipid rafts. Exp. Cell Res. *312*, 3969–3980.

Toyota, M., and Issa, J.P.J. (2005). Epigenetic changes in solid and hematopoietic tumors. Semin. Oncol. *32*, 521–531.

Tucher, J., Linke, D., Koudelka, T., Cassidy, L., Tredup, C., Wichert, R., Pietrzik, C., Becker-Pauly, C., and Tholey, A. (2014). LC-MS based cleavage site profiling of the proteases ADAM10 and ADAM17 using proteome-derived peptide libraries. J. Proteome Res. *13*, 2205–2214.

Wei, X., Prickett, T.D., Viloria, C.G., Molinolo, A., Lin, J.C., Cardenas-Navia, I., Cruz, P., Rosenberg, S.A., Davies, M.A., Gershenwald, J.E., et al. (2010). Mutational and functional analysis reveals ADAMTS18 metalloproteinase as a novel driver in melanoma. Mol. Cancer Res. *8*, 1513–1525.

White, J.M. (2003). ADAMs: Modulators of cell-cell and cell-matrix interactions. Curr. Opin. Cell Biol. *15*, 598–606.

Wick, W., Weller, M., van den Bent, M., Sanson, M., Weiler, M., von Deimling, A., Plass, C., Hegi, M., Platten, M., and Reifenberger, G. (2014). MGMT testing-the challenges for biomarker-based glioma treatment. Nat. Rev. Neurol. *10*, 372–385.

Wilhelm, M., Schlegl, J., Hahne, H., Moghaddas Gholami, A., Lieberenz, M., Savitski, M.M., Ziegler, E., Butzmann, L., Gessulat, S., Marx, H., et al. (2014). Mass-spectrometry-based draft of the human proteome. Nature *509*, 582–587.

Willems, S.H., Tape, C.J., Stanley, P.L., Taylor, N.A., Mills, I.G., Neal, D.E., McCafferty, J., and Murphy, G. (2010). Thiol isomerases negatively regulate the cellular shedding activity of ADAM17. Biochem. J. *428*, 439–450.

Xu, P., and Derynck, R. (2010). Direct Activation of TACE-Mediated Ectodomain Shedding by p38 MAP Kinase Regulates EGF Receptor-Dependent Cell Proliferation. Mol. Cell *37*, 551–566.

Xu, B., Zhang, L., Luo, C., Qi, Y., Cui, Y., Ying, J.-M., Zhang, Q., and Jin, J. (2015). Hypermethylation of the 16q23.1 Tumor Suppressor Gene ADAMTS18 in Clear Cell Renal Cell Carcinoma. Int. J. Mol. Sci. *16*, 1051–1065.

Xu, C., Gagnon, E., Call, M.E., Schnell, J.R., Schwieters, C.D., Carman, C. V., Chou, J.J., and Wucherpfennig, K.W. (2008). Regulation of T Cell Receptor Activation by Dynamic Membrane Binding of the CD3E Cytoplasmic Tyrosine-Based Motif. Cell *135*, 702–713.

Ye, J., Coulouris, G., Zaretskaya, I., Cutcutache, I., Rozen, S., and Madden, T.L. (2012). Primer-BLAST: A tool to design target-specific primers for polymerase chain reaction. BMC Bioinformatics *13*, 134.

Yoda, M., Kimura, T., Tohmonda, T., Morioka, H., Matsumoto, M., Okada, Y., Toyama, Y., and Horiuchi, K. (2013). Systemic overexpression of TNFα-converting enzyme does not lead to enhanced shedding activity in vivo. PLoS One *8*, e54412.

Yoder, J.A., Walsh, C.P., and Bestor, T.H. (1997). Cytosine methylation and the ecology of intragenomic parasites. Trends Genet. *13*, 335–340.

Yuan, J.S., Reed, A., Chen, F., and Stewart, C.N. (2006). Statistical analysis of real-time PCR data. BMC Bioinformatics *7*, 85.

Zeng, W., Corcoran, C., Collins-Racie, L.A., Lavallie, E.R., Morris, E.A., and Flannery, C.R. (2006). Glycosaminoglycan-binding properties and aggrecanase activities of truncated ADAMTSs: comparative analyses with ADAMTS-5, -9, -16 and -18. Biochim. Biophys. Acta *1760*, 517–524.

Zou, J., Lippert, C., Heckerman, D., Aryee, M., and Listgarten, J. (2014). Epigenome-wide association studies without the need for cell-type composition. Nat. Methods *11*, 309–311.

9 Acknowledgement

There are many people whom I wish to thank. Without them, making this thesis would not have been possible. Some are colleagues, but many grew friends over time.

First and foremost, I thank Prof. Karina Reiss for giving me the opportunity to prepare my doctoral thesis in her research group and for her immense support on so various levels regarding my work. I am very grateful for her intensive and passionate guidance over the last three years, her always open door, and being just one grasp away with helping hints and supportive ideas. Many times she re-motivated me and showed me the light on the other side of the microscope, when it was hard to see. Moreover, I am deeply thankful for her support towards my postgraduate project.

I like to thank Prof. Reiner Siebert from the Institute of Human Genetics for warmly welcoming me in his institute and providing tools and ideas for the success of my project. I further thank him for his time and effort in establishing and co-supervising my RTG project.

In regard to the methylation data, I thank Prof. Ole Ammerpohl from the Institute of Human Genetics for kindly providing the access to the cohorts and tirelessly sharing his expertise with me, even before seven in the morning. I especially thank Julia Kolarova from the Institute of Human Genetics for performing the methylation assay for the CRC cohort and the nicest review of my poster.

I am very grateful for the very intensive and productive cooperation with Prof. Joachim Grötzinger from the Biochemistry Department who guided my scientific way with “candies”.

I wish to thank Andre Franke and all other founding members of the RTG1743 for building this interdisciplinary research network and giving young scientists the opportunity to grow in a flourishing environment.

I would like to greatly thank Christian Röder from the Institute for Experimental Cancer Research and his group members for kindly providing the RNA and tissue samples that made this thesis possible.

My special thanks go to my colleague Anselm Sommer for his support in regard to flow cytometry and for performing part of the flow cytometric analyses.

I give special thanks to Pankaj Yadav from the RTG1743 for his support on R programming.

I would like to acknowledge Katrin Masuhr and Marion Kölln from the Anatomy Department for their kind help and effort with the IHC stainings.

My special thanks go to Astrid Evers who welcomed me with wide open arms in the lab and trained me in the first months of my thesis.

I am very grateful for the critical and foremost passionate discussion sessions with Maria Sperrhacke.
I say thank you to Florian Bleibaum for our entertaining, deeply philosophical and not less politically (incorrect) discussions during a white chocolate mocha.
For keeping our lab ordered and smoothly running, I thank Björn Ahrens.
Nancy Speck played an important part for me in motivating me, particularly with Yoda et al. Might the force be with you on your way.

It is a pleasure to thank Ulrich Gerstel and Britta Hansmann for their troubleshooting efforts with Henriette and everything else which refused to work as promised by the advertisement.

I would like to thank all my other colleagues from the Group AG Reiss for the friendly atmosphere, for helping to mutually motivate us and enriching my long days in the lab, and for their help supporting my work. I particularly, would like to thank for our daily lunch time. I cherish this time.

Additionally, I wish to thank Simon, Priya, Wei-Hung and Pankaj for our enjoyable RTG get-togethers.

I am very grateful to Prof. Thomas Roeder from the Zoological Institute for agreeing to be the second supervisor and reviewer of my thesis.

I thank Ian Clark from the School of Biological Sciences, UK, for kindly providing the ADAMTS16 plasmid.

I am grateful to Jan Sonnemann and his wonderful baby daughter for keeping my mood up during each of the 5 crises of the doctoral thesis.

I wish to thank my friends and my family for their support, faith and presence during these challenging years. I especially thank Anna Czabanska for her lovely support and company.

I am deeply grateful to my mother, Birgit Kordowski, for contributing her endless effort and love towards me and my success. I devote this thesis to her.

10 Supplements

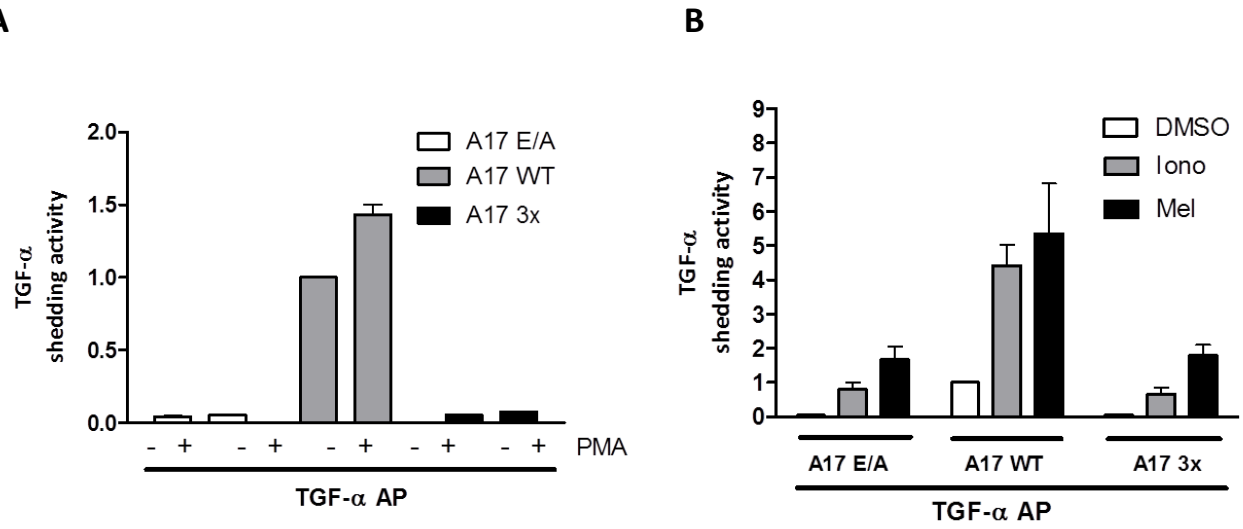

Supplemental Figure 1. Mutations in a polybasic RKK-motif in the membrane-proximal domain of ADAM17 have the same effect as the EE mutations in CANDIS. Substitutions in a polybasic motif of ADAM17 in the MPD (R625G K626G K628G) completely abolished the ability of ADAM17 to shed the transmembrane substrate TGF-α. This motif is proposed to be a phosphatidylserine (PS)-binding motif that is needed for the interaction with exposed PS, to enable shedding. ADAM10/17-double-deficient mouse embryonic fibroblasts (MEFs) were retransfected with inactive ADAM17 E/A variant as control, murine ADAM17 wildtype (A17 WT) or the ADAM17 3x (A17 3x) mutant and plasmids containing alkaline phosphatase coupled TGF-α (TGF-α AP). 24 h after transfection, MEFs were treated or not treated with phorbol 12-myristate 13-acetate (PMA, 200 ng/ml) for 2 h ***(A)*** or ionomycin (Iono, 1 µM) and melittin (Mel, 1 µM) for 30 min ***(B)***. Thereafter, the ADAM17-mediated TGF-α shedding activity was determined. Retransfection of A17 WT rescued constitutive and stimulated TGF-α release. In contrast, retransfection of A17 3x did not rescue constitutive and stimulated TGF-α shedding. Data represent the means +SEM (standard error of mean) of at least three independent experiments (n≥3).

11 Curriculum Vitae

12 Erklärung

Hiermit erkläre ich, Felix Kordowski, dass ich die vorliegende Dissertation eigenständig und nur mit den von mir angegebenen Quellen und Hilfsmitteln bzw. mit der wissenschaftlichen Beratung meiner akademischen Betreuer angefertigt habe. Die vorliegende Arbeit ist unter Einhaltung der Regeln guter wissenschaftlicher Praxis der Deutschen Forschungsgemeinschaft entstanden und wurde bisher in gleicher oder ähnlicher Form an keiner anderen Universität zur Begutachtung im Rahmen eines Prüfungsverfahrens vorgelegt. Weiterhin bestätige ich, dass ich zuvor noch keine Promotionsversuche unternommen habe.

Teile dieser Arbeit wurden in dem folgenden Artikel veröffentlicht:

Düsterhöft*, S., Michalek*, M., **Kordowski*, F.**, Oldefest, M., Sommer, A., Röseler, J., Reiss, K., Grötzinger, J., and Lorenzen, I. (2015). **The extracellular juxtamembrane segment of ADAM17 interacts with membranes and is essential for its shedding activity.** Biochemistry 150908133814005.
*equal contribution

Darüber hinaus befindet sich ein weiteres Manuskript in Revision, welches Daten enthält, die ich im Rahmen meiner Doktorarbeit generiert habe (siehe auch Supplemental Figure 1):

Sommer, A., **Kordowski, F.**, Büch, J., Evers, A., Maretzky, T., Michalek, M., Andrä, J., Blobel, C.P., Jung, S., Schirmeister, T., Kunzelmann, K., Nagata, S., Düsterhöft, S., Nehls, C., Heinbockel, L., Gutsmann, T., Grötzinger, J., Bhakdi, S., Reiss, K. **Phosphatidylserine exposure represents the decisive step of ADAM17-mediated proteolysis.**